

**UCLA**

**UCLA Electronic Theses and Dissertations**

**Title**

Development and Application of New Analytical and Modeling Approaches to Quantify Fatty Acid Metabolism in Cells

**Permalink**

<https://escholarship.org/uc/item/6xp7q81n>

**Author**

Argus, Joseph Patrick

**Publication Date**

2017

Peer reviewed|Thesis/dissertation

UNIVERSITY OF CALIFORNIA

Los Angeles

Development and Application of New Analytical and Modeling Approaches to Quantify Fatty  
Acid Metabolism in Cells

A dissertation submitted in partial satisfaction of the  
requirements for the degree Doctor of Philosophy  
in Molecular and Medical Pharmacology

by

Joseph Patrick Argus

2017

© Copyright by

Joseph Patrick Argus

2017

## ABSTRACT OF THE DISSERTATION

Development and Application of New Analytical and Modeling Approaches to Quantify Fatty  
Acid Metabolism in Cells

by

Joseph Patrick Argus

Doctor of Philosophy in Molecular and Medical Pharmacology

University of California, Los Angeles, 2017

Professor Steven J. Bensinger, Chair

Lipids are a diverse group of molecules that play critical structural, signaling, and energy storage roles in all cells. Fatty acids are key building blocks for many lipids, and the fatty acid content of a lipid species has important effects on its properties and function. As a result, changes in fatty acid metabolism are an essential part of many normal and pathophysiological processes. However, there remain significant gaps in our knowledge of fatty acids and their metabolism, in part due to challenges in measuring fatty acid pool sizes and fluxes. Herein, we demonstrate how stable isotope labeling of cells followed by modeling of gas chromatography-mass spectrometry data from their fatty acids can begin to address these issues and yield important

insights into how fatty acid metabolism affects other aspects of biology. First, we describe a new analytical method optimized for measuring fatty acids and cholesterol from stable isotope-labeled cells. Next, we report a novel mathematical model that allows for measurement of fatty acid elongation, which is particularly useful in analyzing very long chain fatty acids. Finally, we apply our new analytical and modeling approaches to reveal previously unmeasured aspects of cellular fatty acid metabolism and to demonstrate that distinct pro-inflammatory stimuli specifically reprogram fatty acid synthesis and elongation in macrophages. Given the importance of fatty acids and their metabolism both in normal cells and in many diseases, we anticipate that this work will be useful to a wide variety of scientists.

The dissertation of Joseph Patrick Argus is approved.

Heather R. Christofk

Peter J. Tontonoz

Thomas G. Graeber

Steven J. Bensinger, Committee Chair

University of California, Los Angeles

2017

DEDICATION

*To Elvira,  
parents Bill and Mary Ellen,  
and brothers Brian and Kevin*

## TABLE OF CONTENTS

Abstract of the Dissertation .....	ii
Committee.....	iv
Dedication .....	v
Table of Contents .....	vi
List of Figures .....	vii
List of Tables .....	viii
Acknowledgments .....	ix
Vita .....	xii
CHAPTER ONE: Introduction .....	1
References .....	9
CHAPTER TWO: An optimized method to measure fatty acids and cholesterol in stable isotope-labeled cells .....	15
Abstract .....	16
Introduction .....	16
Materials and Methods .....	17
Results .....	18
Discussion .....	22
References .....	23
CHAPTER THREE: Development and application of Fatty Acid Source Analysis (FASA), a new model for quantifying fatty acid metabolism using stable isotope labeling.....	25
Abstract .....	27
Introduction .....	28
Materials and Methods .....	32
Results .....	37
Discussion .....	53
Supplemental Methods .....	58
Figures .....	65
References .....	96
CHAPTER FOUR: Future directions .....	100
References .....	105

## LIST OF FIGURES

### CHAPTER TWO

Figure 2-1 .....	21
Figure 2-2.....	22

### CHAPTER THREE

Figure 3-1 .....	65
Figure 3-2.....	67
Figure 3-3 .....	68
Figure 3-4.....	70
Figure 3-5 .....	72
Figure 3-6.....	74
Figure 3-7.....	76
Figure 3-8.....	78
Supplemental Figure 3-1 .....	80
Supplemental Figure 3-2.....	82
Supplemental Figure 3-3.....	85
Supplemental Figure 3-4.....	88
Supplemental Figure 3-5.....	89
Supplemental Figure 3-6.....	91
Supplemental Figure 3-7.....	93
Supplemental Figure 3-8.....	95

## LIST OF TABLES

### CHAPTER TWO

Table 2-1 .....	17
Table 2-2 .....	19
Table 2-3 .....	20
Table 2-4 .....	21
Table 2-5 .....	22

## ACKNOWLEDGMENTS

The work for this dissertation was performed under the direction of Dr. Steven J. Bensinger. I would like to acknowledge Dr. Bensinger for providing me with outstanding mentorship and resources throughout my graduate studies. In addition, I would like to thank my committee members Dr. Heather R. Christofk, Dr. Thomas G. Graeber, and Dr. Peter J. Tontonoz for their guidance and support.

I am thankful to Dr. Kevin J. Williams, Dr. Autumn G. York, Dr. Moses Q. Wilks, Quan D. Zhou, and other members of the Bensinger lab for their guidance, collaborations, and helpful discussions. I also wish to thank Dr. James A. Wohlschlegel, Dr. Gregory Khitrov, Dr. Heather D. Maynard, and Dr. Samson A. Chow for mentorship and guidance.

I sincerely thank the undergraduate students whom I had the pleasure to mentor since I joined the laboratory: Joohee Sohn, Amy K. Yu, and Eric S. Wang.

I would like to acknowledge the UCLA Chemistry-Biology Interface Training Program (National Institute of General Medical Sciences Grant T32 GM008469) and UCLA Graduate Division (Dissertation Year Fellowship) for providing me with financial support.

### **Chapter Two**

Chapter Two is adapted with permission from Argus, J. P., A. K. Yu, E. S. Wang, K. J. Williams, and S. J. Bensinger. 2017. An optimized method for measuring fatty acids and cholesterol in stable isotope-labeled cells. *J. Lipid Res.* 58: 460–468.

J.P.A. designed/executed experiments, analyzed data, conceptualized the project, and constructed the manuscript. A.K.Y and E.S.W. designed/executed experiments and analyzed data. K.J.W. provided scientific advice. S.J.B. provided resources and supervision, conceptualized the project, and constructed the manuscript. The authors thank Drs. James Wohlschlegel, Catherine Clarke, and Elvira Khialeeva for providing thoughtful analysis. They also thank Joohee Sohn for technical assistance.

This work was supported in part by National Institute of General Medical Sciences Grant T32 GM008469 (J.P.A.), National Institute of Allergy and Infectious Diseases Grant AI093768 (S.J.B.), and National Heart, Lung, and Blood Institute Grant HL126556 (S.J.B.). Other support was provided by the UCLA Graduate Division and the UCLA Dissertation Year Fellowship (J.P.A.). The content is solely the responsibility of the authors and does not necessarily represent the official views of the National Institutes of Health.

### **Chapter Three**

Chapter Three is adapted from Argus, J. P., M. Q. Wilks, Q. D. Zhou, W. Hsieh, E. Khialeeva, V. Bui, S. Xu, A. K. Yu, E. S. Wang, H. R. Herschman, K. J. Williams, and S. J. Bensinger. Development and Application of Fatty Acid Source Analysis (FASA), A New Model for Quantifying Fatty Acid Metabolism Using Stable Isotope Labeling. *Manuscript in Preparation*.

J.P.A. conceptualized the project, designed/executed experiments, analyzed data, and constructed the manuscript. M.Q.W. designed experiments, wrote the script for the models, and analyzed data. Q.D.Z. designed/executed experiments, wrote script for the models, and analyzed data. W.H., E.K., V.B., S.X.,

A.K.Y., E.S.W., and K.J.W. designed/executed experiments and analyzed data. H.R.H. provided scientific advice. S.J.B. conceptualized the project, provided resources and supervision, and constructed the manuscript. The authors thank Drs. James Wohlschlegel, Ajit Divakaruni, and Elvira Khialeeva for providing thoughtful analysis.

This work was supported in part by National Institute of General Medical Sciences Grant T32 GM008469 (J.P.A.), National Institute of Allergy and Infectious Diseases Grant AI093768 (S.J.B.), and National Heart, Lung, and Blood Institute Grant HL126556 (S.J.B.). Other support was provided by the UCLA Graduate Division and the UCLA Dissertation Year Fellowship (J.P.A.). The content is solely the responsibility of the authors and does not necessarily represent the official views of the National Institutes of Health.

## VITA

### Education

- A.B. in Biology, Minor in Chemistry, with College Honors; Washington University in St. Louis, MO: September 2002 – May 2006

### Experience

- Doctoral Student, Laboratory of Steven J. Bensinger, UCLA: 2010-Present
  - Co-managed the laboratory's adoption of existing GC/MS and stable isotope-labeling methods to study mammalian lipid metabolism, resulting in 4 co-authorships.
  - Developed and published novel GC-MS and stable isotope-labeling methods to study mammalian lipid metabolism, resulting in 2 first authorships.
  - Established a GC-MS method for quantifying contaminating organic solvents in water, resulting in 1 co-authorship.
  - Managed and mentored 3 undergraduate students in experimental design, execution, and analysis, resulting in co-authorships or acknowledgements for all 3 students.
- Middle and High School Science Teacher, Thomas Jefferson School, St. Louis, MO: 2007-2010
  - Developed curricula for and taught AP Biology, Intro. Biology, and Intro. Chemistry.
  - Academic advisor/*in loco parentis* for a small group of day and boarding students.
- Technician, Laboratory of Robert G. Kranz, Washington University in St. Louis, MO: 2006-2007
  - Overexpressed, purified, and performed binding studies on a bacterial integral membrane protein required for cytochrome *c* biogenesis, resulting in an acknowledgement.
  - Monitored and maintained selected laboratory common stocks, facilitated ordering.

### Publications

- **Argus, J. P.**, M. Q. Wilks, Q. D. Zhou, W. Hsieh, E. Khialeeva, V. Bui, S. Xu, A. K. Yu, E. S. Wang, H. R. Herschman, K. J. Williams, and S. J. Bensinger. Development and Application of Fatty Acid Source Analysis (FASA), A New Model for Quantifying Fatty Acid Metabolism Using Stable Isotope Labeling. *Manuscript in Preparation*.
- Chao, P. H., J. Collins, **J. P. Argus**, W.-Y. Tseng, J. T. Lee, and R. Michael van Dam. 2017. Automatic concentration and reformulation of PET tracers via microfluidic membrane distillation. *Lab Chip*. **17**: 1802–1816.
- **Argus, J. P.**, A. K. Yu, E. S. Wang, K. J. Williams, and S. J. Bensinger. 2017. An optimized method for measuring fatty acids and cholesterol in stable isotope-labeled cells. *J. Lipid Res.* **58**: 460–468.
- York, A. G., K. J. Williams, **J. P. Argus**, Q. D. Zhou, G. Brar, L. Vergnes, E. E. Gray, A. Zhen, N. C. Wu, D. H. Yamada, C. R. Cunningham, E. J. Tarling, M. Q. Wilks, D. Casero, D. H. Gray, A. K. Yu, E. S. Wang, D. G. Brooks, R. Sun, S. G. Kitchen, T.-T. Wu, K. Reue, D. B. Stetson, and S. J. Bensinger. 2015. Limiting Cholesterol Biosynthetic Flux Spontaneously Engages Type I IFN Signaling. *Cell*. **163**: 1716–1729.
- Mercer, J. L., **J. P. Argus**, D. M. Crabtree, M. M. Keenan, M. Q. Wilks, J.-T. A. Chi, S. J.

Bensinger, C. P. Lavau, and D. S. Wechsler. 2015. Modulation of PICALM Levels Perturbs Cellular Cholesterol Homeostasis. *PLoS One*. **10**: e0129776.

- **Argus, J. P.**, and S. J. Bensinger. 2013. Immunology. Fueling function over expansion in T cells. *Science*. **341**: 37–8.
- Kidani, Y., H. Elsaesser, M. B. Hock, L. Vergnes, K. J. Williams, **J. P. Argus**, B. N. Marbois, E. Komisopoulou, E. B. Wilson, T. F. Osborne, T. G. Graeber, K. Reue, D. G. Brooks, and S. J. Bensinger. 2013. Sterol regulatory element-binding proteins are essential for the metabolic programming of effector T cells and adaptive immunity. *Nat. Immunol.* **14**: 489–99.
- Williams, K. J., **J. P. Argus**, Y. Zhu, M. Q. Wilks, B. N. Marbois, A. G. York, Y. Kidani, A. L. Pourzia, D. Akhavan, D. N. Lisiero, E. Komisopoulou, A. H. Henkin, H. Soto, B. T. Chamberlain, L. Vergnes, M. E. Jung, J. Z. Torres, L. M. Liau, H. R. Christofk, R. M. Prins, P. S. Mischel, K. Reue, T. G. Graeber, and S. J. Bensinger. 2013. An essential requirement for the SCAP/SREBP signaling axis to protect cancer cells from lipotoxicity. *Cancer Res.* **73**: 2850–62.

### Selected Presentations

- UCLA Molecular and Medical Pharmacology Retreat. Title: Developing a Novel Workflow for Quantifying Fatty Acid Metabolism in Mammalian Cells. November 2016. Huntington Beach, CA. Oral Presentation.
- Deuel Conference on Lipids. Title: Developing a Novel Platform for Quantifying Non-Steady State Fatty Acid and Cholesterol Net Synthetic Fluxes In Vitro. March 2015. Monterey Bay, CA. Poster Presentation.
- UCLA Molecular Biology Institute Retreat. Title: Towards Understanding the Importance of SREBP-Mediated Fatty Acid Synthesis in GBM. January 2014. Westwood, CA. Poster Presentation.
- LIPID MAPS Annual Meeting. Title: Towards Understanding the Importance of SREBP-Mediated Fatty Acid Synthesis in GBM. May 2013. La Jolla, CA. Poster Presentation.
- Isotope Tracers in Metabolic Research Course. Title: Using Mass Isotopomer Distribution Analysis to Explore the Impact of SREBP Inhibition on Lipid Metabolism in Glioma. March 2013. Little Rock, AR. Oral Presentation.

### Awards and Honors

- Dissertation Year Fellowship. January 2015 – December 2015 (\$35,000).
- UCLA Chemistry-Biology Interface Training Program Fellowship. July 2011 – June 2014 (\$100,000).
- NSF Graduate Research Fellowship Program, Honorable Mention. June 2011
- Stalker Prize Nominee. June 2006 (for outstanding scientific scholarship as well as contributions to the university in areas of artistic expression and/or community service).
- College Honors in Arts & Sciences. June 2006 (cumulative GPA above 3.5).
- Robert C. Byrd Scholar, September 2002 – June 2006 (\$6,000).
- Summer Research Fellowships, Indiana School of Medicine, Fort Wayne. 2003–2005 (\$5,750).
- National Merit Scholar, September 2002 (\$2,000).

CHAPTER ONE:

Introduction

Lipids are a diverse class of biomolecules with a unifying characteristic of hydrophobicity. On average, lipids make up 15-20% of the dry weight of mammalian cells (1), and can account for more than 80% of total mass in adipose tissue (2, 3). They perform a wide variety of essential biological functions, including energy storage, membrane structure, and signaling (4). Major classes of lipids include free fatty acids, glycerolipids, glycerophospholipids, sphingolipids, eicosanoids, prenols, and sterols (5). Given their critical roles in biology, it is not surprising that modulation of lipids and lipid metabolism are important in many aspects of normal and pathophysiology. Lipids and lipid metabolism are central to a variety of ubiquitous metabolic diseases, including diabetes and obesity (6, 7). More recently, it has been discovered that altered lipid metabolism is a key feature of the modified metabolic profile seen in many cancers (8, 9). Furthermore, immune cells alter their lipid metabolism multiple times during development and in response to pathogens (10, 11). Given the importance of lipids and their metabolism to biology, accurate measurement of these species is a critical aspect of analytical biochemistry (12).

Gas Chromatography-Mass Spectrometry (GC-MS) is an important tool in quantifying lipids (5, 12). However, at its core, GC-MS is a powerful and broadly applicable technique used to identify and quantify organic compounds in complex mixtures (13). Gas chromatography separates mixtures into individual compounds based on their physical properties (14). As these pure compounds exit the chromatograph, they are ionized and detected in the mass spectrometer. The mass-to-charge ratios from the “parent” ions and their “daughter” fragments create characteristic mass spectral “fingerprints” that can be used to identify the compounds (15). For many compounds, parent and/or daughter ion abundance is proportional to the amount of compound over multiple orders of magnitude, allowing for robust quantitation (16). First developed in the

1950s, nearly 70 years of optimization and technological advances have resulted in GC-MS being utilized in a wide variety of fields (17). For example, GC-MS is routinely used in environmental analysis (18), forensics (19), medicine (20), and even astrobiology, where GC-MS instruments have traveled to and analyzed samples on distant planets (21). As part of my dissertation work, I developed a GC-MS method for quantifying residual organic solvents present in water at the end of positron emission tomography (PET) compound synthesis and formulation (22). This is important in assuring tolerable levels of organic solvents before injection of the PET compounds into pre-clinical animal models. However, the large majority of GC-MS work in this dissertation focuses on the analysis of lipids.

GC-MS remains a common tool for quantifying fatty acids and sterols because of its speed, simplicity, accuracy, and cost-effectiveness (23). The main challenge in analyzing lipids by GC-MS is ensuring their evaporation and subsequent stability in the gas phase; as a rule of thumb, these lipids must be neutral and less than 500 Da in weight (5). Fatty acid analysis via derivatization to the methyl ester form has become a quick, simple, and cost-effective way to measure cellular lipids (24). Cholesterol and other sterols can also be measured by GC-MS, particularly when trimethylsilylated (23). These analyses are used extensively in the food/beverage (25), clinical/pharmaceutical (26), and biofuel industries (27). Furthermore, GC-MS is frequently used in discovery settings to answer questions about lipid metabolism in biological systems. For example, we have used these techniques to show that activated T-cells increase cholesterol and fatty acid content during blastogenesis, and that this effect is blunted when signaling from sterol regulatory binding proteins (SREBPs, master regulators of lipid

homeostasis) is inhibited (28). Studies such as these illustrate the continued importance of GC-MS both to lipid quantification and basic biology.

GC-MS is also an important tool in measuring stable isotope incorporation into fatty acids and cholesterol. In the early 1990s, multiple groups developed the mathematics needed to determine the fraction of synthesized and imported fatty acids/cholesterol when the lipogenic acetyl-CoA pool was labeled with stable isotopes such as  $^{13}\text{C}$  and  $^2\text{H}$  (29–31). These studies used GC-MS to produce the fatty acid methyl ester mass isotopomer distributions (MIDs) that were subsequently modeled. The advantage of using GC-MS was twofold. First, as mentioned above, multiple methods had previously been developed for measuring these lipids via GC-MS. Second, electron impact (EI) ionization in positive mode, the most common type of ionization used in GC-MS, generally produces analyte molecular ions with  $m/z$  values that match the uncharged parent species because only a single electron is abstracted (12). Softer ionization techniques often result in the addition of protons or abstraction of hydrides, complicating the resulting MIDs (32). Analyzing lipid MIDs with these mathematical models allowed for the determination of two parameters from the MIDs – the percent contribution of synthesis to a particular fatty acid pool,  $g(t)$ , and the percent contribution of the stable isotope-labeled metabolite to the lipogenic acetyl-CoA pool,  $D$  (29). These models have been used to quantify changes in fatty acid and cholesterol accumulation in a wide variety of physiologic and pathophysiologic conditions (33, 34). For example, we have used a variant of these models to demonstrate that inhibiting SREBPs in cancer cells slows growth not by decreasing de novo fatty acid synthesis itself, but rather by significantly depressing fatty acid desaturation, resulting in an overabundance of saturated fatty acids and lipotoxicity (35). In addition, we have applied this method to show that inhibition of

the protein Phosphatidyl Inositol Clathrin Assembly Lymphoid Myeloid (PICALM) alters the balance of cholesterol synthesis and scavenging, suggesting that PICALM plays a role in cholesterol metabolism (36). Furthermore, we have used this technique to demonstrate that not only do inflammatory stimuli in macrophages result in decreased fatty acid and cholesterol synthesis, but that direct inhibition of these synthetic processes causes an inflammatory phenotype, creating a positive feedback loop (37). These and many other studies have demonstrated the utility of applying stable isotope labeling, GC-MS, and mathematical modeling to quantify lipid metabolism.

The methods and studies mentioned above are focused on analyzing cholesterol and long chain fatty acids (14-18 carbons). However, very long chain fatty acids (VLCFA, 20-24 carbons) also play critical roles in physiology and pathophysiology (38). Very long chain polyunsaturated fatty acids (VLC PUFA) are precursors for lipid signaling molecules essential to both inflammatory and resolving processes (39). VLC saturated fatty acids (SFA) and monounsaturated fatty acids (MUFA) play critical roles in signal transduction as part of sphingolipids enriched in membrane rafts (40). Furthermore, inherited mutations in genes involved in VLCFA metabolism cause a variety of diseases, including macular degeneration, ichthyosis, myopathy, mental retardation, and demyelination (41). As a result, we sought to develop better tools to quantify the metabolism of these important fatty acids using stable isotopes, GC-MS, and modeling.

The first challenge in measuring VLCFA metabolism using stable isotopes, GC-MS, and modeling is generating high quality MID data. Traditionally, as mentioned above, these data would be produced by derivatizing complex cellular lipids into fatty acid methyl esters (FAMES)

and analyzing them via GC-MS. However, there were several aspects of commonly used derivatization and analysis schemes that made it difficult to obtain MIDs for VLCFA. No methods had been demonstrated to quantitatively derivatize all VLCFA from mammalian cells and maintain sufficient sample concentration to visualize low abundance VLCFA molecular ion MIDs (12, 42–44). To address these fundamental issues, we first optimized the derivatization conditions. A large portion of VLC SFA and MUFA are found in sphingolipids, which are much more difficult to derivatize than other complex lipids due to the presence of amide instead of ester linkages (12, 41). We determined reaction conditions harsh enough to result in quantitative yields of VLC SFA and MUFA, without being so stringent as to destroy the more labile VLC PUFA species. Secondly, we maximized yield and sample concentration. A double hexane extraction resulted in quantitative yields of FAMES from the derivatization mix, while a subsequent concentration step and splitless injection onto the GC-MS allowed for collection of robust molecular ion MIDs, even from low abundance and/or highly unsaturated VLCFAs. We anticipate that this method will be useful in better quantifying VLCFA in biological samples (45, Chapter 2). Furthermore, these improvements in data collection for VLCFAs allowed us to develop a new model to interpret the resulting MIDs.

The second challenge in measuring VLCFA metabolism using stable isotopes and GC-MS is the analysis and interpretation of complex MID data. Traditional mathematical models used to analyze FAMES MIDs from stable isotope-labeled cells such as Mass Isotopomer Distribution Analysis (MIDA) and Isotopomer Spectral Analysis (ISA) rely on the assumption that fatty acids are either imported and are unlabeled, or completely synthesized from the lipogenic acetyl-CoA pool (29–31). This assumption largely holds true for 14- and 16-carbon fatty acids because the

single protein fatty acid synthase (FASN) is responsible for making the large majority of synthesized 14 and 16 carbon fatty acids directly from the lipogenic acetyl-CoA (46). However, 18-24 carbon fatty acids are created through elongation using a different set of enzymes, meaning that both FASN-synthesized and imported fatty acids can be subsequently elongated (41, 47). We demonstrated that the traditional two-distribution models (synthesis and import) cannot accurately describe longer fatty acids, as they contain additional distributions representing imported-elongated species. To address this issue, we developed Fatty Acid Source Analysis (FASA), the first model to include multiple distributions for imported-elongated species, which allows for the modeling of VLC SFA and MUFA (48, Chapter 3). We also provided evidence that the model can be applied to PUFA by fixing synthetic and other relevant parameters to 0, in line with well-established biochemical pathways (41, 47). After validating FASA, we then used it to uncover new information about fatty acid metabolism. For example, we provided evidence that, at least under the conditions tested, the lipogenic acetyl-CoA pool is behaving as a single, well-mixed unit. In addition, we showed that shortening followed by elongation contributed in a meaningful way to 18- and 20-carbon n-6 PUFA pools. Finally, we showed that fatty acid elongation in activated macrophages is modulated in different ways depending on the stimulus, suggesting that modulation of fatty acid elongation could be important in enforcing specific inflammatory reactions. Given the importance of VLCFA in normal and pathophysiology, we anticipate that FASA will be useful to scientists in many different fields (48, Chapter 3).

In sum, our work has highlighted the importance of lipid metabolism in biological systems and the advantages of using stable isotopes, GC-MS, and modeling to quantify it. In particular, we have expanded the analytical and mathematical tools available to study VLCFAs. Furthermore,

we have applied these tools to observe unappreciated aspects of fatty acid elongation and its modulation during different biological processes. As VLCFA have been shown to play important structural and signaling roles in a multitude of cell types, we anticipate that our work will advance the study of lipid biology and be useful to a wide variety of scientists.

## References

1. Alberts, B., A. Johnson, J. Lewis, M. Raff, K. Roberts, and P. Walter. 2008. *Molecular Biology of the Cell*. 5th Ed. Garland Science, New York.
2. Martin, A., M. Daniel, D. Drinkwater, and J. Clarys. 1994. Adipose Tissue Density, Estimated Adipose Lipid Fraction and Whole Body Adiposity in Male Cadavers. *Int. J. Obes. Relat. Disord.* **18**: 79–83.
3. Lepage, G., and C. C. Roy. 1984. Improved recovery of fatty acid through direct transesterification without prior extraction or purification. *J. Lipid Res.* **25**: 1391–1396.
4. Nelson, D., and M. Cox. 2005. *Lehninger Principles of Biochemistry*. 4th Ed. W.H. Freeman and Company, New York.
5. McDonald, J. G., P. T. Ivanova, and H. A. Brown. 2016. *In Biochemistry of Lipids, Lipoproteins and Membranes*. 6th Ed., pp. 41–72. , Elsevier, Amsterdam.
6. Adeli, K., J. Taher, S. Farr, C. Xiao, and G. F. Lewis. 2016. *In Biochemistry of Lipids, Lipoproteins and Membranes*. 6th Ed., pp. 549–573. , Elsevier, Amsterdam.
7. Klop, B., J. W. F. Elte, and M. C. Cabezas. 2013. Dyslipidemia in Obesity: Mechanisms and Potential Targets. *Nutrients.* **5**: 1218–1240.
8. Menendez, J. A., and R. Lupu. 2007. Fatty acid synthase and the lipogenic phenotype in cancer pathogenesis. *Nat. Rev. Cancer.* **7**: 763–77.
9. Baenke, F., B. Peck, H. Miess, and A. Schulze. 2013. Hooked on fat: the role of lipid synthesis in cancer metabolism and tumour development. *Dis. Model. Mech.* **6**: 1353–63.
10. O'Neill, L. A. J., and E. J. Pearce. 2016. Immunometabolism governs dendritic cell and macrophage function. *J. Exp. Med.* **213**: 15–23.
11. Gerriets, V. a, and J. C. Rathmell. 2012. Metabolic pathways in T cell fate and function.

- Trends Immunol.* **33**: 168–73.
12. Christie, W. W., and X. Han. 2010. *Lipid Analysis: Isolation, Separation, Identification, and Lipidomic Analysis*. 4th ed. The Oily Press, Bridgwater, England.
  13. Gohlke, R. S., and F. W. McLafferty. 1993. Early gas chromatography/mass spectrometry. *J. Am. Soc. Mass Spectrom.* **4**: 367–71.
  14. Blumberg, L. M. 2011. *In Comprehensive Chromatography in Combination with Mass Spectrometry*. 1st Ed., pp. 13–63. , John Wiley & Sons, Hoboken.
  15. McLafferty, F. W., R. H. Hertel, and R. D. Villwock. 1974. Probability based matching of mass spectra. Rapid identification of specific compounds in mixtures. *Org. Mass Spectrom.* **9**: 690–702.
  16. Crockett, P. W. 1986. Estimation of the Linear Working Range for a Gas Chromatograph/Mass Spectrometer. *Anal. Chem.* **58**: 699–705.
  17. Hites, R. A. 2016. Development of Gas Chromatographic Mass Spectrometry. *Anal. Chem.* **88**: 6955–6961.
  18. Santos, F. J., and M. T. Galceran. 2003. Modern developments in gas chromatography – mass spectrometry-based environmental analysis. *J. Chromatogr. A.* **1000**: 125–151.
  19. Benson, S., C. Lennard, P. Maynard, and C. Roux. 2006. Forensic applications of isotope ratio mass spectrometry - A review. *Forensic Sci. Int.* **157**: 1–22.
  20. Wolthers, B. G., and G. P. B. Kraan. 1999. Clinical applications of gas chromatography and gas chromatography-mass spectrometry of steroids. *J. Chromatogr. A.* **843**: 247–274.
  21. Buch, A., D. P. Glavin, R. Sternberg, C. Szopa, C. Rodier, R. Navarro-González, F. Raulin, M. Cabane, and P. R. Mahaffy. 2006. A new extraction technique for in situ analyses of amino and carboxylic acids on Mars by gas chromatography mass spectrometry. *Planet.*

- Space Sci.* **54**: 1592–1599.
22. Chao, P. H., J. Collins, J. P. Argus, W.-Y. Tseng, J. T. Lee, and R. Michael van Dam. 2017. Automatic concentration and reformulation of PET tracers via microfluidic membrane distillation. *Lab Chip.* **17**: 1802–1816.
23. McDonald, J. G., D. D. Smith, A. R. Stiles, and D. W. Russell. 2012. A comprehensive method for extraction and quantitative analysis of sterols and secosteroids from human plasma. *J. Lipid Res.* **53**: 1399–1409.
24. Carrapiso, A. I., and C. García. 2000. Development in lipid analysis: some new extraction techniques and in situ transesterification. *Lipids.* **35**: 1167–77.
25. Ng, L.-K. 2002. Analysis by gas chromatography/mass spectrometry of fatty acids and esters in alcoholic beverages and tobaccos. *Anal. Chim. Acta.* **465**: 309–318.
26. Brenna, J. T. 2013. Fatty acid analysis by high resolution gas chromatography and mass spectrometry for clinical and experimental applications. *Curr. Opin. Clin. Nutr. Metab. Care.* **16**: 548–54.
27. Knothe, G. 2006. Analyzing biodiesel: Standards and other methods. *JAOCS, J. Am. Oil Chem. Soc.* **83**: 823–833.
28. Kidani, Y., H. Elsaesser, M. B. Hock, L. Vergnes, K. J. Williams, J. P. Argus, B. N. Marbois, E. Komisopoulou, E. B. Wilson, T. F. Osborne, T. G. Graeber, K. Reue, D. G. Brooks, and S. J. Bensinger. 2013. Sterol regulatory element-binding proteins are essential for the metabolic programming of effector T cells and adaptive immunity. *Nat. Immunol.* **14**: 489–99.
29. Kelleher, J. K., and T. M. Masterson. 1992. Model equations for condensation biosynthesis using stable isotopes and radioisotopes. *Am J Physiol Endocrinol Metab.* **262**: E118–

E125.

30. Hellerstein, M. 1991. Measurement of de novo hepatic lipogenesis in humans using stable isotopes. *J. Clin. Invest.* **87**: 1841–1852.
31. Lee, W., E. Bergner, and Z. Guo. 1992. Mass isotopomer pattern and precursor product relationship. *Biol. Mass Spectrom.* **21**: 114–122.
32. Dayhuff, L.-E., and M. J. M. Wells. 2005. Identification of fatty acids in fishes collected from the Ohio River using gas chromatography-mass spectrometry in chemical ionization and electron impact modes. *J. Chromatogr. A.* **1098**: 144–9.
33. Murphy, E. 2006. Stable isotope methods for the in vivo measurement of lipogenesis and triglyceride metabolism. *J. Anim. Sci.*
34. Kelleher, J. K., and G. B. Nickol. 2015. *Isotopomer Spectral Analysis: Utilizing Nonlinear Models in Isotopic Flux Studies*. 1st Ed. Elsevier Inc.
35. Williams, K. J., J. P. Argus, Y. Zhu, M. Q. Wilks, B. N. Marbois, A. G. York, Y. Kidani, A. L. Pourzia, D. Akhavan, D. N. Lisiero, E. Komisopoulou, A. H. Henkin, H. Soto, B. T. Chamberlain, L. Vergnes, M. E. Jung, J. Z. Torres, L. M. Liao, H. R. Christofk, R. M. Prins, P. S. Mischel, K. Reue, T. G. Graeber, and S. J. Bensinger. 2013. An essential requirement for the SCAP/SREBP signaling axis to protect cancer cells from lipotoxicity. *Cancer Res.* **73**: 2850–62.
36. Mercer, J. L., J. P. Argus, D. M. Crabtree, M. M. Keenan, M. Q. Wilks, J.-T. A. Chi, S. J. Bensinger, C. P. Lavau, and D. S. Wechsler. 2015. Modulation of PICALM Levels Perturbs Cellular Cholesterol Homeostasis. *PLoS One.* **10**: e0129776.
37. York, A. G., K. J. Williams, J. P. Argus, Q. D. Zhou, G. Brar, L. Vergnes, E. E. Gray, A. Zhen, N. C. Wu, D. H. Yamada, C. R. Cunningham, E. J. Tarling, M. Q. Wilks, D.

- Casero, D. H. Gray, A. K. Yu, E. S. Wang, D. G. Brooks, R. Sun, S. G. Kitchen, T. T. Wu, K. Reue, D. B. Stetson, and S. J. Bensinger. 2015. Limiting Cholesterol Biosynthetic Flux Spontaneously Engages Type I IFN Signaling. *Cell*. **163**: 1716–1729.
38. Jakobsson, A., R. Westerberg, and A. Jacobsson. 2006. Fatty acid elongases in mammals: their regulation and roles in metabolism. *Prog. Lipid Res.* **45**: 237–49.
39. Smith, W. L., and R. C. Murphy. 2016. *In Biochemistry of Lipids, Lipoproteins and Membranes*. 6th Ed, pp. 259–296. , Elsevier, Amsterdam.
40. Futerman, A. H. 2016. *In Biochemistry of Lipids, Lipoproteins and Membranes*. 6th Ed., pp. 297–326. , Elsevier, Amsterdam.
41. Sassa, T., and A. Kihara. 2014. Metabolism of very long-chain Fatty acids: genes and pathophysiology. *Biomol. Ther. (Seoul)*. **22**: 83–92.
42. Eder, K. 1995. Gas chromatographic analysis of fatty acid methyl esters. *J. Chromatogr. B. Biomed. Appl.* **671**: 113–31.
43. Liu, K.-S. 1994. Preparation of fatty acid methyl esters for gas-chromatographic analysis of lipids in biological materials. *J. Am. Oil Chem. Soc.* **71**: 1179–1187.
44. Lepage, G., and C. C. Roy. 1986. Direct transesterification of all classes of lipids in a one-step reaction. *J. Lipid Res.* **27**: 114–120.
45. Argus, J. P., A. K. Yu, E. S. Wang, K. J. Williams, and S. J. Bensinger. 2017. An optimized method for measuring fatty acids and cholesterol in stable isotope-labeled cells. *J. Lipid Res.* **58**: 460–468.
46. Lehner, R., and A. D. Quiroga. 2016. *In Biochemistry of Lipids, Lipoproteins and Membranes*. 6th Ed., pp. 149–184. , Elsevier, Amsterdam.
47. Bond, L. M., M. Miyazaki, L. M. O'Neill, F. Ding, and J. M. Ntambi. 2016. *In Biochemistry*

of Lipids, Lipoproteins and Membranes. 6th Ed., pp. 185–208. , Elsevier, Amsterdam.

48. Argus, J. P., M. Q. Wilks, Q. D. Zhou, W. Hsieh, E. Khialeeva, V. Bui, S. Xu, A. K. Yu, E. S. Wang, H. R. Herschman, K. J. Williams, and S. J. Bensinger. Development and Application of Fatty Acid Source Analysis (FASA), A New Model for Quantifying Fatty Acid Metabolism Using Stable Isotope Labeling. *Manuscript in Preparation*.

CHAPTER TWO:

An Optimized Method for Measuring Fatty Acids and Cholesterol

in Stable Isotope-Labeled Cells

# An optimized method for measuring fatty acids and cholesterol in stable isotope-labeled cells

Joseph P. Argus,\* Amy K. Yu,\* Eric S. Wang,\* Kevin J. Williams,<sup>†</sup> and Steven J. Bensinger<sup>1,\*†</sup>

Departments of Molecular and Medical Pharmacology\* and Microbiology, Immunology, and Molecular Genetics,<sup>†</sup> David Geffen School of Medicine, University of California, Los Angeles, Los Angeles, CA 90095

**Abstract** Stable isotope labeling has become an important methodology for determining lipid metabolic parameters of normal and neoplastic cells. Conventional methods for fatty acid and cholesterol analysis have one or more issues that limit their utility for in vitro stable isotope-labeling studies. To address this, we developed a method optimized for measuring both fatty acids and cholesterol from small numbers of stable isotope-labeled cultured cells. We demonstrate quantitative derivatization and extraction of fatty acids from a wide range of lipid classes using this approach. Importantly, cholesterol is also recovered, albeit at a modestly lower yield, affording the opportunity to quantitate both cholesterol and fatty acids from the same sample. Although we find that background contamination can interfere with quantitation of certain fatty acids in low amounts of starting material, our data indicate that this optimized method can be used to accurately measure mass isotopomer distributions for cholesterol and many fatty acids isolated from small numbers of cultured cells. **Application of this method will facilitate acquisition of lipid parameters required for quantifying flux and provide a better understanding of how lipid metabolism influences cellular function.**—Argus, J. P., A. K. Yu, E. S. Wang, K. J. Williams, and S. J. Bensinger. **An optimized method for measuring fatty acids and cholesterol in stable isotope-labeled cells.** *J. Lipid Res.* 2017. 58: 460–468.

**Supplementary key words** lipids/chemistry • mass spectrometry • sphingolipids • neutral lipids • stable isotope labeling

Fatty acids and cholesterol perform essential structural, energetic, and signaling roles in all animal cells (1). Renewed interest in understanding how cholesterol and fatty acid homeostasis is dynamically modulated in normal cellular states and during pathophysiologic processes (e.g., oncogenic signaling in cancer) has led to increased

demand for methodologies that can accurately interrogate these lipid classes (2–4). One approach that has gained significant favor is the use of stable isotope labeling to quantify how cellular requirements for cholesterol and fatty acid pool sizes are achieved in normal and neoplastic cells (5). This methodology allows for defining the origin of cellular lipid (e.g., synthesized versus imported from extracellular sources) and determining the carbon source(s) contributing to the acetyl-CoA pool used for the synthesis of lipids (e.g., glucose versus amino acids) (6, 7).

Analysis of stable isotope-labeled fatty acids or cholesterol is commonly performed using GC/MS due to its low cost and relative simplicity (8–10). In this approach, cellular fatty acids or cholesterol are converted to nonpolar derivatives [e.g., fatty acid methyl esters (FAMES) or trimethylsilyl ether (TMSE) cholesterol] before injection to increase volatility and improve chromatography. However, conventional methods are not ideal for analyzing total fatty acids and cholesterol from small amounts of stable isotope-labeled cells for one or more of the following reasons. First, many published methods have been developed for analyzing specific classes of lipids and, as a consequence, may not accurately quantitate total fatty acid or cholesterol content (9, 11, 12). Second, protocols are sometimes not validated for the small amounts of material commonly used in stable isotope-labeling experiments; thus, application of these methods can result in issues with background signal and/or destruction of analytes (e.g., cholesterol or unsaturated fatty acids) (13, 14). Third, stable isotope labeling often requires a large amount of sample to be injected onto the column for accurate determination of the mass isotopomer distribution (MID) of rare molecular ions (7, 15). However, many published methods, which have been optimized for nonlabeled samples,

*This work was supported in part by National Institute of General Medical Sciences Grant T32 GM008469 (J.P.A.), National Institute of Allergy and Infectious Diseases Grant AI093768 (S.J.B.), and National Heart, Lung, and Blood Institute Grant HL126556 (S.J.B.). Other support was provided by the UCLA Graduate Division and the UCLA Dissertation Year Fellowship (J.P.A.). The content is solely the responsibility of the authors and does not necessarily represent the official views of the National Institutes of Health.*

*Manuscript received 14 May 2016 and in revised form 12 December 2016.*

*Published, JLR Papers in Press, December 14, 2016  
DOI 10.1194/jlr.D069336*

Abbreviations: AFA, amidified fatty acid; BHT, butylated hydroxytoluene; BSTFA, *N,O*-bis(trimethylsilyl)trifluoroacetamide; CE, cholesterol ester; CRB, galactocerebroside; FAME, fatty acid methyl ester; FEFA, free and esterified fatty acid; LCFA, long chain fatty acid; MID, mass isotopomer distribution; PC, phosphatidylcholine; TMCS, trimethylchlorosilane; TMSE, trimethylsilyl ether; VLCFA, very long chain fatty acid.

<sup>1</sup>To whom correspondence should be addressed.  
e-mail: sbensinger@mednet.ucla.edu

cannot inject enough material onto the column to visualize these MIDs (16–18). Finally, few methods allow for efficient measurement of both fatty acids and cholesterol from the same sample (19).

To address these challenges, we developed a method optimized for analysis of total fatty acids and cholesterol from small numbers of cultured stable isotope-labeled cells. In this approach, cells are derivatized in situ (without initial lipid extraction) using a short acid-catalyzed methanolysis reaction. FAMES and cholesterol are extracted and concentrated. FAMES are subsequently analyzed by a rapid GC/MS program. The sample is then dried, further derivatized using *N,O*-bis(trimethylsilyl)trifluoroacetamide (BSTFA):trimethylchlorosilane (TMCS) (99:1) and pyridine, and reanalyzed by GC/MS to quantify TMSE cholesterol. In validation experiments, we demonstrate that long chain fatty acid (LCFA; 14–18 carbons) and very long chain fatty acid (VLCFA; 20–24 carbons) yields are near 100% for representatives from all major animal lipid classes (FFA, TG, cholesteryl ester (CE), phosphoglycerolipid, phosphosphingolipid, and glycosphingolipid), while maintaining cholesterol yields at approximately 80–90%. Our data indicate that background fatty acid and cholesterol contamination can be a limiting factor when small amounts of starting material are used, depending on the analytes of interest. Nevertheless, we found that application of this method can generate robust MIDs for cholesterol and many fatty acids from a relatively wide range of cell numbers ( $0.4\text{--}2.5 \times 10^6$  H1299 lung cancer cells), representing approximately 20–125  $\mu\text{g}$  of total fatty acid and cholesterol. Thus, we anticipate that utilization of this method will facilitate the application of stable isotope labeling to model lipid metabolic parameters in normal and disease states.

## MATERIALS AND METHODS

### Reagents

Optima grade methanol, Optima grade water, Optima grade *n*-hexane, and ACS plus grade hydrochloric acid were purchased from Fisher. Chromosolv Plus grade toluene,  $\geq 99.0\%$  butylated hydroxytoluene (BHT), ACS grade sodium carbonate, 99:1 BSTFA, TMCS, and anhydrous 99.8% pyridine were purchased from Sigma-Aldrich. The 99+% acetyl chloride was purchased from Alfa Aesar. FAMES, FFAs, glyceryl trionadecanoate, and cholesteryl heneicosanoate were purchased from NuChek Prep. The 1,2-ditricosanoyl-*sn*-glycero-3-phosphocholine,

*N*-lignoceroyl-D-*erythro*-sphingosylphosphorylcholine, and D-galactosyl- $\beta$ -1,1'-*N*-nervonoyl-D-*erythro*-sphingosine were purchased from Avanti Polar Lipids. Cholesterol, stigmastanol, stigmasterol, and cholesterol- $d_6$  were purchased from Sigma-Aldrich. H1299 (also referred to as NCI-H1299) cells were purchased from ATCC.  $^{13}\text{C}_6$ -glucose was purchased from Cambridge Isotope Laboratories. FBS was purchased from Omega Scientific. All other cell culture reagents were purchased from Gibco.

### Internal standards, lipid class standards mix, and standard curves

FAMES and sterols (17:1 *n*-9, 19:0, 19:1 *n*-12, 23:0, 23:1 *n*-9, cholesterol- $d_6$ , stigmastanol, and stigmasterol) were used as internal standards in one or more experiments, as described in the text. The mass of internal standards used per tube was varied based on the nature of the experiment; for experiments with  $0.4\text{--}2.5 \times 10^6$  H1299 cells, 1–3  $\mu\text{g}$  of each relevant internal standard were used. Internal standards were generally added in 10  $\mu\text{l}$  of toluene. The lipid class standards mix contained equal masses of the six lipids listed in **Table 1**. Lipid (150  $\mu\text{g}$ ) was added to each sample in 50  $\mu\text{l}$  of toluene. The standard curve for the lipid class standards mix was GLC-14A (methyl ester version; NuChek Prep) supplemented with 23:0, 24:0, and 24:1 *n*-9 methyl esters in a 62.5:12.5:12.5:12.5 mass ratio. The standard curve used to test for nonhydrolytic FAME loss and to quantify fatty acids and cholesterol in H1299 cells was designed to roughly mimic the content of animal cells. It consisted of GLC-96 (methyl ester version; NuChek Prep), 18:1 *n*-7 methyl ester, and cholesterol in an 83.2:7.0:9.2 mass ratio.

### Cell culture

Unlabeled H1299 cells were cultured at 37°C (5%  $\text{CO}_2$ ) in RPMI supplemented with antibiotic and 10% heat-inactivated FBS. Cells were trypsinized and counted in RPMI supplemented with antibiotic and 2.5% FBS using trypan blue exclusion and a Nexelcom Cellometer K2. Cells were then aliquoted into glass tubes containing 1.5–3.5 ml of PBS (used to dilute out FBS) and pelleted. The supernatant was aspirated until 50–100  $\mu\text{l}$  remained in the tube. H1299 cells were labeled at 37°C (5%  $\text{CO}_2$ ) using glucose-free DMEM supplemented with 25 mM  $^{13}\text{C}_6$ -glucose, antibiotic, and 5% FBS. Labeled medium was refreshed daily and cells were maintained in a subconfluent state by splitting as necessary. After  $\geq 5$  divisions in labeled medium (to ensure metabolic and isotopic steady state), cells were collected with trypsin and 2 ml of PBS directly into glass tubes and pelleted. The supernatant was aspirated until 50–100  $\mu\text{l}$  remained in the tube. All cell pellets were held at  $-20^\circ\text{C}$  until derivatization.

### Free and esterified fatty acid method derivatization

Derivatization was as described previously (13) with minor modifications. Briefly, 200  $\mu\text{l}$  of toluene, 1.5 ml of methanol, and 300  $\mu\text{l}$  of methanolic HCl (8.0% w/v) were added, in that order,

TABLE 1. Lipid class standards mix representative of major animal lipid classes containing fatty acids

Lipid Class (Subclass)	Properties		Specific Standard Used	
	Relative Polarity	Fatty Acid Linkage	Full Name	Abbreviation
FFA	More	None	Heptadecanoic acid	17:0 FFA
TG	Less	Ester	Glyceryl trionadecanoate	19:0 TG
Cholesteryl Ester	Less	Ester	Cholesteryl heneicosanoate	21:0 CE
Phosphoglycerolipid (PC)	More	Ester	1,2-Ditricosanoyl- <i>sn</i> -glycero-3-phosphocholine	23:0 PC
Phosphosphingolipid (SM)	More	Amide	<i>N</i> -lignoceroyl-D- <i>erythro</i> -sphingosylphosphorylcholine	24:0 SM
Glycosphingolipid (cerebroside)	More	Amide	D-galactosyl- $\beta$ -1,1'- <i>N</i> -nervonoyl-D- <i>erythro</i> -sphingosine	24:1 <i>n</i> -9 CRB

Each sample contained 25  $\mu\text{g}$  of each specific standard (150  $\mu\text{g}$  total lipid per sample).

to samples in glass tubes. Methanolic HCl was prepared by adding 1.9 ml concentrated aqueous HCl to 8.1 ml methanol. Tubes were capped, shaken, and incubated at 100°C for 1.5 h in a closed fume hood or at 45°C for 16 h on the benchtop.

#### Amidified fatty acid method derivatization

Derivatization was as described previously (9, 20) with minor modifications. Briefly, 2 ml of methanolic HCl (5:1 v/v) were added to samples in glass tubes. Methanolic HCl was prepared by adding 4 ml concentrated aqueous HCl to 20 ml methanol. Tubes were capped, shaken, and incubated at 80°C for 5 h in a closed fume hood or at 50°C for 24 h on the benchtop.

#### Current method derivatization

Two milliliters of current method master mix were added to samples in glass tubes. The current method master mix contained 9% acetyl chloride, 18% toluene, and 73% methanol by volume. The master mix was made by slowly adding acetyl chloride to pre-mixed toluene and methanol on ice to avoid splashing. Reaction mixes were supplemented to contain approximately 100  $\mu$ l of "sample" water unless otherwise stated. Tubes were capped, shaken, and incubated at 100°C for 2 h or overnight in a closed fume hood. Tubes were shaken again after 1 h for the 2 h incubation, and after several hours for the overnight incubations.

#### Neutralization, extraction, and concentration

After incubation, tubes were cooled to room temperature. To neutralize, 2.5 ml of 0.31 M [free and esterified fatty acid (FEFA) method], 0.99 M [amidified fatty acid (AFA) method], or 0.66 M (current method) aqueous sodium carbonate was added to yield a final aqueous layer of approximately 0.1 M sodium carbonate. After adding 2 ml of n-hexane, the tubes were shaken and centrifuged at 2,000 *g* for 5 min. The organic layer was extracted to a new tube, and the 2 ml n-hexane extraction was repeated. The combined organic layers were evaporated to dryness using the EZ-2 Elite Speedvac ("Low BP Mix" program, 50 min to final stage, 0 min final stage, lamp off). The dried lipids were redissolved in a small amount of toluene appropriate for the sample (75  $\mu$ l recommended for 0.4–2.5  $\times 10^6$  stable isotope-labeled H1299 cells) and transferred to robovials containing 300  $\mu$ l glass inserts for GC/MS analysis.

#### GC/MS analysis

For FAMES, an Agilent 7890A/5975C GC/MS equipped with a 27.75 m, 0.25 mm ID, 25  $\mu$ m film, DB-Wax column (Agilent) was used. Sample (0.5–2  $\mu$ l) was injected in splitless mode into an inlet held at 275°C. The oven program was as follows: 95°C for 1 min, followed by 40°C/min to 115°C for 0 min, 30°C/min to 190°C for 2 min, 4°C/min to 218°C for 3 min, 4°C/min to 250°C for 7.8 min (31.8 min total). Helium was the carrier gas, and the column flow rate was 1 ml/min for 23.75 min followed by 1.7 ml/min for the remainder of the run. The MS was run in EI mode (70 eV). The transfer line, EI source, and quadrupole were maintained at 250, 230, and 150°C, respectively. For experiments without <sup>13</sup>C labeling, analyte most abundant ions were collected in SIM mode (*m/z* 74.1 saturated FAMES, *m/z* 55.1 monounsaturated FAMES, *m/z* 67.1 diunsaturated FAMES, *m/z* 79.1 polyunsaturated FAMES). For experiments with <sup>13</sup>C labeling, molecular ions were collected in SIM mode. For analytes, MIDs were collected; whereas for internal standards, only M+0 was collected. Specifically, the SIM windows were as follows (start time in minutes: *m/z* range): 0:242.2–257.2; 8:270.3–287.3; 8.55:268.3–285.3; 9.4:282.3 and 284.3; 10.6:298.3–317.3; 11.15:296.3–315.3; 11.8:292.3–300.3; 12.3:310.3 and 312.3; 13.8:326.3–347.3; 14.25:324.3–345.3; 14.85:322.3–341.3; 15.65:318.3–326.3; 16.25:316.3–324.3;

18:354.4–377.4; 18.55:352.4–375.4; 19.4:350.4–370.4; 20.2:344.4–352.4 and 368.4; 22:382.4–407.4; 22.7:380.4–405.4; 24:74.1, 79.1, 386.4, 396.4 and 416.4.

For TMSE sterols, an Agilent 7890A/5975C GC/MS equipped with a 28 m, 0.25 mm ID, 25  $\mu$ m film, ZB-MR1 column (Phenomenex) was used. One microliter of sample was injected in split mode (1:10 split ratio) into an inlet held at 300°C. The oven program was as follows: 280°C for 5 min, 5°C/min to 292.5°C for 0 min, 23.75°C/min to 340°C for 0 min (9.5 min total). Helium was the carrier gas; column flow rate was 1 ml/min. The MS was run in EI mode (70 eV). The transfer line, EI source, and quadrupole were maintained at 300, 230, and 150°C, respectively. For experiments without <sup>13</sup>C labeling, M+0 molecular ions were collected in SIM mode (*m/z* 458.4 for TMSE cholesterol, *m/z* 464.4 for TMSE cholesterol-d<sub>6</sub>, *m/z* 488.5 for TMSE stigmastanol, *m/z* 486.5 for TMSE stigmastanol). For experiments with <sup>13</sup>C labeling, TMSE cholesterol molecular ions were collected in SIM from M-2 to M+27, while M+0 molecular ions (listed previously) were collected for internal standards. Chromatographic and spectral analyses were performed using ChemStation and MassHunter (Agilent).

#### Statistics

All statistical analyses were performed using a two-tailed heteroscedastic Student's *t*-test.

## RESULTS

#### Difficulties in completely derivatizing fatty acids from representatives of all major animal lipid classes

In cells, the majority of fatty acids are either esterified or amidified into complex lipids (1). A variety of methods have been developed to derivatize cellular fatty acids into FAMES (9, 11). Historically, one strategy involves extraction of lipids from the biological source material followed by base-catalyzed hydrolysis (saponification) and extraction of the resultant FFAs. These FFAs are then methylated in a second reaction and extracted for subsequent analysis (12, 21). However, we chose to pursue *in situ* acid-catalyzed methanolysis because it only requires a single derivatization reaction followed by a single extraction step (8). Multiple *in situ* acid-catalyzed methanolysis methods have been developed for derivatization of FEFAs (8, 13, 22), but it remains unclear whether these methods can efficiently derivatize AFAs. To begin testing this, we applied a commonly used FEFA method to a lipid class standards mix containing equal masses of standards representing the major fatty acid-containing lipid classes in animal cells (1, 9), spanning a range of polarities and fatty acid linkages (Table 1). One hundred and fifty micrograms of the lipid class standards mix were derivatized using 2 ml of 0.39 M methanolic HCl containing 10% toluene at 45°C for 16 h (13). One hundred microliters of water were added to mimic the water present in typical biological samples. As expected, FEFAs [FA, TG, CE, and phosphatidylcholine (PC)] were efficiently derivatized (absolute yield of 89–98%; Table 2). However, yields from AFAs [SM and galactocerebroside (CRB)] were far lower (9–20%; Table 2). Increasing the temperature and decreasing the time of the reaction improved yield (49–62%; Table 2), but still failed to fully

TABLE 2. Current method derivatizes representatives of all major classes of animal lipids containing fatty acids

	FEFA Method (Percent Yield)		AFA Method (Percent Yield)		Current Method (Percent Yield)	
	45°C, 16 h	100°C, 1.5 h	50°C, 24 h	80°C, 5 h	100°C, 2 h	100°C, 21 h
FFA	98 ± 1	99 ± 0	95 ± 1	95 ± 1	96 ± 1	95 ± 1
TG	89 ± 1	96 ± 2	4 ± 1	35 ± 4	98 ± 1	96 ± 0
CE	96 ± 1	96 ± 4	14 ± 3	47 ± 2	101 ± 1	99 ± 1
PC	92 ± 0	95 ± 1	92 ± 0	92 ± 1	95 ± 1	93 ± 0
SM	20 ± 0	62 ± 8	94 ± 2	98 ± 3	98 ± 4	98 ± 3
CRB	9 ± 0	49 ± 7	88 ± 1	90 ± 1	96 ± 1	94 ± 1

One hundred and fifty micrograms of lipid class standards mix were added to each tube and reacted as described in the Materials and Methods. Samples were normalized to a 23:1 n-9 methyl ester internal standard added before extraction. Yield was determined by comparing samples to a FAME external standard curve. Values reported are the mean ± SD (n = 3).

derivatize SM and CRB. These data support the notion that methods optimized to derivatize FEFAs may not be able to fully derivatize fatty acids from amidified lipids, likely because amide bonds are more resistant to methanolysis than ester bonds (9, 16).

We next tested two variants of a representative method specifically developed for derivatizing AFAs by reacting 150 µg of lipid class standards mix with 2 M methanolic HCl at 50°C for 24 h or 80°C for 5 h (9, 20). One hundred microliters of water were added to mimic the water content commonly present in biological sample preparations. Both variants of this AFA method resulted in sufficient yields (≥88%) from polar lipids (FFA, PC, SM, CRB; Table 2). However, both of the AFA methods had significantly decreased yields (4–47%) from nonpolar lipids (TG, CE; Table 2), likely due to their insolubility in a water-methanol mix (13). Taken together, these results indicate that methods developed for specific lipid classes may not be able to completely derivatize fatty acids from representatives of other major animal lipid classes. As a result, using these methods could result in an incomplete assessment of total cellular fatty acid content.

#### Development of a method for derivatization of fatty acids from representatives of all major animal lipid classes

One previously published method used an in situ acid-catalyzed methanolysis approach that completely derivatized fatty acids from CE, PC, and SM (16). In this method, 1.3 M HCl and 100°C incubation were used to fully derivatize the AFAs in SMs. Neutral CEs were brought into solution by including benzene in the reaction mix and by using acetyl chloride as an anhydrous source of acid (in place of aqueous HCl). This method increased the range of complex lipids derivatized in a single reaction; however, there are several aspects of this derivatization that do not make it ideal. Benzene is a regulated carcinogen, and acetyl chloride (due to its reactivity) was added dropwise on a per sample basis, greatly increasing labor time. Furthermore, other important lipid classes (TG, FFA, glycosphingolipids) were not directly tested. To address this, we modified the derivatization by replacing benzene with noncarcinogenic toluene, and added the reagents in a single master mix (2 ml of 9:18:73 acetyl chloride:toluene:methanol, v/v). Reaction time was extended from 1 to 2 h at 100°C to ensure complete derivatization of AFAs. To test whether these changes allowed for the derivatization of fatty acids

from representatives of all major animal lipid classes, 150 µg of our lipid class standards mix were reacted in the presence of 100 µl of water. We found that FFA, TG, CE, PC, SM, and CRB were all efficiently derivatized at 95–101% of theoretical yield (Table 2). Extending the reaction to 21 h did not change the results, further demonstrating the completion of the reaction at 2 h (Table 2).

#### Optimizing extraction and GC/MS analysis for limiting amounts of stable isotope-labeled FAMEs

One intrinsic challenge with stable isotope labeling of lipids is that it requires intensive analysis of the molecular ion mass isotopomers to gain useful information about synthesis (6, 7). For fatty acids, the molecular ion mass isotopomers are rare (<2% of all ions created), particularly for PUFAs (9). Furthermore, the high cost of stable isotope-enriched metabolites limits the amount of starting material that can be feasibly generated from in vitro labeling experiments. As a result, many published methods, which are optimized for large amounts of unlabeled starting material, do not produce enough signal to be used for analysis of stable isotope-labeled lipids. To address this, we improved extraction efficiency and concentrated the final samples by drying under vacuum. After derivatization, samples were neutralized with 2.5 ml of 0.66 M aqueous Na<sub>2</sub>CO<sub>3</sub> and extracted twice with 2 ml of n-hexane. We observed extraction efficiencies of greater than or equal to 95% for FAMEs derivatized from the lipid class standards mix described above. The combined organic layers were then dried under vacuum and subsequently redissolved in as low as 75 µl of toluene before GC/MS analysis. As a result of our extraction, drying, and redissolving steps, we were able to significantly increase the final sample concentration.

Published FAME GC/MS programs can also be problematic when applied to stable isotope-labeled samples. Programs often call for the GC/MS inlet to be run in “split” mode, which is simple, rapid, and yields sharp peaks because only a small fraction (1–10%) of the injected sample is loaded onto the column (9, 11, 16). This may be sufficient for large amounts of unlabeled starting material, but usually will not result in adequate signal for analysis of FAMEs from small numbers of stable isotope-labeled cells. Furthermore, run times can be an issue (sometimes exceeding 90 min) because of challenges in chromatographically separating FAME isomers and the slow elution of cholesterol (16, 19). To overcome signal deficiencies, we used a “splitless” injection

paired with solvent focusing to load the entire injected sample onto the column while still resolving FAME isomers. An extended final bake out of the column is avoided by allowing sterols to elute in empty or noncritical areas of subsequent chromatograms, decreasing run time to 32 min. Taken together, these results show that our method has been optimized for rapid analysis of limiting amounts of stable isotope-labeled FAMEs by increasing signal (up to 150-fold) and reducing run time (up to 3-fold) compared with conventional methods (11, 16, 19).

#### Minimal losses of FAMEs due to hydrolysis, oxidation, or evaporation

Excess water can interfere with methyl ester derivatization by both driving nonpolar lipids out of solution and hydrolyzing methyl esters to free acids (13). Conversely, insufficient water has been reported to hinder sphingolipid derivatization (16). Because we designed the current method to work *in situ*, we sought to determine the water tolerance of the reaction. To that end, we derivatized the lipid class standards mix described above using the new procedure in the presence of 0–200  $\mu\text{l}$  of water, approximating the range of residual water commonly found in pellets of cultured cells. Yields for FAMEs from all lipid classes were 92–101% when 50–200  $\mu\text{l}$  of water were present, indicating that this amount of water is well-tolerated in the reaction. In agreement with previous results (16), we also observed that a completely anhydrous reaction modestly decreased yield from sphingolipids (approximately 85% of theoretical yield), but not other lipid classes. Additionally, increasing the water content in the reaction mixture resulted in a dose-dependent decrease in FAME yields, however this decrease was less than 5% and affected all fatty acids analyzed equally.

Evaporative loss of low molecular weight FAMEs during drying and destruction of PUFAs under harsh acid-catalyzed methanolysis conditions has been reported (9, 14, 16, 23). To address these issues, we analyzed 20–125  $\mu\text{g}$  of a FAME/cholesterol mix designed to roughly mimic the content of animal cells (see the Materials and Methods). Samples were analyzed by GC/MS directly (external standard curve) or after being subjected to the current derivatization reaction (internal standard curve). Water (50, 100, or 200  $\mu\text{l}$ ) was added before derivatization to mimic sample water. A 19:0 methyl ester internal standard added before derivatization was used to correct for minor losses due to hydrolysis. When yield was determined using the ratio of internal to external standard curve slopes, we observed losses of less than or equal to 5% for all fatty acids measured, with the exception of 7% for 14:0 with 200  $\mu\text{l}$  of water present. We found that performing derivatization under argon and in the presence of the antioxidant BHT (100 mg/l) did not result in significant improvement of the yield of PUFAs, likely because loss in the reaction was already low (<5%). Thus antioxidants and inert gas can be included, but they do not appear to be necessary to preserve PUFAs in the current method with the amounts of lipid used. In sum, these data demonstrate that FAME losses due to hydrolysis, evaporation, and oxidation are minimal when 50–200  $\mu\text{l}$  of water is present and lipid mass exceeds 20  $\mu\text{g}$ .

#### Complete derivatization of LCFAs and VLCFAs from all major animal lipid classes in cellular matrix

Cellular matrix can interfere with acid-catalyzed methanolysis by neutralizing acid or protecting complex lipids. Thus, we tested whether this method could completely derivatize fatty acids in the presence of cellular matrix. To that end, the yield from our lipid class standards mix was determined when spiked into matrix from  $2.5 \times 10^6$  H1299 lung cancer cells. We observed that yields were nearly identical in the presence or absence of cellular matrix (Table 3). We also considered the possibility that endogenous lipids from the cellular matrix might behave differently than exogenously added lipid. To test for this, we reacted cellular matrix from  $2.5 \times 10^6$  H1299 cells for 2 h or overnight (15 h). Incubation for both 2 and 15 h resulted in nearly identical yields of endogenous fatty acids (<5% difference), suggesting that, similar to the lipid class standards, endogenous lipids are fully derivatized in the first 2 h of the reaction. We also observed that the method is linear for  $\geq 17$  fatty acids over a range of cancer cell numbers ( $0.4$ – $2.5 \times 10^6$  H1299), with  $R^2$  values greater than 0.99 (Table 4).

To further demonstrate the importance of fully derivatizing fatty acids from all major classes of lipid in animals, we assessed fatty acid content from cultured cells (H1299) using the current method and a commonly used FEFA method (13). The two methods yielded similar results for LCFAs, but the current method resulted in an increase of 1.5- to 3-fold for 22:0, 24:0, and 24:1 n-9 (Fig. 1). This is likely due to significant enrichment of saturated and mono-unsaturated VLCFAs in sphingolipids (24, 25), which can be poorly derivatized by FEFA methods (Table 2). Taken together, these results demonstrate that the current method fully derivatizes LCFAs and VLCFAs from all major animal lipid classes in the presence of cellular matrix, and that failure to completely derivatize fatty acids from these different classes can result in significant underestimation of the fatty acid content of cultured cells.

#### Efficient quantitation of cholesterol from the same sample

It is difficult to analyze both fatty acids and cholesterol using a single derivatization and GC column (9). To address this, we developed an integrated approach where we

TABLE 3. Complete derivatization of lipid class standards in cellular matrix

	Without Cellular Matrix (Percent Yield)	With Cellular Matrix (Percent Yield)
FFA	97 $\pm$ 1	96 $\pm$ 1
TG	99 $\pm$ 1	97 $\pm$ 1
CE	103 $\pm$ 1	103 $\pm$ 1
PC	96 $\pm$ 1	97 $\pm$ 1
SM	100 $\pm$ 4	103 $\pm$ 6
CRB	98 $\pm$ 1	98 $\pm$ 1

One hundred and fifty micrograms of lipid class standards mix were added to tubes containing 0 or  $2.5 \times 10^6$  H1299 cells. All tubes were analyzed using the current method. Samples were normalized to a 19:1 n-12 methyl ester internal standard added after dry down. Yield was determined by comparing samples to a FAME external standard curve. The contribution of cellular fatty acids was corrected for. Values reported are the mean  $\pm$  SD (n = 3).

TABLE 4. Fatty acid and cholesterol response is linear with cell number

	Slope ( $\mu\text{g}/10^6$ Cells)	y-Intercept ( $\mu\text{g}$ )	R <sup>2</sup>
14:0	0.70	0.02	1.000
16:0	9.27	0.06	1.000
16:1 n-7	2.06	0.04	1.000
18:0	4.65	0.06	1.000
18:1 n-9	12.55	-0.06	1.000
18:1 n-7	3.71	0.00	1.000
18:2 n-6	1.24	0.00	1.000
20:0	0.08	0.00	0.999
20:1 n-9	0.35	0.00	0.999
20:2 n-6	0.08	0.00	0.999
20:3 n-6	0.49	0.01	1.000
20:4 n-6	2.78	0.01	1.000
22:0	0.14	0.00	0.999
22:4 n-6	0.18	-0.01	0.999
22:6 n-3	1.30	0.02	1.000
24:0	0.67	0.02	1.000
24:1 n-9	0.57	0.01	1.000
Cholesterol	9.70	0.22	0.998

H1299 cells ( $0\text{--}2.5 \times 10^6$ ) were added to tubes and analyzed using the current method. Linear regression was performed after analyte responses were normalized to 19:0 methyl ester (fatty acids) or cholesterol- $d_6$  (cholesterol) internal standards (added before derivatization) and fit to an internal standard curve. Cellular samples were performed in technical triplicate.

could analyze cholesterol content after FAME analysis. Samples were dried and rederivatized in 1:1 (99:1 BSTFA:TMCS):pyridine to produce TMSE sterols and a new rapid GC/MS program was run on a ZB-MR1 column (<10 min per sample, see the Materials and Methods). Fatty acids are also trimethylsilylated, but they do not interfere with TMSE sterol quantitation because they elute at much lower temperatures. One potential concern was that a harsh acid methanolysis reaction could result in the destruction of cholesterol (13, 19, 26). To determine the yield of cholesterol in our method, we processed three concentrations of deuterated cholesterol (cholesterol- $d_6$ ) alone or in the presence of cellular matrix ( $2.5 \times 10^6$  H1299 cells). We found that the yield of cholesterol- $d_6$  was 77–

80% in the absence of cellular matrix and 86–90% in the presence of cellular matrix (Table 5). Though we saw modest destruction of cholesterol in this method, in unlabeled samples it could be accounted for by using cholesterol- $d_6$  as an internal standard to control for any differences in destruction between samples (Table 4). In sum, these data demonstrate that this method can be used to quantify fatty acids and cholesterol from the same sample.

#### Successful application of method to small numbers of stable isotope-labeled cells

To determine whether the current method was capable of measuring MIDs from small numbers of stable isotope-labeled cells, H1299 cells were brought to metabolic and isotopic steady state in glucose-free DMEM supplemented with 25 mM  $^{13}\text{C}_6$ -glucose and 5% FBS. In applying the current method to these samples, LCFA data was collected from a 0.5  $\mu\text{l}$  injection, while data from rarer VLCFAs were collected using a 2  $\mu\text{l}$  injection. Dilution tests indicated that consistent MIDs can be collected for cholesterol and many fatty acid species down to the equivalent of  $0.4 \times 10^6$  H1299 cells (approximately 20  $\mu\text{g}$  of total cellular fatty acid and cholesterol). The 14 fatty acid species included nonessential LCFAs (14:0, 16:0, 16:1 n-7, 18:0, 18:1 n-9, 18:1 n-7), PUFAs (18:2 n-6, 20:3 n-6, 20:4 n-6, 22:4 n-6), and nonessential VLCFAs (20:0, 22:0, 24:0, 24:1 n-9) (Fig. 2 and data not shown).

Background contamination can be an issue for fatty acid and cholesterol analysis from small numbers of cells. Fatty acids are present even in the purest solvents and the cleanest glassware, and can cause inaccurate quantitation. Cholesterol contamination is less common than fatty acid contamination, but it can also be an issue when serum is used in collection media. Furthermore, in stable isotope-labeled samples, unlabeled background contamination can distort MIDs. Thus, we assessed fatty acid and cholesterol background using the y-intercept of the H1299 linearly test (Table 4, modified to include only points from 0 to

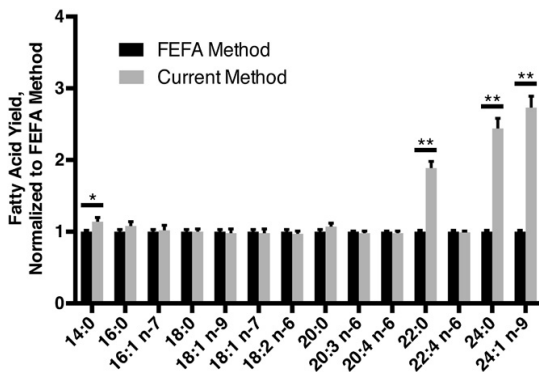


Fig. 1. The current method results in a significantly higher yield of VLC saturates and monounsaturates from cultured cells. H1299 cells were collected at 85% confluency from 60 mm plates in triplicate and were analyzed using the current method or a FEFA method (45°C, 16 h). Values represent micrograms on the plate normalized to a 19:0 methyl ester added before derivatization, then further normalized to the average result of the FEFA method. Data are presented as the mean  $\pm$  SD ( $n = 3$ ). \* $P \leq 0.05$ , \*\* $P \leq 0.01$

TABLE 5. Cholesterol yield in the current method

		Micrograms of Total Sterol Added (Percent Yield)		
		4.4	8.8	27.5
Cholesterol-d <sub>6</sub>	Sterol alone	77 ± 1	79 ± 3	80 ± 1
	Sterol + cells	90 ± 0	86 ± 2	88 ± 2
Stigmasterol	Sterol alone	98 ± 1	98 ± 1	100 ± 1
	Sterol + cells	103 ± 2	99 ± 0	99 ± 0

Variable amounts of sterol (10:1 mix of cholesterol-d<sub>6</sub> and stigmasterol by mass) were added to empty tubes (sterol alone) or tubes containing  $2.5 \times 10^6$  H1299 cells (sterol + cells) and analyzed using the current method. Analytes were normalized to a stigmasterol internal standard added after the initial dry down. Absolute yield was determined by comparing to a “sterol alone” tube that only went through the second dry down and trimethylsilylation. Values are reported as average ± SD (n = 3).

$1 \times 10^6$  H1299 cells). For low numbers of cells ( $0.4 \times 10^6$  H1299 cells), background contamination was 5% or less for cholesterol and the 14 fatty acids reported above, with the exception of 18:0, 20:0, and 22:0, which had 9%, 18%, and 11% contamination, respectively. Similar results were obtained when measuring background using mock tubes (cell collection and derivatization reagents only). Stigmasterol was used as an internal standard for cholesterol studies and was not subject to significant destruction with the new methodology (Table 5). In combination with the dilution test above, we conclude that in these labeling conditions, MIDs for cholesterol and 11 fatty acids can be determined from  $0.4 \times 10^6$  H1299 cells. Increased sample size would be required for measuring MIDs of fatty acids with higher background, such as 18:0, 20:0, and 22:0 (approximately  $0.8 \times 10^6$ ,  $1.6 \times 10^6$ , and  $1.2 \times 10^6$  H1299 cells, respectively). Taken together, these data demonstrate that

the current method provides an approach for quantifying LCFAs, VLCFAs, and cholesterol from limited amounts of stable isotope-labeled cells.

## DISCUSSION

There has been reinvigorated interest in how lipid metabolism affects the fate and function of cells. Because of this, stable isotope labeling of lipids, which can give unique insights into metabolic flux, is rapidly becoming an important tool for assessing changes in lipid homeostasis. As such, development of new techniques that facilitate the isolation and analysis of lipids is an important objective. Herein, we describe a method that can be used to analyze both fatty acids and cholesterol from small numbers of stable isotope-labeled cultured cells. To our knowledge, this is the first method optimized to quantify cholesterol as well as LCFAs and VLCFAs from all major animal lipid classes. Importantly, the current method also addresses the critical challenge in analysis of stable isotope-labeled lipids, obtaining sufficient molecular ion mass isotopomer signal from limited starting material and low abundance analytes. We acknowledge that quantitation of thermally labile lipids (e.g., eicosanoids), endogenous lipid species that may also be generated by ex vivo oxidation (e.g., oxysterols), or highly volatile fatty acids (e.g., short or medium chain FAs) may require alternate methodology (10, 23, 27). Nevertheless, we anticipate that this new method will be useful to a wide variety of scientists investigating the impact of fatty acid and cholesterol homeostasis on cell biology.

Due to the high cost of stable isotope-labeled metabolites, in vitro stable isotope labeling experiments are usually done on the smallest scale feasible. As a result, we validated our method from  $0.4$ – $2.5 \times 10^6$  H1299 cells (approximately 20–125  $\mu\text{g}$  total fatty acids and cholesterol), which represent one 50% confluent well in a 6-well plate to a fully confluent T-25 flask. This is within the range of many in vitro stable isotope-labeling experiments (22, 28–30). It is important to note that different cell lines may have different lipid content and stable isotope labeling properties. Also, our data indicate that background contamination is a limiting factor in decreasing starting material. Thus, when using the current method to analyze other conditions or cell lines, it will be important to verify that the total fatty acid and cholesterol content is above 20  $\mu\text{g}$

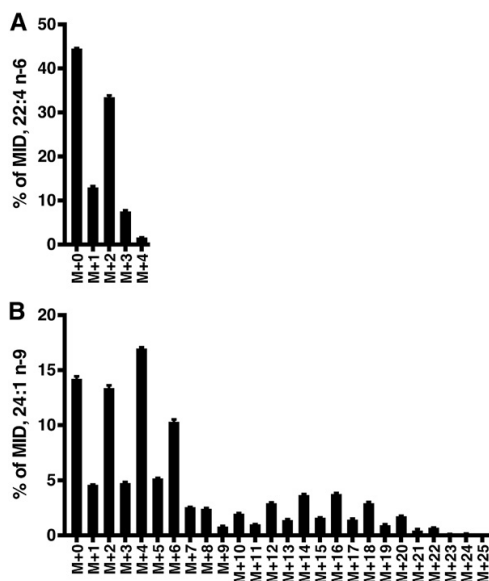


Fig. 2. FAME MIDs collected from stable isotope-labeled cells using the current method. H1299 cells were brought to isotopic steady state in DMEM containing 100%  $^{13}\text{C}_6$ -glucose and 5% FBS. Cells were collected at 85% confluency from 60 mm plates in triplicate and were analyzed using the current method. A: 22:4 n-6. B: 24:1 n-9. Data are presented as the mean ± SD (n = 3).

and to include appropriate controls to visualize background and limit of detection for each analyte. For example, we have found that in low numbers of cultured cells, background contamination significantly interferes with quantitation of 22:1 n-9. As a result, accurately measuring that fatty acid would require increased sample material.

Fatty acids can be incorporated into a wide variety of complex lipid species. Thus, fully derivatizing fatty acids from all the major classes of complex lipids in animals is critical for accurately quantifying fatty acid pool sizes. For example, our data indicate that poor derivatization of sphingolipids can result in significant errors in quantifying the amount of VLC saturates and monounsaturates in cultured cancer cells (Fig. 1). This issue would likely be amplified in cells with higher concentrations of sphingolipids, such as neurons, glia, or cancer cells of neural origin (31). Additionally, we expect that the current method can facilitate accurate quantification of fatty acid pool sizes in cells containing large amounts of neutral lipids, such as hepatocytes and adipocytes (32, 33). Finally, we hypothesize that this new method will be particularly useful in ensuring accurate quantification of MIDs of fatty acids. Metabolic channeling has been shown to be important in the fluxes of metabolites, including selective incorporation of fatty acid species into particular complex lipids (34). Underrepresenting the labeled fatty acids from one or more classes of lipid as a result of poor extraction or derivatization could interfere with the accuracy of mass isotopomer modeling studies designed to determine a cell's reliance on synthesis or import in achieving fatty acid homeostasis.

Cholesterol can be subject to degradation under harsh derivatization procedures (9, 13) and, in our methodology, we did observe modest destruction (Table 5). In unlabeled samples, this issue is remedied by the use of cholesterol- $d_6$  as an internal standard (Table 4). In stable isotope-labeled samples, cholesterol- $d_6$  cannot be used because it cannot be fully distinguished from  $^{13}C$ -labeled sample cholesterol chromatographically or by mass using our instrumentation. Thus, we used stigmastanol as the internal standard when analyzing  $^{13}C$ -labeled samples. We found that stigmastanol was resistant to degradation in the current reaction, likely due to its lack of double bonds (Table 5). One potential consequence of using stigmastanol as an internal standard in the current method is that absolute cellular cholesterol content may be overestimated by up to 15% if a matrix-free internal standard curve is applied. However, we anticipate that relative error in cholesterol content between cellular samples will be significantly reduced as cellular matrix concentrations become closer. Thus, we strongly recommend using similar amounts of cellular matrix to maintain accuracy when assessing cholesterol in isotopic labeling studies. Alternatively, one could employ milder methods developed specifically for cholesterol analysis if small changes in cholesterol parameters are expected or very accurate absolute quantitation is required (35). Finally, when using the current method to observe MIDs of cholesterol, we strongly recommend culturing cells in an amount of  $^{13}C$ -labeled substrate that results in modest labeling of the cellular acetyl-CoA pool (no more than 35%

$^{13}C$ ). This results in a more accurate molecular ion MID by limiting potential interference by the MID of the largest fragment ion, M-15 (36). Use of modest labeling also reduces the possibility of kinetic isotope effects selectively stabilizing  $^{13}C$ -labeled cholesterol in the derivatization reaction (37).

In conclusion, we believe that the broad range of input sample material that this method can accommodate, combined with heightened efficiencies of lipid derivatization and sample usage, make this new approach highly amenable to a variety of biologic applications, and will facilitate studies interrogating lipid homeostasis. 

The authors thank Drs. James Wohlschlegel, Catherine Clarke, and Elvira Khialeeva (University of California, Los Angeles) for providing thoughtful analysis. They also thank Joo Hee Sohn (University of California, Los Angeles) for technical assistance.

## REFERENCES

- Vance, D. E., and J. E. Vance, editors. 2008. *Biochemistry of Lipids, Lipoproteins and Membranes*. 5th edition. Elsevier B.V., Oxford, UK.
- Currie, E., A. Schulze, R. Zechner, T. C. Walther, and R. V. Farese. 2013. Cellular fatty acid metabolism and cancer. *Cell Metab.* **18**: 153–161.
- Cyster, J. G., E. V. Dang, A. Reboldi, and T. Yi. 2014. 25-Hydroxycholesterols in innate and adaptive immunity. *Nat. Rev. Immunol.* **14**: 731–743.
- Lee, S. D., and P. Tontonoz. 2015. Liver X receptors at the intersection of lipid metabolism and atherogenesis. *Atherosclerosis*. **242**: 29–36.
- Buescher, J. M., M. R. Antoniewicz, L. G. Boros, S. C. Burgess, H. Brunengraber, C. B. Clish, R. J. DeBerardinis, O. Feron, C. Frezza, B. Ghesquiere, et al. 2015. A roadmap for interpreting  $^{13}C$  metabolite labeling patterns from cells. *Curr. Opin. Biotechnol.* **34**: 189–201.
- Hellerstein, M. K., and R. A. Neese. 1992. Mass isotopomer distribution analysis: a technique for measuring biosynthesis and turnover of polymers. *Am. J. Physiol.* **263**: E988–E1001.
- Kelleher, J. K., and T. M. Masterson. 1992. Model equations for condensation biosynthesis using stable isotopes and radioisotopes. *Am. J. Physiol.* **262**: E118–E125.
- Carrapiso, A. I., and C. García. 2000. Development in lipid analysis: some new extraction techniques and in situ transesterification. *Lipids*. **35**: 1167–1177.
- Christie, W. W., and X. Han. 2010. *Lipid Analysis: Isolation, Separation, Identification, and Lipidomic Analysis*. 4th edition. The Oily Press, Bridgwater, UK.
- McDonald, J. G., D. D. Smith, A. R. Stiles, and D. W. Russell. 2012. A comprehensive method for extraction and quantitative analysis of sterols and secosteroids from human plasma. *J. Lipid Res.* **53**: 1399–1409.
- Eder, K. 1995. Gas chromatographic analysis of fatty acid methyl esters. *J. Chromatogr. B Biomed. Appl.* **671**: 113–131.
- Liu, K-S. 1994. Preparation of fatty acid methyl esters for gas-chromatographic analysis of lipids in biological materials. *J. Am. Oil Chem. Soc.* **71**: 1179–1187.
- Ichihara, K., and Y. Fukubayashi. 2010. Preparation of fatty acid methyl esters for gas-liquid chromatography. *J. Lipid Res.* **51**: 635–640.
- Palmquist, D. L., and T. C. Jenkins. 2003. Challenges with fats and fatty acid methods. *J. Anim. Sci.* **81**: 3250–3254.
- Kelleher, J. K., A. T. Kharroubi, T. A. Aldaghas, I. B. Shambat, K. A. Kennedy, A. L. Holleran, and T. M. Masterson. 1994. Isotopomer spectral analysis of cholesterol synthesis: applications in human hepatoma cells. *Am. J. Physiol.* **266**: E384–E395.
- Lepage, G., and C. C. Roy. 1986. Direct transesterification of all classes of lipids in a one-step reaction. *J. Lipid Res.* **27**: 114–120.
- Masood, M. A., and N. Salem. 2008. High-throughput analysis of plasma fatty acid methyl esters employing robotic transesterification and fast gas chromatography. *Lipids*. **43**: 171–180.

18. Lin, Y. H., N. Salem, E. M. Wells, W. Zhou, J. D. Loewke, J. A. Brown, W. E. M. Lands, L. R. Goldman, and J. R. Hibbeln. 2012. Automated high-throughput fatty acid analysis of umbilical cord serum and application to an epidemiological study. *Lipids*. **47**: 527–539.
19. Meier, S., S. A. Mjøs, H. Joensen, and O. Grahl-Nielsen. 2006. Validation of a one-step extraction/methylation method for determination of fatty acids and cholesterol in marine tissues. *J. Chromatogr. A*. **1104**: 291–298.
20. Sweeley, C. C., and E. A. Moscatelli. 1959. Qualitative microanalysis and estimation of sphingolipid bases. *J. Lipid Res.* **1**: 40–47.
21. Lowenstein, J. M., H. Brunengraber, and M. Wadke. 1975. Measurement of rates of lipogenesis with deuterated and tritiated water. *Methods Enzymol.* **35**: 279–287.
22. Tumanov, S., V. Bulusu, and J. J. Kamphorst. 2015. Analysis of fatty acid metabolism using stable isotope tracers and mass spectrometry. *Methods Enzymol.* **561**: 197–217.
23. Lepage, G., and C. C. Roy. 1984. Improved recovery of fatty acid through direct transesterification without prior extraction or purification. *J. Lipid Res.* **25**: 1391–1396.
24. Sassa, T., and A. Kihara. 2014. Metabolism of very long-chain fatty acids: genes and pathophysiology. *Biomol. Ther. (Seoul)*. **22**: 83–92.
25. Laviad, E. L., L. Albee, I. Pankova-Kholmyansky, S. Epstein, H. Park, A. H. Merrill, and A. H. Futerman. 2008. Characterization of ceramide synthase 2: tissue distribution, substrate specificity, and inhibition by sphingosine 1-phosphate. *J. Biol. Chem.* **283**: 5677–5684.
26. Morrison, W. R., and L. M. Smith. 1964. Preparation of fatty acid methyl esters and dimethylacetals from lipids with boron fluoride-methanol. *J. Lipid Res.* **5**: 600–608.
27. Deems, R., M. W. Buczynski, R. Bowers-Gentry, R. Harkewicz, and E. A. Dennis. 2007. Detection and quantitation of eicosanoids via high performance liquid chromatography-electrospray ionization-mass spectrometry. *Methods Enzymol.* **432**: 59–82.
28. Grassian, A. R., S. J. Parker, S. M. Davidson, A. S. Divakaruni, C. R. Green, X. Zhang, K. L. Slocum, M. Pu, F. Lin, C. Vickers, et al. 2014. IDH1 mutations alter citric acid cycle metabolism and increase dependence on oxidative mitochondrial metabolism. *Cancer Res.* **74**: 3317–3331.
29. Metallo, C. M., P. A. Gameiro, E. L. Bell, K. R. Mattaini, J. Yang, K. Hiller, C. M. Jewell, Z. R. Johnson, D. J. Irvine, L. Guarente, et al. 2011. Reductive glutamine metabolism by IDH1 mediates lipogenesis under hypoxia. *Nature*. **481**: 380–384.
30. Kamphorst, J. J., J. R. Cross, J. Fan, E. de Stanchina, R. Mathew, E. P. White, C. B. Thompson, and J. D. Rabinowitz. 2013. Hypoxic and Ras-transformed cells support growth by scavenging unsaturated fatty acids from lysophospholipids. *Proc. Natl. Acad. Sci. USA*. **110**: 8882–8887.
31. Posse de Chaves, E., and S. Sipione. 2010. Sphingolipids and gangliosides of the nervous system in membrane function and dysfunction. *FEBS Lett.* **584**: 1748–1759.
32. Berk, P. D., and E. C. Verna. 2016. Nonalcoholic fatty liver disease: lipids and insulin resistance. *Clin. Liver Dis.* **20**: 245–262.
33. Rutkowski, J. M., J. H. Stern, and P. E. Scherer. 2015. The cell biology of fat expansion. *J. Cell Biol.* **208**: 501–512.
34. Grevengoed, T. J., E. L. Klett, and R. A. Coleman. 2014. Acyl-CoA metabolism and partitioning. *Annu. Rev. Nutr.* **34**: 1–30.
35. Verleyen, T., M. Forcades, R. Verhe, K. Dewettinck, A. Huyghebaert, and W. De Greyt. 2002. Analysis of free and esterified sterols in vegetable oils. *J. Am. Oil Chem. Soc.* **79**: 117–122.
36. Linstrom, P. J., and W. G. Mallard, editors. NIST Chemistry WebBook: NIST Standard Reference Database Number 69. National Institute of Standards and Technology, Gaithersburg, MD.
37. Lynn, K. R., and P. E. Yankwich. 1961. Isotope fractionation at the methyl carbon in the reactions of cyanide ion with methyl chloride and methyl bromide. *J. Am. Chem. Soc.* **83**: 3220–3223.

CHAPTER THREE:

Development and Application of Fatty Acid Source Analysis (FASA),

A New Model for Quantifying Fatty Acid Metabolism

Using Stable Isotope Labeling

## **Development and Application of Fatty Acid Source Analysis (FASA), A New Model for Quantifying Fatty Acid Metabolism Using Stable Isotope Labeling**

**Authors:** Joseph P. Argus<sup>1</sup>, Moses Q. Wilks<sup>2</sup>, Quan Zhou<sup>1</sup>, Wayne Hsieh<sup>3</sup>, Elvira Khialeeva<sup>4</sup>, Viet Bui<sup>3</sup>, Shili Xu<sup>1</sup>, Amy K. Yu<sup>1</sup>, Eric S. Wang<sup>1</sup>, Harvey R. Herschman<sup>1</sup>, Kevin J. Williams<sup>3</sup>, and Steven J. Bensinger<sup>1,3\*</sup>

### **Affiliations:**

1. Department of Molecular and Medical Pharmacology, David Geffen School of Medicine, University of California, Los Angeles, 615 Charles E Young Dr. E, Los Angeles, CA 90095, USA
2. Gordon Center for Medical Imaging, Massachusetts General Hospital, Harvard Medical School, 149, 13<sup>th</sup> Street, Charlestown, MA 02129
3. Department of Microbiology, Immunology and Molecular Genetics, David Geffen School of Medicine, University of California, Los Angeles, 615 Charles E Young Dr. E, Los Angeles, CA 90095, USA
4. Molecular Biology Institute, University of California, Los Angeles, 615 Charles E Young Dr. E, Los Angeles, CA 90095, USA

\*Corresponding Author: Steven J. Bensinger

e-mail: [sbensinger@mednet.ucla.edu](mailto:sbensinger@mednet.ucla.edu)

Running title: A New Model to Quantify Fatty Acid Metabolism

## **Abstract**

It is well understood that fatty acids can be synthesized, imported, and modified to meet requisite demands in cells. However, quantifying the movement of fatty acids through the multiplicity of these metabolic steps has remained elusive. To address this, we developed Fatty Acid Source Analysis (FASA), a new model that quantifies the contribution of synthesis, import and elongation pathways to fatty acid homeostasis in saturated, monounsaturated, and polyunsaturated fatty acid pools. Application of FASA revealed several previously unmeasured aspects of cellular fatty acid homeostasis, and demonstrated that distinct pro-inflammatory stimuli (e.g., Toll-like receptor 2, 3 or 4) specifically reprogram the fluxes of fatty acids through the synthetic and elongation pathways in macrophages. In sum, this new modeling approach significantly advances our ability to quantify cellular fatty acid metabolism, and brings new insights as to how cells dynamically reshape their lipidome in response to metabolic or inflammatory signals.

## **Introduction**

Fatty acids are a diverse group of acyl tail carboxylic acids that perform essential structural, energetic, and signaling roles in all cells (1, 2). Perturbations in cellular fatty acid homeostasis drive pathogenesis of a broad array of human diseases (3, 4). Despite the clear importance of preserving fatty acid homeostasis, we have a surprisingly poor understanding of how cells achieve and maintain their fatty acid composition under normal conditions. Nor do we understand how fatty acid homeostasis is dynamically modulated in response to instructional signals or pathologic states.

Individual cells meet their fatty acid requirements through a combination of synthesis, import, and modification pathways (1). Long chain fatty acids (LCFAs) are synthesized through the enzymatic action of Fatty Acid Synthase (FASN), producing primarily palmitic acid (16:0) and, to a lesser extent, 14:0 and 18:0 through the condensation of acetyl-CoA with malonyl-CoA (1, 5). These direct LCFA products of FASN can be further modified by both elongation and desaturation. The fatty acid desaturation pathways selectively oxidize fatty acids, introducing desaturations into the acyl tails. The fatty acid elongation pathways lengthen a wide variety of fatty acids by 2 carbons per cycle through addition of malonyl-CoA (derived from acetyl-CoA) (1). In addition to synthesis, elongation, and desaturation, fatty acids can be imported directly into distinct fatty acid pools, where they then can flux through cellular elongation or desaturation pathways as required (1, 6). In combination, these metabolic pathways allow cells to generate a wide variety of fatty acids ranging from 14 to 24 (or greater) carbons. Thus, the cellular pool of any given fatty acid species likely represents an admixture of fatty acids that were 1) directly synthesized, 2) synthesized and then enzymatically modified, 3) directly imported, and 4)

imported and then enzymatically modified. This intrinsic complexity in fatty acid metabolism makes understanding how cells maintain their fatty acid composition difficult. Consequently, development of novel methodologies and models that will help to unravel the complex nature of fatty acid homeostasis is essential for elucidating how cells achieve their cellular lipid composition, and how these pathways might become deranged in pathologic states.

The multiplicity of metabolic pathways contributing to fatty acid pools makes identifying the “source” of a lipid nearly impossible without the use of labeling strategies. Isotopomer Spectral Analysis (ISA) and Mass Isotopomer Distribution Analysis (MIDA) are independent modeling approaches that infer fatty acid metabolic parameters using mass spectrometry data from cells or tissues cultured with stable isotope-labeled metabolites such as glucose or glutamine (7, 8). In classical ISA and MIDA models, there is an underlying assumption that fatty acids are either directly synthesized by FASN (oft termed *de novo* synthesized) or directly imported. This assumption results in modeling the empirical mass isotopomer distribution as two sub-distributions, a “light” distribution representing imported fatty acid, and a “heavy” distribution representing directly synthesized fatty acid. From these distributions, one determines the relative contribution of the *de novo* synthesis and import pathways to fatty acid pools. However, elongation of imported fatty acids is not incorporated into these models. Thus, the utility of these models is largely restricted to fatty acids for which the contribution of elongation to the pool is minimal (e.g., 14- and 16-carbon species). Subsequent iterations of these models include single elongation of imported 16-carbon fatty acid species, extending utility to 18-carbon fatty acids (9–11). However, it is likely that very long chain fatty acid pools (e.g., 20:0, 22:0, etc.), and even 18-carbon fatty acid pools (e.g., stearate and oleate) can include multiply elongated fatty acids.

This complexity makes modeling metabolism of these lipid species inaccurate, and consequently limits the ability to interrogate how homeostasis of these biologically important fatty acid pools is regulated.

To address this scientific barrier, we have developed a new model, termed Fatty Acid Source Analysis (FASA), that accommodates elongation of fatty acids in addition to classical modeling of fatty acid synthesis and import. Application of FASA allows for accurate tracing of the movement of fatty acids through synthesis and elongation pathways in the cell, thereby significantly increasing the accuracy in defining the flux and sources of fatty acids contributing to the saturated, monounsaturated, and polyunsaturated fatty acid pools within the cell. Application of FASA at metabolic and isotopic steady state revealed previously unmeasured aspects of fatty acid metabolism in cells. We find that, under standard culture conditions, a remarkably high percentage of 18- to 24-carbon fatty acid species in cells are subject to flux through the elongation machinery. We also provide evidence that the acetyl-CoA pools contributing to both fatty acid synthesis and elongation behave as a single, well-mixed pool rather than distinct pools. Finally, we apply FASA to primary macrophages to model the impact of Toll-like receptor (TLR)-driven metabolic reprogramming on fatty acid homeostasis. Unexpectedly, FASA revealed that different TLRs drive distinct reprogramming modifications of fluxes of long chain and very long chain fatty acids through the synthetic and elongation machinery. These observations suggest potential physiologic importance in differentially regulating elongation during specific inflammatory responses. We suggest the development and application of FASA will significantly advance the ability to model cellular fatty acid metabolic

fluxes, and we anticipate that FASA utilization will be broadly useful to a wide variety of fields interrogating the impact of fatty acids in health and disease.

## **Materials and Methods**

### **Reagents**

Optima grade methanol, optima grade water, optima grade n-hexane, and ACS plus grade hydrochloric acid were purchased from Fisher. Chromosolv Plus grade toluene, ACS grade sodium carbonate, 99+% acetyl chloride was purchased from Alfa Aesar. Fatty acid methyl esters were purchased from NuChek Prep. H1299 (also referred to as NCI-H1299) cells were purchased from ATCC. Primary human fibroblasts were obtained from the Coriell Institute.  $^{13}\text{C}_6$ -glucose and  $^{13}\text{C}_5$ -glutamine (MPT grade) were purchased from Cambridge Isotope Laboratories. Fetal bovine serum (FBS) was purchased from Omega Scientific, Atlanta Biosciences, and Hyclone. LPS, Poly:IC, and Pam3CSK4 were purchased from Invivogen. MHV-68 was a gift from Ting-Ting Wu (UCLA). Calcein AM was purchased from Santa Cruz Biotechnology. All other cell culture reagents were purchased from Gibco.

### **Mice**

C57BL/6 mice were purchased from Jackson Labs.

### **Lentiviral Transduction**

Commercial short hairpin RNAs (shRNA) were obtained from Sigma. Lentiviruses were generated using 3rd generation system with puromycin selection (plasmids available upon request). The doxycycline induction of knockdown is controlled by the Tet repressor (TetR) protein expressed from the pLenti0.3/EF/GW/IVS-Kozak-TetR-P2A-Bsd vector, which was constructed by Dr. Ethan Abel and was kindly provided by Dr. Diane M. Simeone (University of

Michigan, Translational Oncology Program). Additional details of the shRNA system are available in supplemental methods.

### **Cell Culture**

For experiments using the H1299 shCON line without induction, cells were plated in 24-well dishes at  $t = -16$  hr and changed into labeling media at  $t = 0$  hr. Labeling media consisted of DMEM containing 2% FBS, antibiotic, and indicated percentages of U- $^{13}\text{C}_6$ -glucose and U- $^{13}\text{C}_5$ -glutamine. Cells were counted and collected at  $t = 48$  hrs. For experiments using H1299 shCON and shSCAP lines with induction, cells were induced in 10cm plates at  $t = -48$  hr and re-plated in 12-well dishes at  $t = -16$  hr. At  $t = 0$  hr, a set of replicate wells were counted, and the remaining wells changed into labeling media. Labeling media consisted of DMEM containing 5% FBS, antibiotic, and 100% U- $^{13}\text{C}_6$ -glucose and U- $^{13}\text{C}_5$ -glutamine. At  $t = 48$  hr, the labeled cells were counted and collected. For experiments measuring parental H1299 cells at pseudo-steady state, cells were cultured in DMEM containing 5% FBS, antibiotic, and 100% U- $^{13}\text{C}_6$ -glucose for 5 days (approximately 5 cell divisions). Media was refreshed every 12 hours, and cells were maintained in a sub-confluent state. After 5 days, the labeled cells were counted and collected.

For experiments using primary human fibroblasts, cells were plated into 12-well dishes containing labeling media ( $3 \times 10^5$  cells per well). Labeling media consisted of DMEM containing 5% FBS, antibiotic, and 100% U- $^{13}\text{C}_6$ -glucose and U- $^{13}\text{C}_5$ -glutamine. After three days, the labeled cells were collected.

For experiments using bone marrow derived macrophages (BMDMs), bone marrow from C57BL/6 mice were differentiated into macrophages in DMEM containing 10% FBS (Atlanta Biosciences or HyClone), 5% M-CSF conditioned media, 1% pen/strep (GIBCO), 1% glutamine (Invitrogen), and 0.5% sodium pyruvate (Invitrogen) for 7 days prior to experimental use. At day 5 (t = -48 hr), macrophages were scraped, counted, and replated into 12-well dishes using the same differentiation media. At day 7 (t = 0 hr), a set of replicate wells were counted and collected, while the remaining wells were changed into labeled media containing no treatment, PAM3, PIC, LPS, or MHV-68 (MOI = 1). At day 9 (t = 48 hr), cells were collected and counted.

### **Cell Counting and Collection**

Immediately prior to counting, 1.25 $\mu$ M Calcein-AM (final concentration) was added to each well and incubated for 15 minutes. The plates were then imaged on a Molecular Devices ImageXpress XL. 21 high magnification fluorescence images were captured for each well (23.9% of total well surface area) using a 10x Objective (Nikon Plan Fluor, 0.3 NA). Cell number was assessed using MetaXpress Software with Powercore using the Multi-wavelength cell scoring module. Following imaging, cells were dissolved in 6M aqueous guanidine HCl and transferred to glass tubes for derivatization with 3M methanolic guanidine HCl. Samples were prepared alongside internal standard curve samples made up of FAMES (Nu-chek Prep).

### **Lipid Derivatization and GC-MS**

For experiments using the H1299 shCON line without induction, FAMES were prepared as described previously (12). For all other experiments, FAMES were prepared as described previously (13) with the following modifications. The final reaction volume of 725  $\mu$ L

contained 10.5% acetyl chloride, 10% toluene, and 6% water in methanol (v/v) as well as methyl nonadecanoate as an internal standard. The reaction proceeded at 45C for 24 hrs, and was neutralized with 775  $\mu$ L of 0.87M sodium carbonate in water. After addition of 1 mL of hexane, inversion, and centrifugation, the organic layer was extracted and dried. The remaining FAMES were redissolved in 250  $\mu$ L hexane for analysis by GC-MS.

Complete GC-MS configurations and running programs are available upon request. Integration and quantification of all ions was performed on MassHunter Quantitative Analysis Program (Agilent Technologies, B.06.00). Fatty acid pool sizes were determined by taking the sum of the area under the curve (AUC) for all isotopomers of the molecular ion, normalizing to internal standard (19:0 methyl ester), and comparing to a FAMES internal standard curve.

### **ISA and FASA Modeling**

See supplemental methods for a full explanation of ISA and FASA modeling.

### **Gene expression analysis**

RNA was extracted from all cells with Trizol using manufacturer's protocol. cDNA was synthesized with iScript cDNA Synthesis Kit (Bio- Rad) as per manufacturer's instructions (700ng/ $\mu$ L RNA per cDNA synthesis reaction). Quantitative PCR (qPCR) was conducted on the Roche LightCycler 480 using SYBR Green Master Mix (Kapa Biosciences) and 0.5  $\mu$ mol/L primers. Relative expression values are normalized to control gene (*36B4*) and expressed in terms of linear relative mRNA values. Primer sequences are available upon request.

**Statistics:**

Statistical analyses were performed using a two-tailed heteroscedastic Student's t-test ns – not significant,  $p > .05$ ; \* -  $.01 < p \leq .05$ ; \*\* -  $.001 < p \leq .01$ ; \*\*\* -  $p \leq .001$ . In some instances, log-likelihood ratio tests (LLRTs) between ISA and FASA were performed as described in supplemental methods.

## Results

### **Classical Models Fail to Accurately Model Fatty Acids Greater than 16 Carbons in Length**

Cells maintain their fatty acid composition through a complex mixture of synthetic, import, and modification (e.g., desaturation and elongation) pathways (1). Stable isotope labeling and subsequent modeling of mass isotopomer distributions of fatty acids using classical approaches (e.g., Isotopomer Spectral Analysis (ISA) and Mass Isotopomer Distribution Analysis (MIDA)) allows for the accurate identification of the source (i.e. directly synthesized by fatty acid synthase (FASN) versus imported) of long chain fatty acids within the cellular pool (7, 8, 14). FASN-synthesized and imported fatty acids which are subsequently elongated are not traditionally modeled using these classical approaches. Thus, we sought to ask if application of ISA would accurately model a range of fatty acid pools that likely have significant contributions from elongation pathways (for example, very long chain fatty acids).

To this end, H1299 lung cancer cells were cultured in DMEM containing isotope label (100% U- $^{13}\text{C}_6$  glucose and 100% U- $^{13}\text{C}_5$  glutamine) for 48h. After labeling, cells were collected and subjected to *in situ* acid methanolysis (12). Fatty acid methyl esters were then extracted, and run on GC-MS to determine the mass isotopomer distributions (MIDs) for individual long chain and very long chain fatty acids (LCFAs and VLCFAs, respectively). ISA was employed to determine the contribution of synthesis and import to the indicated cellular fatty acid pools (7, 15). Our ISA-based algorithm utilizes a grid search approach to determine the parameter values that minimize the sum of squared error (SSE) between the empirical MID and the modeled MID for individual fatty acids in each sample (see supplemental methods for further explanation).

As expected, ISA model fits were excellent for 14 and 16 carbon LCFA species (Figure 1a and Supplemental Figure 1a). However, we observed that ISA model fits deteriorate as fatty acid carbon chains become longer (i.e. 18-24 carbons; Figure 1b and 1c, and Supplemental Figure 1c and 1e). For example, inspection of the best fit for the fatty acid 20:0 revealed that ISA could not find the true FASN-synthesized (referred to hereafter as DNS or *de novo* synthesized) distribution (Figure 1b, blue bracket), and instead fit intermediate masses as a component of the DNS distribution (Figure 1b, red bracket). Additional examples of this ambiguity can be observed in longer fatty acids (e.g., 24:0; Figure 1c, see red and blue brackets, respectively). Similar results were seen with murine BMDMs and primary human fibroblasts (Supplemental Figures 2d-f and 3c-f). Analysis of the sum of squared error (SSE) between the empirical data sets and the ISA model fitting confirmed significant error in the modeled data for fatty acids longer than 16 carbons (Figure 1d). Similar SSE results were seen with murine BMDMs (Supplemental Figure 2g), but the trend was less pronounced in primary human fibroblasts (Supplemental Figure 3d-g). Taken together, these data demonstrate that classical ISA provides accurate modeling of LCFA containing up to 16 carbons, but becomes less accurate as fatty acid chain length increases.

### **Development of FASA, a New Model That More Accurately Defines LCFAs and VLCFA Metabolism in Cells**

Classical ISA modeling assumes that fatty acids are either synthesized by FASN or fully imported. Parameter  $D$  represents the fractional contribution of  $^{13}\text{C}$ -labeled metabolite to the lipogenic acetyl-CoA pool (Figure 2a). Correspondingly,  $1-D$  represents the fractional contribution to the lipogenic acetyl-CoA pool from natural metabolites. Parameter  $g(t)$

represents the percentage (%) of a given fatty acid that accumulates in the fatty acid pool over time that is necessarily fluxed through the synthetic enzymatic machinery (Figure 2a) (7, 16). For simplicity, we designate  $g(t)$  as  $S$  for “synthesized fatty acids” (also defined as *de novo* synthesized by FASN).  $1-g(t)$  defines the naturally labeled fraction of a given fatty acid pool, and is representative of  $I$  for imported fraction of a fatty acid pool under isotopic steady state conditions. The imported pool  $I$  is a mixture of imported and pre-existing lipids under non-isotopic steady state conditions (17).

We reasoned that the intermediate masses observed in the MIDs of VLCFAs (e.g., Figure 1b and 1c) were due to shorter, imported fatty acids that were subsequently elongated to fill VLCFA pools. This elongation flux would result in the incorporation of  $^{13}\text{C}$ -labeled carbons from the acetyl-CoA pool into otherwise unlabeled fatty acids, thereby creating intermediate distributions in the MIDs, which would interfere with accurate model fitting using ISA. To accommodate this elongation pathway flux, we created a new model, Fatty Acid Source Analysis (FASA), that allows for fatty acids to be either synthesized ( $S$ ), imported ( $I$ ), or elongated from imported fatty acid species (designated  $IE_n$ , where  $n$  is the number of elongations after import) from fatty acids as short as 14:0 (Figures 2b, 3a). Incorporation of the imported-elongated parameters ( $IE_n$ ) results in one additional distribution per two-carbon increase in length from 14:0.

In FASA, we also directly modeled the lipogenic acetyl-CoA pool. Multiple turns of the tricarboxylic acid (TCA) can result in a lipogenic acetyl-CoA that contains one carbon from a labeled metabolite and a second carbon from an unlabeled metabolite in a phenomenon we term “carbon shuffling”. This “carbon shuffling” would cause an overestimation of even numbered

ions with an underestimation of odd numbered ions in the synthesized distribution, a problem we observed in the classical ISA model (Figure 1b, red bracket). To ameliorate this issue, instead of modeling the dilution of the  $^{13}\text{C}$ -stable isotope into the acetyl-CoA pool (parameter  $D$ ), we directly modeled the frequency of acetyl-CoAs with 0, 1 and 2  $^{13}\text{C}$ s using parameters  $D_0$ ,  $D_1$ , and  $D_2$ . The same  $D$  from ISA can still be calculated from  $D_0$ ,  $D_1$ , and  $D_2$  (see supplemental methods); however, this addition also allows us to measure changes in carbon shuffling. To determine the metabolic parameter values (e.g.,  $D$ ,  $S$ ,  $I$ ,  $IE_n$ ) that resulted in the best fit for MIDs, we developed a Matlab-based script that uses a constrained gradient descent (Levenberg-Marquardt) to minimize the sum of squared error (SSE) between the empirical and modeled MIDs for each fatty acid in each sample. Monte Carlo replicates with random parameter starting points were performed to ensure the global minimum of the SSEs function was found (see supplemental methods).

Analysis of 14-16 carbon fatty acid MIDs using FASA demonstrated equivalent or slightly improved best fits when compared to classical ISA (Figure 3b). Accordingly, model derived parameters such as  $S$ ,  $I$ , and  $D$  were nearly identical between ISA and FASA (Figure 3c, 3g and Supplemental Figure 1a). Using FASA, we did observe a consistent contribution of elongation parameters ( $IE_n$ ) to the 16:0 and 18:0 pools, indicative of a contribution of fatty acid elongation flux from shorter fatty acids, likely via the activity of ELOVL6 (Figure 3e and Supplemental Figure 1b). Similar results were seen with murine BMDMs (Supplemental Figure 2b-c) and primary human fibroblasts (Supplemental Figure 3b-c).

Importantly, reanalysis of MIDs for VLCFA with FASA resulted in significantly better visual fits when compared to ISA, ameliorating the issues with modeling the intermediate masses (Figure 3d, red and blue brackets). Model derived parameters (e.g.,  $S$  and  $I$ ) were significantly adjusted, and contributions of elongation to the fatty acid pool were now quantifiable. For example, in 20:0, single, double, and triple elongation of unlabeled shorter fatty acids made up a significant portion ( $\approx 30\%$ ) of the pool (Figure 3e). Similar results were seen with murine BMDMs ( $\approx 50\%$ , Supplemental Figure 2d) and primary human fibroblasts ( $\approx 55\%$ , Supplemental Figure 3d). Consistent with better visual fits, the SSE compared to empirical data was significantly lower for 18-carbon or greater fatty acid species using a log likelihood ratio test, indicating that the observed better fits were not solely a function of increased parameter number in our new model (Figure 3f). These results demonstrate the importance of including elongation as a parameter when modeling fatty acids, particularly for fatty acids longer than 16 carbons.

Finally, in applying FASA to H1299 cells, we observed that the modeled values indicating the percentage of synthesized fatty acid carbon originating from  $^{13}\text{C}$ -labeled metabolites (otherwise defined as parameter  $D$ -see above) remained remarkably constant across all LCFA and VLCFA species measured (Figure 3g). Similar results for  $D$  were seen in studies on murine macrophages and primary human fibroblasts (Supplemental Figures 2h and 3h). This observation is consistent with the concept that the acetyl-CoA and malonyl-CoA pools available to both FASN and elongation machinery (i.e. ELOVL1-7), are equivalently labeled from the isotope-labeled metabolite precursors (in this case,  $\text{U-}^{13}\text{C}_6$ -glucose and  $\text{U-}^{13}\text{C}_5$ -glutamine). Thus, we conclude that the acetyl-CoA pool contributing to both the fatty acid synthetic and elongation pathways is behaving as a single, well-mixed pool, rather than distinct pools with different contributions of

isotope label. Although spatially separated acetyl-CoA pools exist within the cell (e.g., cytosolic (1), ER (18), mitochondrial (1), peroxisomal (19), and nuclear (20)), these different pools are either 1) isotopically equivalent to the lipogenic acetyl-CoA pool or 2) do not significantly contribute to fatty acid synthetic processes in the conditions tested here.

### **Modification of FASA to Accommodate Polyunsaturated Fatty Acid Elongation**

In mammals, essential polyunsaturated fatty acids (PUFAs) are not synthesized *de novo* (21), and mammalian cells rely on import of these fatty acids from the diet (e.g. 18:2n-6, 18:3n-3). Upon import, these fatty acids are elongated and/or desaturated to create a wide variety of requisite PUFAs (1). Consequently, classical ISA and MIDA, which are predicated on modeling two distributions (synthesized and imported), are not well suited to model PUFA metabolism (7, 8). Because FASA allows for import and elongation of fatty acids, we thought it possible that FASA would be able to model components of PUFAs metabolism. Furthermore, we designed FASA to allow users to pre-set any model parameter to any specific value *a priori*. For example, one can set the *S* parameter (representing synthesized fatty acids) to zero because mammalian cells cannot *de novo* synthesize n-6 and n-3 PUFAs. Additionally, one can also set the *D* parameters to values previously determined from abundant species (for example, using *D* from 16:0 to model other fatty acids in the same sample). While defining these parameters *a priori* adds additional assumptions, it effectively constrains the parameter space when only a few mass isotopomers are measurable, a common occurrence with PUFA.

With these concepts in mind, we asked if FASA would be capable of modeling n-6 PUFA metabolism in cells. Linoleic acid (18:2n-6) is an essential PUFA that serves as the starting point

for the synthesis of other n-6 PUFA (1). As such, we set the parameters for synthesis ( $S$ ) and import-elongation from 14 and 16 carbons ( $IE_2$ - $IE_3$  for 20-carbon PUFA and  $IE_3$ - $IE_4$  for 22-carbon PUFA) to zero (Figure 4a). We also fixed the  $D_0$ ,  $D_1$ , and  $D_2$  parameter values to reflect the parameters obtained from an abundant, easily modeled fatty acid (e.g., 16:0 or 18:0). In combination, these changes allowed for a single global minimum for the SSE function to be found more easily. Inspection of MIDs generated for n-6 PUFAs 20:4 and 22:4 revealed good visual fits when compared to empirical data (Figure 4b and Supplemental Figure 4a). Similar results could be seen with primary murine macrophages and primary human fibroblasts (Supplemental Figures 5a-b and 6a-b). Correspondingly, model parameters indicated that  $\approx 55\%$  of the pool was imported directly whereas  $\approx 40\%$  of the 22:4 pool was elongated once, and  $\approx 5\%$  was double elongated (Figure 4b).

Unexpectedly, we consistently observed evidence of double elongation in 20:3n-6 pool in several cell lines tested. Inspection of the 20:3n-6 MIDs revealed that the M+4 abundance was consistently and significantly overrepresented (Supplemental Figure 5c and 6c), and in some cases, the M+4 abundance was even greater than that of M+3 (Figure 4d, black bracket). This mass isotopomer distribution indicates a non-zero contribution of double elongation to the 20:3n-6 pool, despite an expectation of only single elongation in this fatty acid pool, based on well described biochemical pathway descriptions of 18:2n-6 fluxing into the 18:3n-6 pool (via desaturation by FADS2), followed by a single elongation into 20:3n-6. We also observed a modest increase in M+2 in 18:2n-6 from labeled samples (20-40% higher than expected for unlabeled 18:2n-6), indicating single elongation into that pool. Therefore, we added an extra import-elongation distribution for these PUFAs (18:2n-6 and 20:3n-6) to accommodate

elongation from 16 carbons when applying FASA (Figure 4d-e). Similar results could be seen with primary murine macrophages and primary human fibroblasts (Supplemental Figures 5c-d and 6c-d).

One potential explanation for double elongation into 20:3 is that 16:2n-6 is present in the serum used in culture, and is elongated after import into the 16:2 pool. However, 16:2n-6 does not appear to be present in FBS (22). An alternative explanation is that 18:2n-6 was imported into the cell, shortened into a 16:2n-6 species, and then subject to flux through the elongation pathway. Taken together, these studies provide proof-of-concept that application of FASA can model PUFAs and can uncover previously unrecognized fluxes of fatty acids within a cell.

### **Determining Minimum Labeling Levels for Accurate Modeling of Elongation Parameters**

One limitation of any stable isotope modeling approach for lipid metabolism occurs when isotope labeling of the lipid of interest is low. As the amount of stable isotope label in the acetyl-CoA pool decreases, the synthesis ( $S$ ) and import-elongated ( $IE_n$ ) distributions will approach the imported ( $I$ ) distribution, making model fitting progressively more difficult. Therefore, we sought to determine the minimal amount of labeling of the acetyl-CoA pool (parameter  $D$ ) required for FASA to effectively fit the distributions in LCFA and VLCFA MIDs.

To this end, H1299 cells were cultured in media containing increasing percentages of  $^{13}\text{C}$ -labeled glucose and glutamine. After the cells were collected, fatty acids were derivatized and analyzed by GC-MS to obtain MIDs. Modeling of MIDs using FASA revealed that model parameter  $D$  behaved in a linear fashion with respect to the percentage of  $^{13}\text{C}$  labeled metabolites in the media

down to approximately 30% ( $D \approx 25\%$ ). Below this level, the relationship between  $D$  and the percentage of  $^{13}\text{C}$  labeled metabolite in the media became non-linear, particularly for the longest fatty acids tested (Supplemental Figure 7a). Accordingly, the  $S$  and  $I$  model parameters (FASN-synthesized and imported, respectively) were consistent down to a  $D$  of  $\approx 30\%$  (Supplemental Figure 7b). However, for elongation parameters ( $IE_n$ ), we observed that a variable level of labeling in the lipogenic acetyl-CoA pool ( $D$ ) was required for consistent determination of elongation parameters. For example, in examining the elongation parameters of 20:0, we observed that the  $IE_1$  parameter consistently modeled down to a  $D$  of  $\approx 30\%$  (Supplemental Figure 7b). In contrast,  $IE_2$  and  $IE_3$  required higher levels of labeling to achieve good fits ( $D \approx 45\%$ ) (Supplemental Figure 7b). Thus, we conservatively conclude that FASA will most consistently model VLCFAs when the lipogenic acetyl-CoA pool labeling is at 45% or greater (Supplemental Figure 7c-d).

### **Application of FASA reveals significant contribution of flux through elongation pathways in fatty acid homeostasis.**

Translation of labeling data and modeling parameters into metabolic information is complex, and depends on both the system and the labeling conditions (17). Interpretation of FASA parameters, as well as parameters from many other stable isotope labeling models, is simplified when measurements are made at isotopic and metabolic steady state (iSS and mSS, respectively) (17). A metabolite pool reaches iSS when its MID remains constant with time, whereas a metabolite pool reaches mSS when its size and fluxes remain constant over time (17). The key advantage for applying FASA when at iSS and mSS is that pre-existing, and therefore unlabeled, pools of fatty acids have been diluted out, and fluxes are constant. This allows us to unambiguously

identify unlabeled fatty acids as imported and to determine the relative contribution of different sources to a fatty acid pool (e.g., FASN-synthesized and imported) (17). While these steady state conditions are hard to ensure in any system, cells cultured over an extended period of time in the presence of stable isotope metabolite are considered to be in pseudo-iSS and pseudo-mSS (17).

To study cells at iSS and mSS pseudo steady state, H1299 cells were cultured in DMEM containing 5% FBS and 100% U-<sup>13</sup>C<sub>6</sub>-glucose for 5 days (approximately 5 cell divisions). Culture media were refreshed every 12 hours, and cells were maintained in a sub-confluent state. After collection, fatty acids were extracted and derivatized and run on GC-MS. MIDs were determined for individual fatty acids and modeled using FASA. In line with our previous data (Figure 3g), *D* was remarkably consistent across all measured saturated fatty acids (SFA) and monounsaturated fatty acid (MUFAs) (Figure 5a). Analysis of individual SFA and MUFA species from 16 to 24 carbons in length revealed that individual fatty acid pools are an admixture of imported, synthesized and imported-elongated fatty acids (Figure 5b). For example, modeling of the 20:0 fatty acid pool indicates that  $\approx 50\%$  of the pool is derived from fatty acids which have been synthesized by FASN and subsequently elongated,  $\approx 15\%$  is imported, and  $\approx 35\%$  are fatty acids which were imported as shorter species (14:0, 16:0, or 18:0) and then fluxed through the elongation machinery ( $IE_1 \approx 20\%$  (18:0 to 20:0),  $IE_2 \approx 15\%$  (16:0 to 20:0), and  $IE_3 \approx 5\%$  (14:0 to 20:0)). Similar patterns were seen in other SFA and MUFA (Figure 5b). This result underscores the importance of using a model that includes not only import-elongation but the possibility of multiple elongations after import, particularly when analyzing longer fatty acids.

In ISA, steady state  $S$  and  $I$  represent the contribution of *de novo* synthesis and import to a particular fatty acid pool (16, 23). In addition, the ratio of  $S$  to  $I$  represents the ratio of the synthetic and import fluxes if two additional assumptions are made, 1) that *de novo* synthesis and import are the only influxes to the pool, and 2) that there is no preferential loss from the pool (17). These concepts can be generalized in FASA; contribution of import and elongation to a particular fatty acid pool can be determined by comparing  $I$  to the sum of the other source parameters (Figure 5c). Relative import and elongation fluxes can also be determined if the same additional assumptions are made (see supplemental methods). For fatty acid pools that are direct products of desaturation instead of elongation (e.g. 18:1n-9), elongation contribution can still be determined, but import will include both direct import and import followed by desaturation. For example, in the 18:1n-9 pool, “import” will include both directly imported 18:1n-9 and imported 18:0 that has subsequently been desaturated. Though the final product of FASN is primarily 16:0, it has been reported to produce 14:0 and 18:0 at lower frequency (1, 5). One challenge that these metabolic pathways create is that ISA and FASA cannot differentiate a FASN-synthesized 18:0 from a FASN-synthesized 16:0 that is subsequently elongated. For simplicity, we assume that with the exception of the 14:0 pool, all FASN products are 16:0. As a result, at iSS and mSS,  $IE_I$  will underestimate the contribution of elongation for 16 carbon fatty acids, while  $1-I$  will overestimate the contribution of elongation for 18 carbon fatty acids (see supplemental methods).

Summation of the fatty acid subject to synthesis and elongation in the SFA and MUFA pools (both long chain and very long chain) revealed that flux through the elongation pathways contributes roughly 50-75% of the 18-carbon species in the cell and 80-95% for 20- to 24-carbon

species (Figure 5d). Examination of n-6 PUFAs revealed that linoleic acid and arachidonic acid were minimally elongated whereas other species (e.g., 22:4) were elongated at least once in approximately 70% of pool (Figure 5d). These data indicate that the elongation pathways provide an important metabolic conduit to meet a cell's fatty acid requirements.

### **Interpretation of FASA Parameters When Applied Pre-Steady State**

Though FASA can provide a significant amount of information about fatty acid origin and flux at steady state, it is difficult to achieve and/or maintain steady state for the required labeling period (often multiple days) in many model systems (17, 23). Thus, we determined what biological information can be ascertained from application of FASA when cells have not achieved isotopic steady state in the fatty acid pools. To this end, H1299 cells were cultured in medium containing 100% U-<sup>13</sup>C<sub>6</sub>-glucose and 100% U-<sup>13</sup>C<sub>5</sub>-glutamine to maximize isotope label into the acetyl-CoA pool for 48h. H1299 cells divided approximately 2-times over this culture period; this time period is sufficient to achieve iSS in the lipogenic acetyl-CoA pool, but not sufficient to achieve iSS for the fatty acid pools of the cells (23). After 48h in culture, cells were counted, lipids extracted, and analysis of MIDs was performed using FASA.

Before iSS in the fatty acid pools is achieved, it is difficult to use FASA or other isotope labeling analysis to determine the contribution of import to a given fatty acid pool, because the unlabeled fatty acid population of the cell is an unknown mixture of newly imported and pre-existing unlabeled fatty acids. We can, however, use FASA pre-steady state to quantify the accumulation of both FASN-synthesized and elongated fatty acids during the labeling period. For example, pre-steady state FASA parameters can be used to determine the accumulation of SFA and MUFA

that were directly elongated from 18 to 20 carbons, including those that remained in the 20 carbon fatty acid pools as well as those that further fluxed through subsequent elongations and/or desaturations. This process is shown schematically in Figure 6a-c.

First, we determined all SFA + MUFA origins that require elongation from 18 to 20 carbons; this analysis included direct products of that elongation step (i.e. 20:0 and 20:1 that were *de novo* synthesized or imported-elongated) as well as the downstream elongation/desaturation products (i.e. 22:0 and 22:1 that were *de novo* synthesized or imported-elongated 2-4 times; 24:0 and 24:1 that were *de novo* synthesized or imported-elongated 3-5 times) (Figure 6a). Multiplying these values by the final measured amount of each fatty acid pool divided by the average cell number on the plate during labeling results in the contributions that each fatty acid made to the total accumulation of 18 to 20 SFA + MUFA elongation products over the labeling period (Figure 6b). Summing these individual contributions gave the total accumulation of 18 to 20 SFA + MUFA elongation products (nmol/1e6 cells) during the labeling period (Figure 6c). This process can be repeated similarly for other elongation steps as well as FASN-synthesized (*S*) for all fatty acids to define the relative contribution of the elongation machinery to fatty acid homeostasis in the cell over the labeling time (Figure 6d-f).

For proof-of-concept, we then applied this approach to H1299 cells which have the sterol regulatory element binding protein (SREBP) transcriptional axis acutely disrupted using a doxycycline-inducible shRNA targeting the SREBP chaperone SCAP (24). The SREBPs are master transcriptional regulators of lipid homeostasis, driving a cassette of genes regulating fatty acid homeostasis and are reliant on SCAP expression for their proper function (25). Cells were

treated with doxycycline for 96h; in the final 48h of doxycycline treatment they were also labeled with 100% U-<sup>13</sup>C<sub>6</sub>-glucose and 100% U-<sup>13</sup>C<sub>5</sub>-glutamine as above. Cells were then collected and analyzed for gene expression and fatty acid content. Knockdown efficiency for SCAP was approximately 90% of control cells, and accordingly, expression of SREBP target genes involved in fatty acid metabolism were also significantly decreased (Figure 7a) (25).

Application of FASA, followed by the analytical approach as described in Figure 5b and c, demonstrated that loss of SREBP activity significantly decreased the accumulation of SFA and MUFAs that were synthesized by FASN and/or fluxed through the elongation machinery (Figure 7b and 7c). A less significant impact of SREBP on PUFA elongation was observed, despite the decreases in the expression of the elongases and desaturases that impact PUFA metabolism in SREBP loss-of-function cells (Figure 7d). Thus, application of FASA under non-steady state conditions can reveal an integrated picture of the net biochemical activity of a cell's fatty acid machinery in response to perturbations, and can offer significantly greater insights than gene expression studies alone.

### **Macrophages Specifically Reprogram Elongation in Response to Inflammatory Stimuli**

Macrophages rapidly reprogram their lipid metabolism in response to inflammatory signals. These changes in metabolism are critical for proper differentiation and function (12, 26, 27). To date, little is known about how these TLR signals influence the fluxes of fatty acid through elongation pathways. To investigate this question, BMDMs were stimulated with a panel of TLR agonists (TLR 2, 3, or 4) for 48h in <sup>13</sup>C-labeling media, followed by fatty acid extraction, derivatization, and injection onto GC-MS. MIDs for LCFA and VLCFA were obtained from

quiescent and activated macrophages and then modeled using FASA. Modeling revealed that TLR2 activation significantly increased the accumulation of labeled SFA and MUFA which had fluxed through FASN and/or the elongation machinery (Figure 8a-b). In contrast, TLR3-stimulation resulted in the opposite metabolic program, with a profound decrease in the accumulation of labelled SFA and MUFA that had fluxed through FASN and/or the elongation pathways (Figure 8a, b). Interestingly, TLR4 stimulation produced more modest changes in accumulation through the FASN and/or elongation pathways, resulting in an elongation phenotype that most resembles that of untreated cells (Figure 8a, b).

Analysis of n-6 PUFAs revealed similarly distinct metabolic reprogramming in response to these different pro-inflammatory stimuli (Figure 8c). In contrast to SFA and MUFA metabolism, TLR3 stimulation resulted in the significant accumulation of n-6 PUFAs that fluxed through elongation pathways into the 22:4 pool. TLR2 and 4 variably impacted n-6 PUFA accumulation due to elongation pathways, with minimal to modest changes depending on the step. Of note, we find that gene expression studies alone would not be able to predict the complex accumulation pattern we observed in the reprogramming of fatty acid elongation machinery. For example, we find that TLR2 activation did not significantly change expression levels of *Elovl6* and *Elovl3* (Figure 8d), while our model indicated significant accumulation of fatty acids which are the products of these enzymes. In other cases, the gene expression and modeling data are concordant, such as upregulation of *Elovl2* in response to TLR3 activation (Figure 8d) and the accumulation of *Elovl2* product 22:4. In combination, these data demonstrate that pro-inflammatory stimuli can reprogram the fluxes of fatty acids through the elongation pathways,

but that there is a high degree of specificity in the changes to elongation by different inflammatory signals.

Finally, we asked if the reprogramming of elongation driven by TLR3 stimulation could also be observed during viral infections. BMDMs were challenged with the  $\gamma$ -herpes virus MHV68 (MOI=1) in labeling media for 48h before lipids were collected and analyzed as above. We observed a similar pattern of elongation in PUFAs to that of TLR3 stimulated macrophages (Figure 8e, f). Likewise, gene expression studies also indicated a significant upregulation of *Elovl2* in response to infection (Supplemental Figure 8b), suggesting that reprogramming the elongation machinery is a physiologic response by the host to viral infection of cells. Taken together, these studies illustrate how our new model can be applied to determine how fatty acid homeostasis is reprogrammed in cells in response to metabolic or inflammatory signals.

## Discussion

Understanding how lipids flux through metabolic pathways under normal and disease states is of significant importance. Herein, we developed a new model, Fatty Acid Source Analysis (FASA), which better represents the flow of fatty acids through cellular metabolic pathways. FASA provides the ability to analyze synthesis, elongation, and import of fatty acids ranging from 14-24 carbons in length and 0-4 double bonds, covering the majority of fatty acids found in animal cells. FASA improves on previous systems by including three additional features relevant to modeling cellular fatty acid metabolism. First, we incorporate elongation of imported fatty acids. Second, we directly model the lipogenic acetyl-CoA pool. Third, we allow users to set any parameter *a priori*, facilitating the modeling of fatty acids (i.e. PUFA) and conditions (i.e. TLR3 stimulation) with little or no *de novo* synthesis. In combination, these improvements have allowed application of FASA to uncover novel aspects of cellular fatty acid metabolism and to delineate the movement of fatty acids through the elongation pathway under steady state or in response to changes in metabolic and inflammatory signals. We anticipate that this model will be useful for further interrogation of cellular fatty acid metabolism in a wide variety of normal and disease models.

In the current study, we demonstrate how the new model can be applied to uncover novel or previously unmeasured aspects of cellular fatty acid metabolism. For example, we show that elongated fatty acids can make up a large majority of 20- to 24-carbon SFA and MUFA pools under standard culture conditions. We also find that a significant fraction of these VLCFAs are derived from the FASN-synthesized pool of fatty acids. Thus, we provide evidence for considerable metabolic flux through the elongation machinery to deliver requisite fatty acids to

cells in culture. We also observed surprising fluxes of fatty acids. In modeling PUFAs, we routinely measured M+4 label in 20:3n-6, consistent with double elongation from 16:2. This event can be observed both in H1299 cells and, in particular, in the TLR3 activated macrophages. The origin of 16:2 in these systems remains to be determined. Nor is it clear which elongase enzyme(s) would be involved in the flux of 16:2. It is important to note that the exact specificity of many of the elongases remains poorly defined, and we outline the elongation enzymes as they are classically described. However, the relative promiscuity of ELOVLs complicate assigning a specific elongation protein to an elongation product. We anticipate that application of FASA will allow for future mechanistic work on these very interesting and poorly understood enzymes. Finally, we provide proof-of-concept studies that this model can be applied to elucidate the impact of metabolic reprogramming on the movement of fatty acids in dynamically regulated systems, such as TLR induced metabolic reprogramming.

One of the largest challenges in stable isotope labeling is the appropriate interpretation of often complicated MIDs (17). Even when models, such as the one developed here, are used to determine the fractional contribution of different sources to the metabolite pool, the metabolic implications must be carefully interpreted. For the current model, examining cells at metabolic and isotopic steady states will result in the simplest analysis. In this case, the key parameters for elongated fatty acids (18-24 carbons) are  $I$  and  $1-I$ , which represent the contribution of import and elongation to a particular fatty acid pool, respectively. These parameters could also be combined with absolute quantitation of the fatty acid of interest to yield net fluxes of synthesis, import, and elongation. However, one should be aware that these calculations are predicated on assumptions about the system; it will be important in applying this model to understand these

assumptions and be aware of how specific elements of their model may impact interpretation of data. Additionally, the model is unable to detect some fatty acid modification events, such as shortening,  $\beta$ -oxidation, or futile cycles of elongation and shortening; accordingly, these changes would not be visible in flux calculations. Thus any flux calculations determined using this modeling approach should be considered representative of the “net” flux of the system. It is our expectation that, as this model is applied to more model systems, additional metabolic parameters will be incorporated to improve the model, and eventually approach absolute rate calculations for these complicated fatty acid metabolic pathways.

In many systems, achieving metabolic and isotopic steady state is not practically achievable. However, as we and others have shown, useful biological data can still be obtained (Figures 6-8) (17). Information about the contribution of fatty acid import may be difficult to obtain due to the confounding factor of cells containing pre-existing unlabeled fatty acid pools. Nevertheless, accumulation of isotope label in newly synthesized and imported then elongated fatty acids can still be easily measured, providing a quantitative assessment of the accumulation of isotope label containing fatty acids over the experimental period. Thus, it is possible to define the general flow of fatty acids through the synthesis elongation pathways, providing evidence for underlying changes in flux. However, these values must be treated with caution. Similar to steady state studies, one cannot assess all of the modifications to fatty acids that may be occurring (e.g.,  $\beta$ -oxidation) or the flow into unmeasured pools. As a result of these confounding factors it is possible, and indeed likely, that the non-steady state accumulation described here will be an underestimation of the absolute enzymatic flux. We recommend that additional studies, such as gene expression or protein expression studies, be undertaken in dynamic systems to provide

complementary information. The issue of flux underestimation could potentially be ameliorated through shorter labeling times to approach true enzymatic rates, but this approach becomes technologically challenging, as isotope labeling of synthesized or elongated fatty acids becomes more difficult to measure due to scarcity of the newly labelled fatty acid product. An alternate approach would involve further modifying the model to decrease unaccounted loss from  $\beta$ -oxidation and export. Though FASA does come with the aforementioned caveats, to our knowledge this is the most complete and accurate way to measure *de novo* synthesis, elongation, and import, containing significant improvements over radioassays and other stable isotope assays (16).

Finally, one assumption common to ISA, MIDA, and the current method is that the acetyl-CoA pool contributing to lipogenesis will have a uniform labeling pattern (7, 8). FASN is the major source of 14-16 carbon saturates, and the elongases (ELOVL1-7) are the major source of 18-24 carbon fatty acids (1). Given that FASN is a cytosolic enzyme and that ELOVLs are embedded in the ER, it is not unreasonable to assume that the cytosolic acetyl-CoA pool is the major lipogenic acetyl-CoA pool in the cell (1). Though other groups have identified conditions in which the mitochondrial (19), nuclear (20), or peroxisomal (19) acetyl-CoA pools can differ in labeling pattern from that of the cytosolic acetyl-CoA pool, the contribution of those organelles to *de novo* synthesis is often relatively small (1). Furthermore, the data from FASA is consistent with the hypothesis that the lipogenic acetyl-CoA is behaving as a single, well-mixed pool. The *D* values calculated independently for 14-24 carbon SFAs and MUFAs are remarkably consistent, indicating that this assumption is valid (Figures 3g and 5a, Supplemental Figures 2h, 3h). However, it is possible that this assumption would not hold true with all cell lines or culture

conditions. Consequently, it will be important to validate that all analyzed fatty acids from a single condition yield similar  $D$  values when different experimental systems are used. We show that successful application requires a fairly significant level of labeling in the acetyl-CoA pool ( $\approx 45\%$ ) to obtain good fits for the data. Thus, it will also be important for those applying FASA to ensure that manipulations do not reduce labeling within the lipogenic acetyl-CoA pool below recommended levels and/or to develop alternative strategies to ensure appropriate levels of isotope labeling (i.e. use both glucose and glutamine labeling).

In conclusion, we provide herein a novel model, FASA, that allows for in depth characterization of fatty acid elongation in cells. Using FASA, we have demonstrated that fatty acid elongation pathways significantly contribute to LC and VLCFA homeostasis of cells. We also show that these pathways are dynamically and specifically regulated by different inflammatory signals, suggesting an importance in regulating these pathways during responses to different classes of pathogens. We expect that application of this new method will continue to uncover novel aspects of fatty acid metabolism and be useful to a wide variety of fields endeavoring to elucidate how fatty acid homeostasis impacts cellular fate and function.

## Supplemental Methods

### Steady State and FASA Parameter Definitions

We define metabolic steady state (mSS) as the point at which per cell fluxes and pool sizes for a given metabolite remain constant for the average cell in a population (17). We define isotopic steady state (iSS) as the point at which MIDs remain constant for a given metabolite (17). mSS and iSS for fatty acids can be approximated by culturing cells in a sub-confluent state in stable isotope-labeled media for enough that the original fatty acids have been diluted out (17, 23). In an idealized system (mSS, no fatty acid losses, acetyl-CoA pool reaches iSS within a few hours), 5 divisions in is sufficient to dilute pre-existing fatty acid contribution to below 5%. In practice, losses may cause iSS to be reached more quickly.

For FASA at mSS and iSS,  $I$  represents the contribution of import for a given fatty acid. If fatty acid shortening is non-negligible,  $I$  will be a mixture of directly imported fatty acid and imported-shortened fatty acid.

### Log-Likelihood Ratio Test

The log-likelihood ratio test (LLRT) was used to compare the goodness of fit between FASA and ISA, as ISA can be considered to be a special case of FASA. p-values were determined using the test statistic  $T$  and the right-tailed chi-square distribution with degrees of freedom  $f$  as defined below.

$$T = \frac{SSE_{ISA} - SSE_{FASA}}{\sigma^2}, f = m_{FASA} - m_{ISA}$$

$$T = 2[\text{LogL}(FASA) - \text{LogL}(ISA)] = 2\left[\frac{SSE_{ISA}}{2\sigma^2} - \frac{SSE_{FASA}}{2\sigma^2}\right], f = m_{FASA} - m_{ISA}$$

$SSE_n$  represents the sum of squared errors for the best fit using model  $n$ .  $\sigma$  represents the standard deviation of the individual mass isotopomers in an MID of a sample injected 20 times (a measurement of instrument noise).  $m_n$  represents the number of parameters in model  $n$ .

### Calculating $D$ from $D_0$ , $D_1$ , and $D_2$

When using FASA,  $D$ , the percent contribution of stable isotope-labeled metabolites to the lipogenic acetyl-CoA pool, is calculated from the directly modeled parameters  $D_0$ ,  $D_1$ , and  $D_2$  using the following formula.

$$D = \frac{.5D_1 + D_2 - q}{e - q}$$

$q$  represents the  $^{13}\text{C}$  enrichment of natural metabolites (.011), while  $e$  represents the  $^{13}\text{C}$  enrichment of stable isotope-labeled metabolites (.99). Note that for both ISA and FASA, as the acetyl CoA pool approaches iSS,  $D$  will transition from representing direct contribution of stable isotope-labeled metabolites (e.g.  $^{13}\text{C}$  glucose to  $^{13}\text{C}$  acetyl-CoA) to both direct and indirect contributions (e.g.  $^{13}\text{C}$  glucose to  $^{13}\text{C}$  amino acids to  $^{13}\text{C}$  acetyl-CoA).

### Calculating Average Cell Number During the Labeling Period

Average cell number during the labeling period ( $c_{avg}$ ) is calculated assuming exponential growth between starting and final cell counts ( $c_i$  and  $c_f$ , respectively) using the following formulae.

$$c_{avg} = \frac{c_i \theta \left( \frac{t_f}{2^\theta} - \frac{t_i}{2^\theta} \right)}{\ln 2 (t_f - t_i)}, \text{ where } \theta = \frac{t \ln 2}{\ln \frac{c_f}{c_i}}$$

$\theta$  represents the exponential doubling time, and  $t_f$  and  $t_i$  represent final and initial times, respectively.

## Calculating Accumulation of FASN and Elongation Products Pre-iSS Using FASA

### Parameters

FASA pre-steady state parameters can be used to quantify the accumulation of both DFP and elongated fatty acids during the labeling period. Note that SFA and MUFA of the same length were combined in this analysis because in general the relevant elongases are similar (1, 6). For a particular elongation step, we first determined all FA origins that require having passed through that elongation step to exist (see tables below).

	FASN	16=>18	18=>20	20=>22	22=>24
14:0	S				
16:0	S				
16:1n-7	S				
18:0	S	S, IE1-IE2			
18:1n-9	S	S, IE1-IE2			
18:1n-7	S	S, IE1-IE2			
20:0	S	S, IE2-IE3	S, IE1-IE3		
20:1*	S	S, IE2-IE3	S, IE1-IE3		
22:0	S	S, IE3-IE4	S, IE2-IE4	S, IE1-IE4	
22:1n-9	S	S, IE3-IE4	S, IE2-IE4	S, IE1-IE4	
24:0	S	S, IE4-IE5	S, IE3-IE5	S, IE2-IE5	S, IE1-IE5
24:1n-9	S	S, IE4-IE5	S, IE3-IE5	S, IE2-IE5	S, IE1-IE5

	16=>18	18=>20	20=>22
18:2n-6	IE1		
20:3n-6	IE2	IE1-IE2	
20:4n-6		IE1	
22:4n-6		IE2	IE1-IE2

All of the fatty acids measured and used the accumulation experiments are listed in these tables. Note that the 20:1 MID was a sum of three peaks; 20:1n-9 was identified using a standard, and the other two species were presumed to be 20:1n-11 and 20:1n-7 based on relative retention time and mass spectra. 18:3n-6 was not abundant enough to be quantified, which has been previously reported for mammalian cells cultured in FBS (22). Also note that n-6 PUFA beyond 22:4 were not modeled due to lack of signal. It is possible that including these fatty acids in our PUFA accumulation calculations could change results, but we think it unlikely, given that these products are a) low abundance and/or b) direct products of desaturation or beta oxidation, suggesting that the contribution of elongation would be low.

Multiplying the selected parameter values by the final amount of each FA divided by the average cell number on the plate during labeling resulted in the contributions that each FA made to the total accumulation of elongation products through a particular elongation step over the labeling period. Summing these individual contributions gave the total accumulation of elongation products for a particular elongation step (nmol/1e6 cells) during the labeling period. This process was the same for DFP, except that only *S* for all FA was used.

Though the final product of FASN is primarily 16:0, it has been reported to produce 14:0 and 18:0 at lower frequency (1, 5). One challenge this creates is that, for example, ISA and FASA cannot differentiate a FASN-synthesized 18:0 from a FASN-synthesized 16:0 that is subsequently elongated. For simplicity, we assume that with the exception of the 14:0 pool, all FASN products are 16:0. When applying FASA pre-steady state, calculation of the accumulation of FASN products will not be affected, as we assume that any molecule comprised

of all carbons from the lipogenic acetyl CoA pool was synthesized by FASN (regardless of whether the direct FASN product was 14:0, 16:0, or 18:0). The accumulation of 14 to 16 elongation products (SFA+MUFA) will be underestimated because our calculations do not include the elongation of FASN-synthesized 14:0. The accumulation of 16 to 18 elongation products (SFA+MUFA) will be overestimated because our calculations includes direct FASN synthesis of 18:0.

### **Creation of Inducible-shRNA Cell Lines**

Plasmids were transfected with either Lipofectamine 2000 (Invitrogen) or DNAfectin 2100 (Lambda Biosciences). Oligonucleotides were annealed and ligated into pENTR<sup>TM</sup>/H1/TO vector (Invitrogen #K4920-00) following the BLOCK-iT<sup>TM</sup> Inducible H1 RNAi Entry Vector Kit manual. Resulting shRNA constructs were recombined into pLentipuro/BLOCK-iT-DEST using Gateway<sup>®</sup> LR Clonase II<sup>®</sup> (Invitrogen #11791-020). pLentipuro/BLOCK-iT-DEST is a modification of pLenti4/BLOCK-iT-DEST (Invitrogen #K4925-00) wherein the SV40 promoter/zeocin resistance cassette was replaced with the human PGK promoter/puromycin resistance gene and the cPPT/WPRE elements were added, and was kindly provided by Dr. Andrew Aplin (Thomas Jefferson University, Kimmel Cancer Center). Recombinant lentiviruses were packaged in 293FT cells (Invitrogen #R700-07) by co-transfecting  $9 \times 10^6$  cells with 4  $\mu\text{g}$  each of lentivirus plasmid, and packaging plasmids pLP1, pLP2, and pLP/VSV-G (Invitrogen #K4975-00), using 48  $\mu\text{l}$  FuGENE<sup>®</sup>6 (Promega #E2691, Fitchburg, Wisconsin) as a transfection reagent. Viral supernatants were collected 72 hours after transfection. Indicated cells were transduced with viral supernatant for 72 hours, followed by selection with puromycin (2  $\mu\text{g}/\text{ml}$ ) for 10 days. The doxycycline induction of knockdown is control by the Tet repressor (TetR)

protein expressed from the pLenti0.3/EF/GW/IVS-Kozak-TetR-P2A-Bsd vector, which was constructed by Dr. Ethan Abel and was kindly provided by Dr. Diane M. Simeone (University of Michigan, Translational Oncology Program).

### Non-Elongation Model

The distribution of heavy carbons incorporated into a lipid with  $N$  total carbons,  $L_N(n|q, s, p, e)$ , was modeled as a multinomial mixture of two distributions: synthesized,  $C_N(n)$ , and non-synthesized,  $B_N(n)$ , lipid (Eqs. 1), as described previously in Williams et al. These distributions are functions of total carbons in the lipid ( $N$ ), background  $^{13}\text{C}$  abundance ( $q$ ), amount of *de novo* synthesis ( $s$ ), usage of glucose as an AcCoA source ( $p$ ), and  $^{13}\text{C}$  enrichment of heavy glucose ( $e$ ). Non-synthesized lipids can be simply modeled as a binomial with  $N$  trials and success rate  $q$ ,  $B_N(n|q)$ , as each carbon has an independent probability  $q$ , of being a heavy isotope. Because synthesized lipids are built using 2-carbon blocks of AcCoA, that distribution is modeled as a sum of  $\frac{N}{2}$  2-carbon-units, each described as i.i.d. random variables  $A(q, p, e)$ . The number of heavy carbons in each 2 carbon units is modeled as a mixture of two binomial distributions, with success rates  $e$  for AcCoA originating from glucose, and  $q$  for all other sources (Eq. 1c). The parameter  $e$  is known *a priori* and maximum likelihood estimates (MLE) of  $q$  can be calculated from control cell lines grown with unlabeled media. The distribution of  $^{13}\text{C}$  incorporated into lipid, as measured from GC/MS, was used to calculate maximum likelihood estimates for  $p$  and  $s$  in each cell line and replicate.

$$L_N(n|q, s, p, e) = s * C_N(n|q, p, e) + (1 - s) * B_N(n|q) \quad (1a)$$

$$C_N(q, p, e) = \sum_1^{\frac{N}{2}} [A(q, p, e)] \quad (1b)$$

$$A(n|q, p, e) = p * B_2(n|e) + (1 - p) * B_2(n|q) \quad (1c)$$

Small corrections are made to account for the possible incorporation of  $^{13}\text{C}$  in the methylation of lipids in GC/MS processing.

### Elongation Model

We expand on the model described above to account for intracellular remodeling and modification of FAs. To account for elongation of existing FAs, we treat the distribution of heavy carbon incorporation as a slightly more complex mixture of distributions: the fully-synthesized, and non-synthesized ( $C_N(n)$  and  $B_N(n)$ , respectively), distributions, as well as several elongated distributions,  $E_N(n)$  (Eq. 2a). Because a synthesized FA that is modified to a longer form is indistinguishable from a fully synthesized version of the longer FA, here we only consider elongation of scavenged FAs. Therefore, the multinomial distribution of a  $N$ -carbon FA after undergoing  $i$  elongations ( $E_N(q, \vec{p}, i)$ ) is the sum of the binomial distribution (of the original FA), and a "synthesized" distribution of  $i$  AcCoAs (Eq 2b). The relative amount of fully synthesized, scavenged, and elongated FAs is defined by  $\vec{s}$ , where  $s_{\text{synth}}$  is the amount of fully synthesized lipid, and  $s_i$  is the amount of lipid that has been elongated by  $i$  AcCoAs. In this model, we do not consider elongation of lipids shorter than myristoleate.

Additionally, to account for remodeling of the AcCoA pool, the relative abundance unlabeled, single-, and double-labeled AcCoA are defined explicitly, as  $\vec{p} = [p_0, p_1, p_2]$ . This therefor changes the formulation of the synthesized distribution to  $C_N(\vec{p})$  as described by Eq. 2c. As in the non-elongation model, small corrections are made for the possible incorporation of  $^{13}\text{C}$  in the methylation of lipids in GC/MS processing. Based on these models, maximum likelihood estimates are acquired for the  $(M+2) \times 1$  parameter vector,  $\vec{b} = [p_0, p_1, s_0, s_1, \dots, s_M]$ , using an iterative optimization algorithm. To ensure convergence to the global maxima, each data set is fit multiple times with random initial conditions.

$$L_N(n|q, \vec{s}, \vec{p}) = s_{\text{synth}} * C_N(n|\vec{p}) + s_0 * B_N(n|q) + \sum_{i=1}^M s_i * E_N(n|q, \vec{p}, i) \quad (2a)$$

$$\vec{s} = [s_{\text{synth}}, s_0, s_1, \dots, s_M], \text{ where } M = \frac{N - 14}{2}$$

$$E_N(q, \vec{p}, i) = B_{N-2*i}(q) + C_{i*2}(\vec{p}) \quad (2b)$$

$$C_N(\vec{p}) = \sum_1^{\frac{N}{2}} [A(\vec{p})], \text{ where } A(n|\vec{p}) = \begin{cases} p_0 & \text{if } n = 0 \\ p_1 & \text{if } n = 1 \\ p_2 & \text{if } n = 2 \end{cases} \quad (2c)$$

# Figures

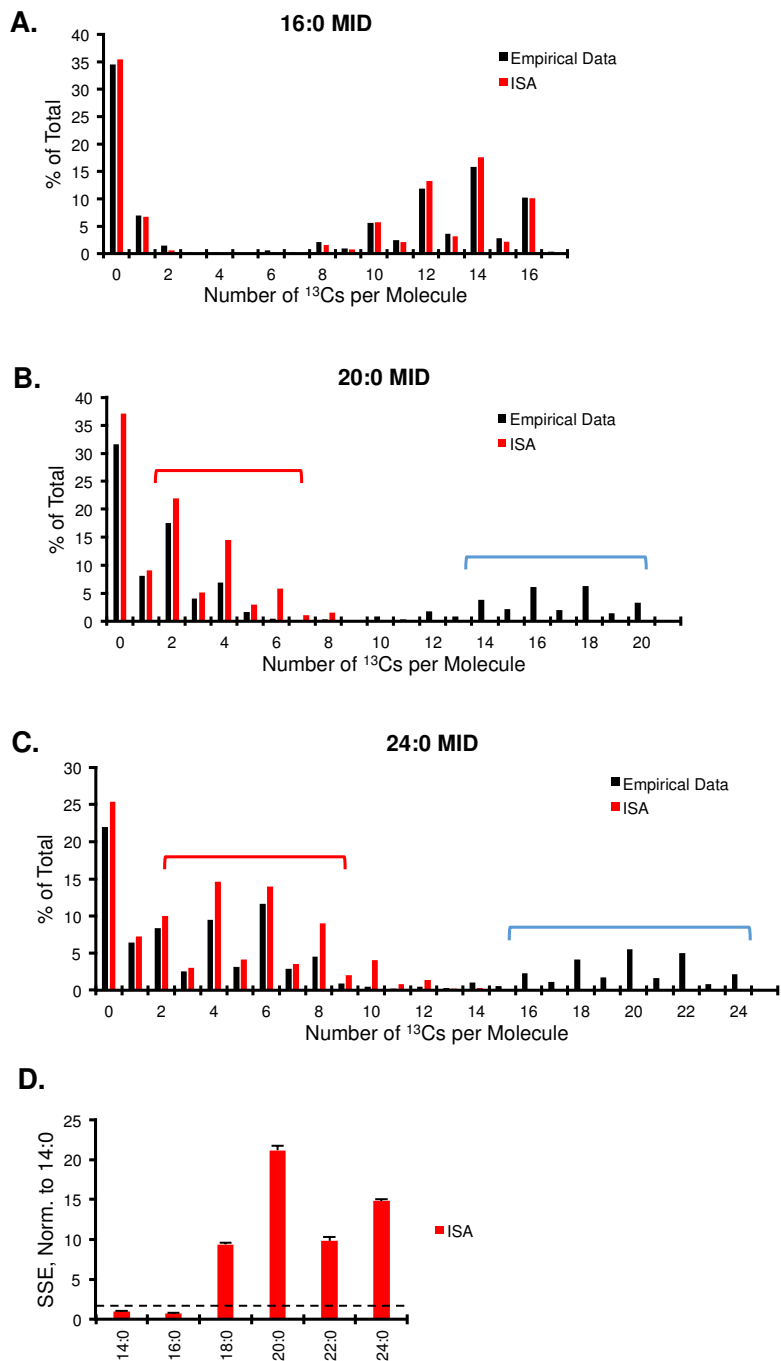


**Figure 1. Traditional ISA Can Yield Suboptimal Fits for Fatty Acids Containing 18-24 Carbons.**

H1299 cells were cultured for 48 hours in DMEM containing 2% FBS, 100% U-<sup>13</sup>C<sub>6</sub>-glucose, and 100% U-<sup>13</sup>C<sub>5</sub>-glutamine. After labeling, cells were collected, derivatized, and analyzed as described in materials and methods. Representative Mass Isotopomer Distributions (MIDs) for indicated fatty acids (in black) and modeled data using Isotopomer Spectral Analysis (ISA, in red). Red brackets indicate overestimation of empirical data by ISA modeling and blue brackets indicate underestimation. A) Representative empirical and ISA-derived MIDs for 16:0. B) Representative empirical and ISA-derived MIDs for 20:0. C) Representative empirical and ISA-derived MIDs for 24:0. D) ISA Sum of Squared Error (SSE) for indicated fatty acids normalized to 14:0. Values represent the average +/- standard deviation of biological quadruplicates.

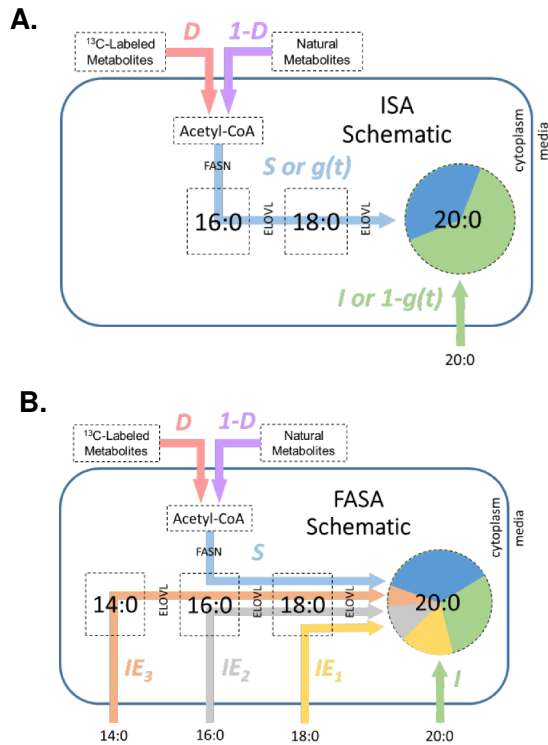


**Figure 2. Schematic of ISA and FASA Models.**

Schematic for traditional Isotopomer Spectral Analysis- ISA (A) and Fatty Acid Source Analysis –FASA (B).  $^{13}\text{C}$ -labeled and natural metabolites flow into the lipogenic acetyl-CoA pool. The relative contribution of  $^{13}\text{C}$ -labeled metabolites to the lipogenic acetyl-CoA pool is defined as parameter  $D$ , whereas the relative contribution of natural metabolites is defined as  $1-D$ . Saturated fatty acids (e.g., 16:0 SFA) are generated by the enzymatic action of Fatty Acid Synthase (FASN) and the accumulation of labeled SFA in the SFA pool is defined as  $g(t)$  or  $S$ . Imported SFA into this pool is defined as  $1-g(t)$  for ISA or  $I$  parameter in FASA. For FASA, imported fatty acids that are subsequently enter the elongation pathways are defined by parameter  $IE_n$ .

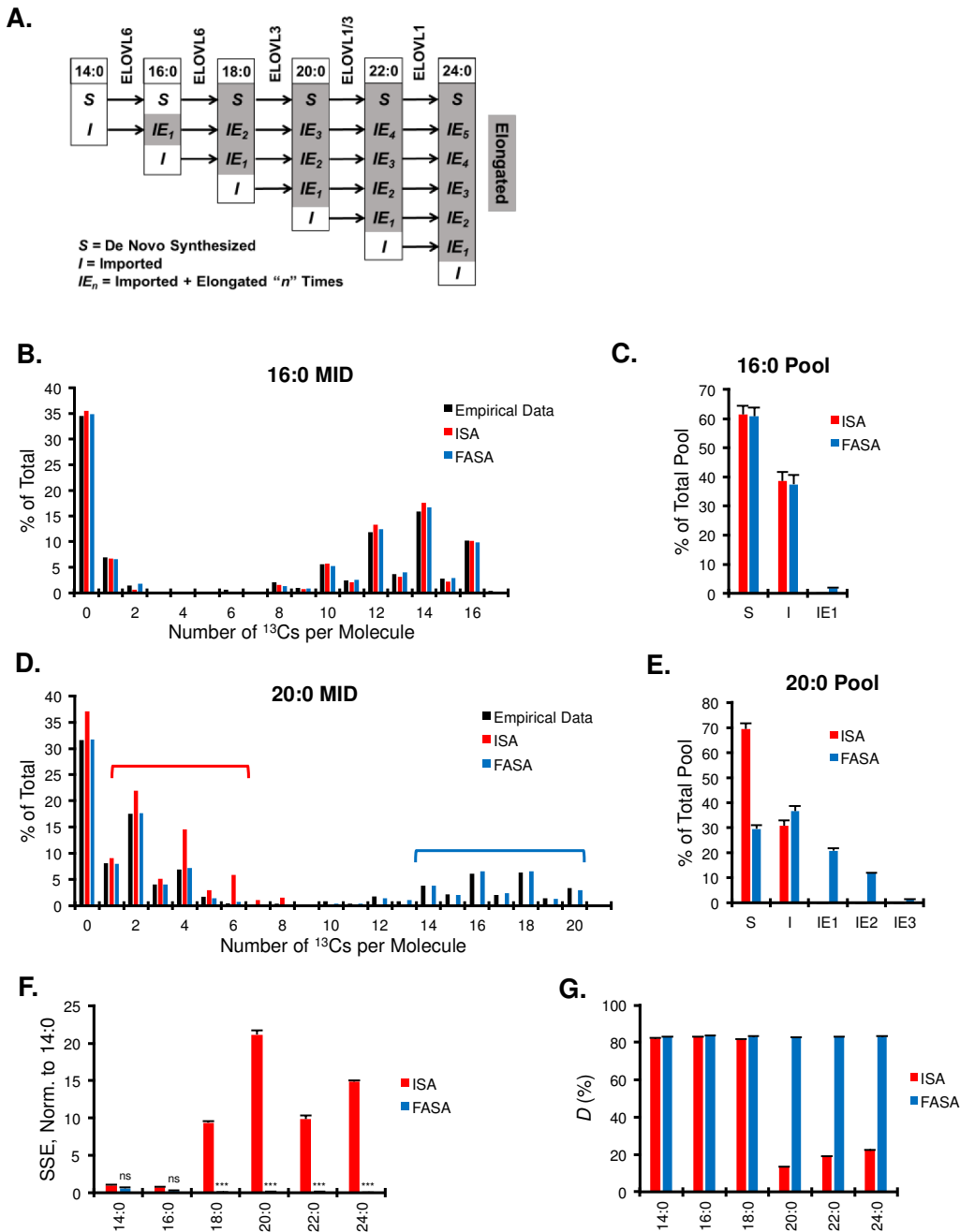


**Figure 3. FASA Significantly Improves Fits for Fatty Acids Containing 18-24 Carbons.**

H1299 cells were cultured for 48 hours in DMEM containing 2% FBS, 100% U-<sup>13</sup>C<sub>6</sub>-glucose, and 100% U-<sup>13</sup>C<sub>5</sub>-glutamine. After labeling, cells were collected, derivatized, and analyzed as described in materials and methods. A) Saturated Fatty Acid (SFA) elongation schematic for

FASA. Representative Mass Isotopomer Distributions (MIDs) for indicated fatty acid (in black) and modeled data using Isotopomer Spectral Analysis (ISA in red) and Fatty Acid Source Analysis FASA in blue). B) Representative empirical, ISA-derived, and FASA-derived MIDs for 16:0. C) Contributions parameters for 16:0 pool. D) Representative empirical, ISA-derived, and FASA-derived MIDs for 20:0. Red brackets indicate overestimation of empirical data by ISA modeling and blue brackets indicate underestimation. These over- and underestimations are corrected by FASA modeling. E) Contributions parameters for 20:0 pool. F) Sum of Squared Error (SSE) for ISA and FASA, normalized to 14:0. G) Acetyl-CoA enrichment parameter (*D*) for indicated fatty acids using ISA (red) or FASA (blue). Data shown for MIDs are representative singlets of biological quadruplicates. Data shown for pool contribution parameters, SSEs, and *D* are the average +/- standard deviation of biological quadruplicates. \*\*\*  $p \leq .001$  using log-likelihood ratio test (see supplemental methods for additional detail).

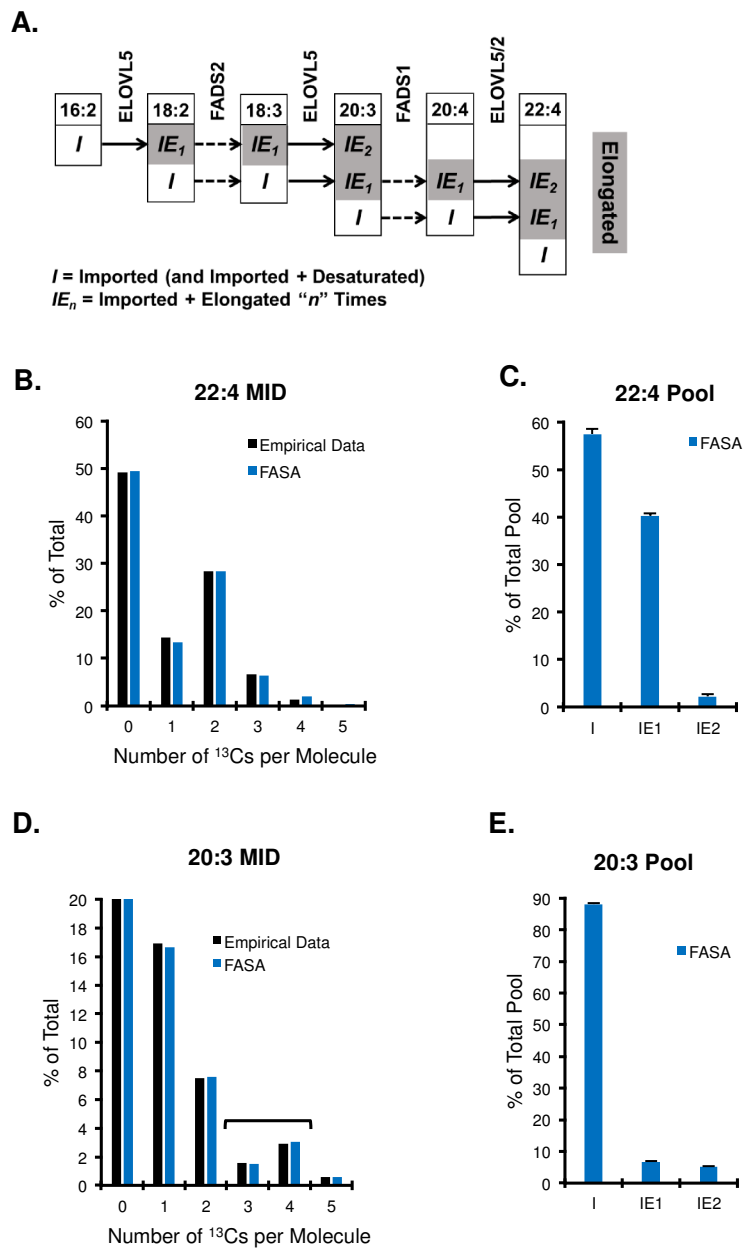


**Figure 4. FASA Provides Excellent Fits for Polyunsaturated Fatty Acids.**

H1299 cells were cultured for 48 hours in DMEM containing 2% FBS, 100% U-<sup>13</sup>C<sub>6</sub>-glucose, and 100% U-<sup>13</sup>C<sub>5</sub>-glutamine. After labeling, cells were collected, derivatized, and analyzed as described in materials and methods. A) n-6 PUFA elongation schematic for FASA. B) Representative MID and FASA modeling for 22:4n-6. C) Contribution parameters defined by

FASA for the 22:4n-6 pool. D) Representative MIDs and FASA modeling for 20:3n-6. Black bracket highlights higher than expected M+4 in MID for 20:3. E) Contribution parameters defined by FASA for 20:3n-6 pool. Data shown for MIDs are representative singlets. Data shown for pool contribution parameters are the average +/- standard deviation of biological quadruplicates.

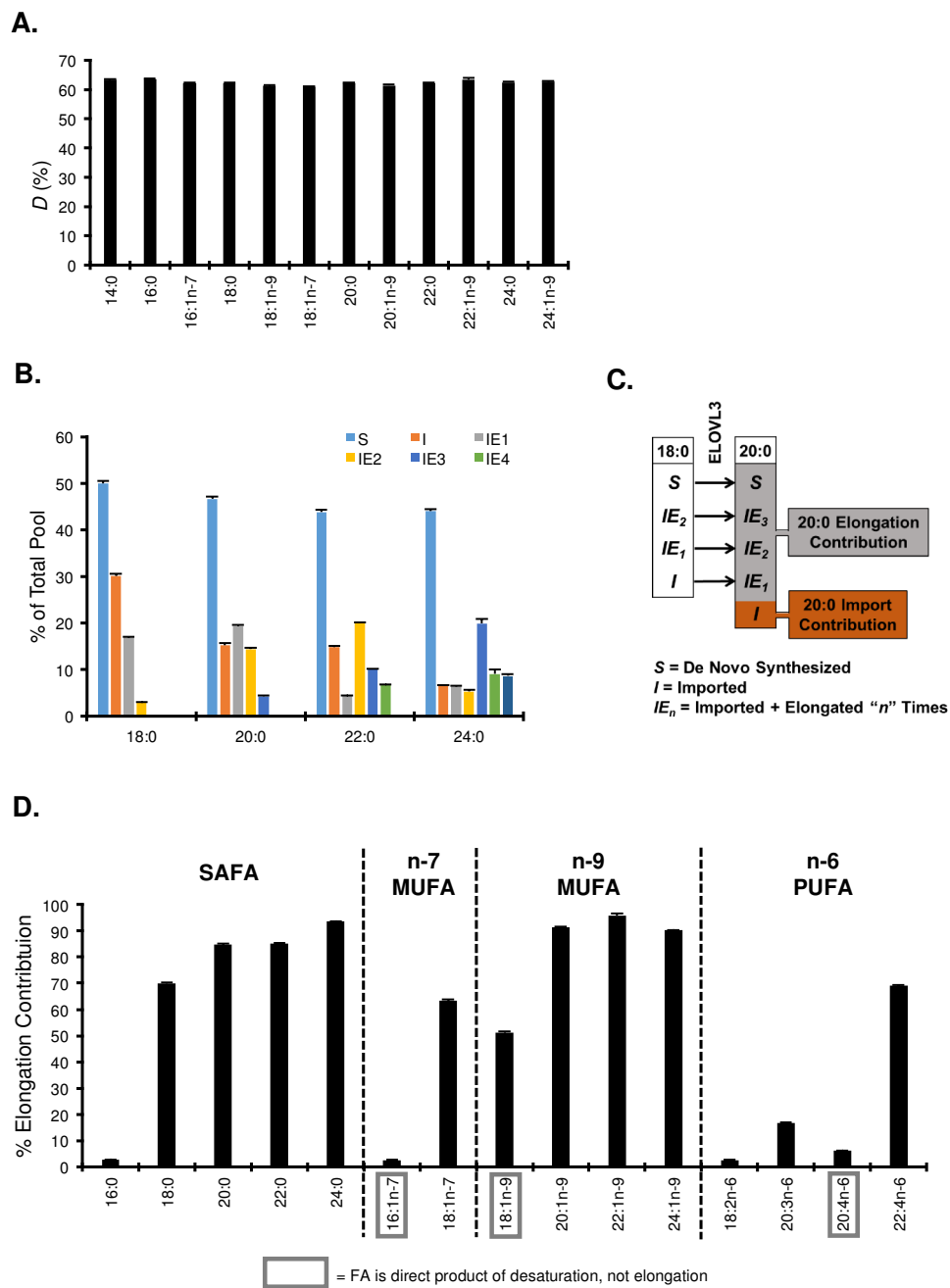


**Figure 5. Application of FASA to Cells at Steady State Reveals a Significant Role for Elongation.**

H1299 cells were cultured in a subconfluent state for 5 days in DMEM containing 5% FBS and 100% U-<sup>13</sup>C<sub>6</sub>-glucose. After labeling to steady state, cells were collected, derivatized, and

analyzed as described in materials and methods. A) *D* for the independently modeled SFA and MUFA. B) Contribution parameters for selected SFA modeled by FASA. C) Diagram for determining elongation and import contribution for 20:0. D) Elongation contribution for indicated saturated, monounsaturated and polyunsaturated fatty acids. Note that for 16:0 and 16:1n-7, *S* is not considered elongated, whereas for 18:0 and 18:1n-9, *S* is considered elongated (see supplemental methods for additional detail). Data shown are the average +/- standard deviation of biological triplicates.

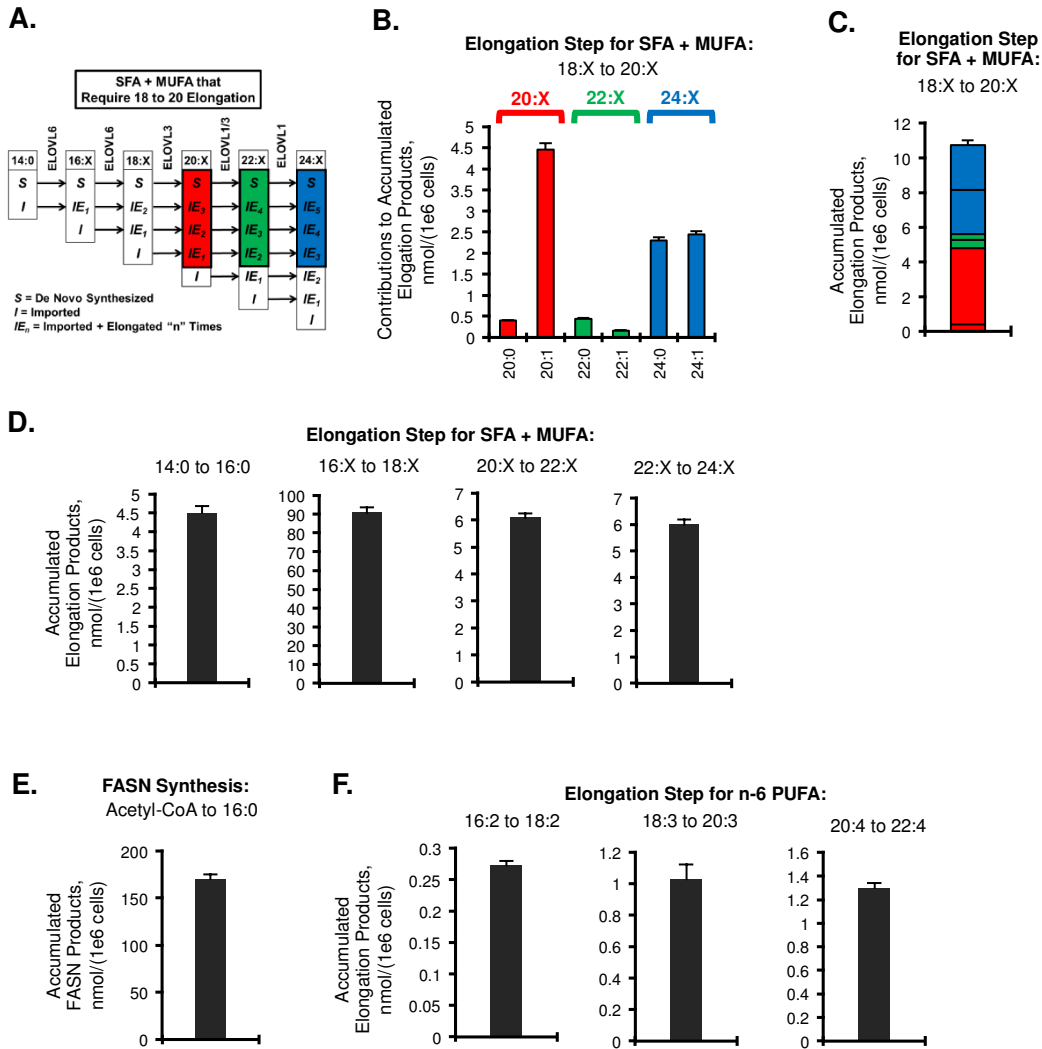


**Figure 6. Interpretation of FASA Parameters When Applied Pre-Steady State.**

H1299 cells were cultured for 48 hours in DMEM containing 5% FBS. These cells were then labeled for 48 hours in DMEM containing 100% U-<sup>13</sup>C<sub>6</sub>-glucose and U-<sup>13</sup>C<sub>5</sub>-glutamine, 5% FBS. After labeling, cells were derivatized and analyzed as described in materials and methods. When applying FASA, values for *D* were fixed using results for 16:0 to facilitate modeling. Values represent average ± standard deviation of biological quadruplicate. A) Schematic for which SFA and MUFA origins require 18 to 20 elongation. X = 0 or 1 desaturations in fatty acids. B) Lipid

that has accumulated in 20, 22, and 24 carbon SFA and MUFA pools that was subject to 18 to 20 elongation during the labeling period (48h). C) Summation of all accumulated 18 to 20 elongation product as described in B. D) Accumulated SFA + MUFA elongation products. E) Accumulated FASN products. F) Accumulated n-6 PUFA elongation products. See supplemental methods for a complete description of all fatty acid origins included for each summation.

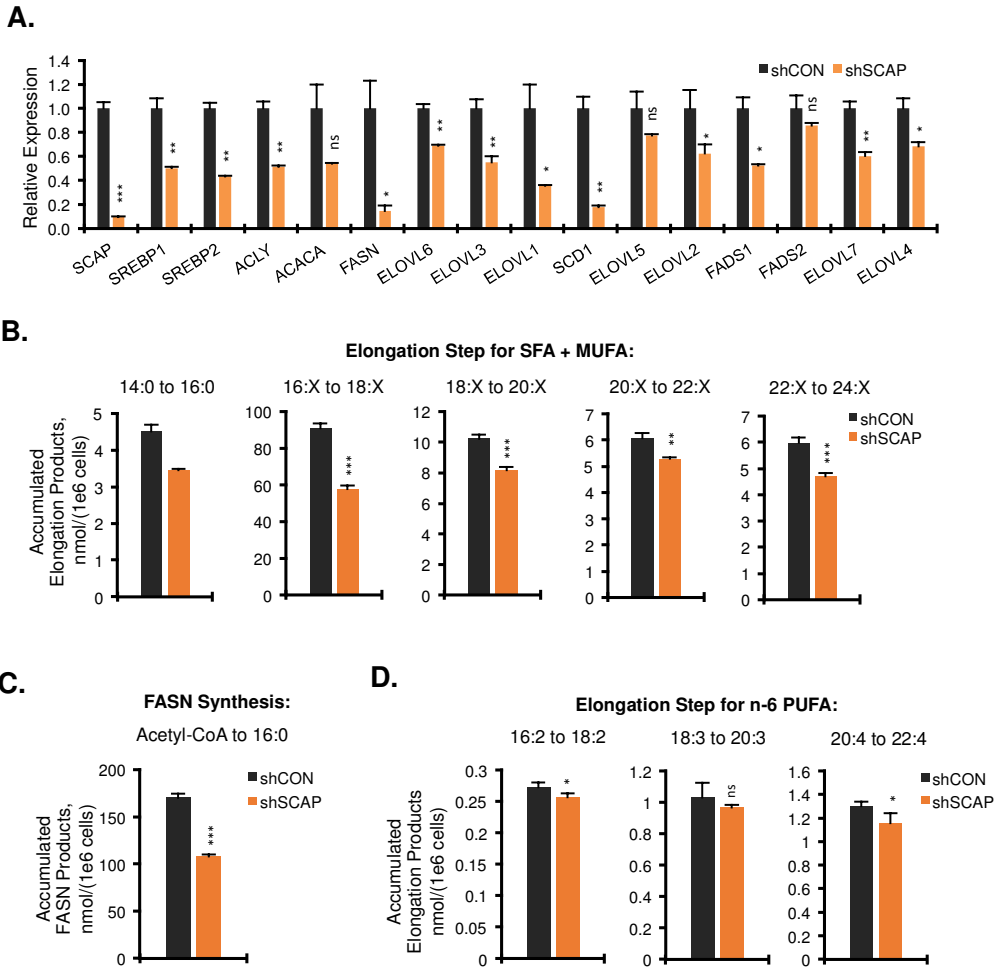


**Figure 7. Application of FASA to cells with acute silencing of SREBP.**

H1299 cells with a stably incorporated, doxycycline-inducible shCON or shSCAP were cultured for 48 hours in DMEM containing 5% FBS with 15 ug/mL doxycycline. These cells were then labeled for 48 hours in DMEM containing 100% U-<sup>13</sup>C<sub>6</sub>-glucose and U-<sup>13</sup>C<sub>5</sub>-glutamine, 5% FBS, and 15 ug/mL doxycycline. After labeling, cells were derivatized and analyzed as described in materials and methods. When applying FASA, values for *D* were fixed using results for 16:0 to facilitate modeling. Values represent average ± standard deviation (n = 3 for RNA, n = 4 for fatty acids). A) mRNA expression of SCAP and selected SREBP targets with doxycycline. B)

Accumulated SFA + MUFA elongation products. C) Accumulated FASN products. D) Accumulated n-6 PUFA elongation products. See supplemental methods for a complete description of all fatty acid origins included for each summation.

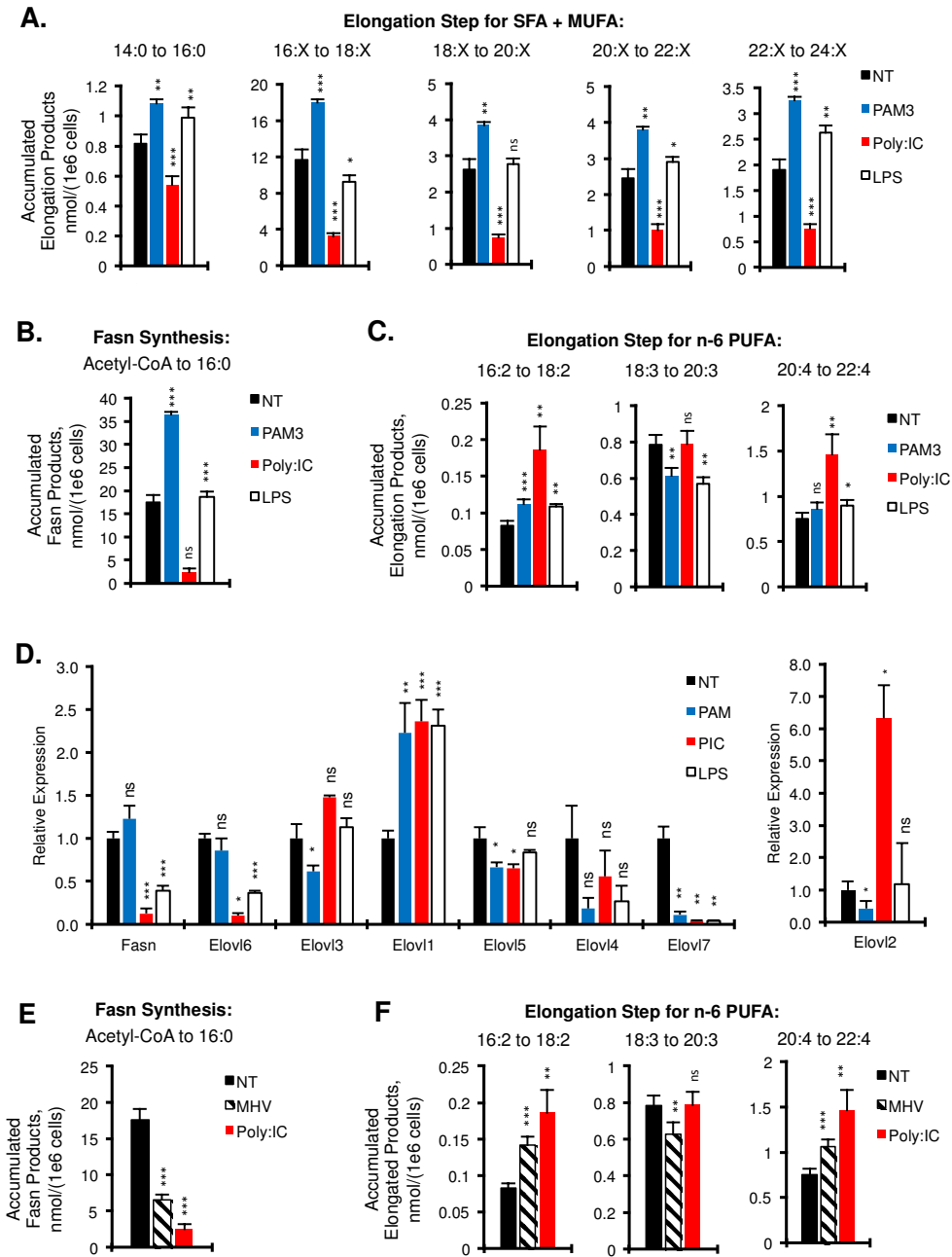
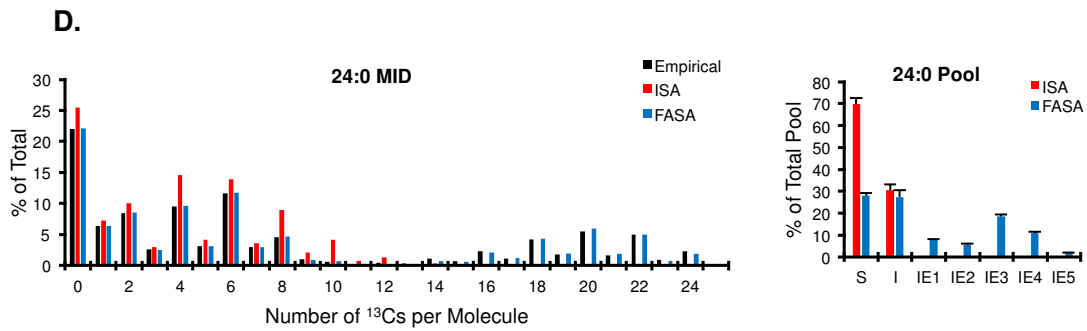
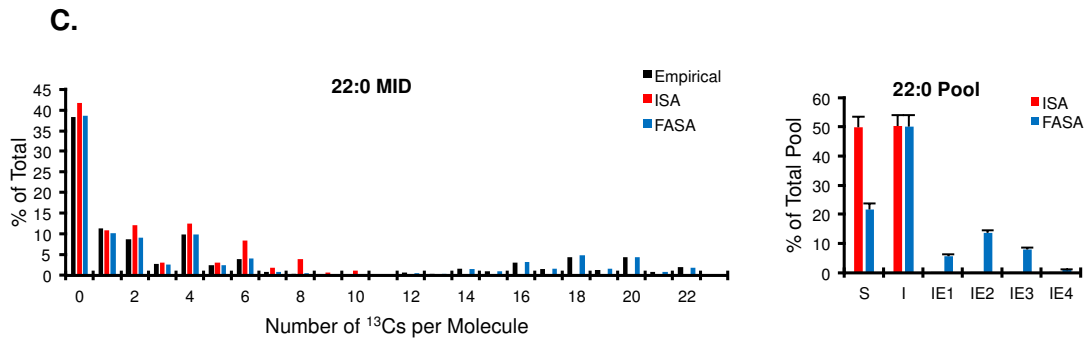
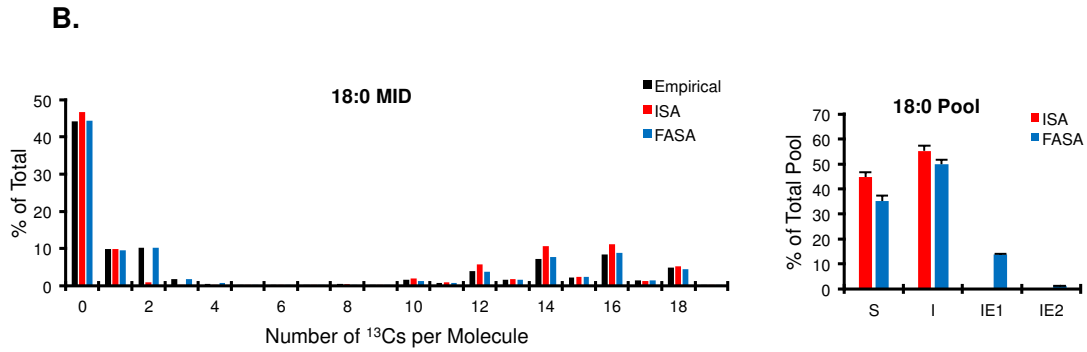
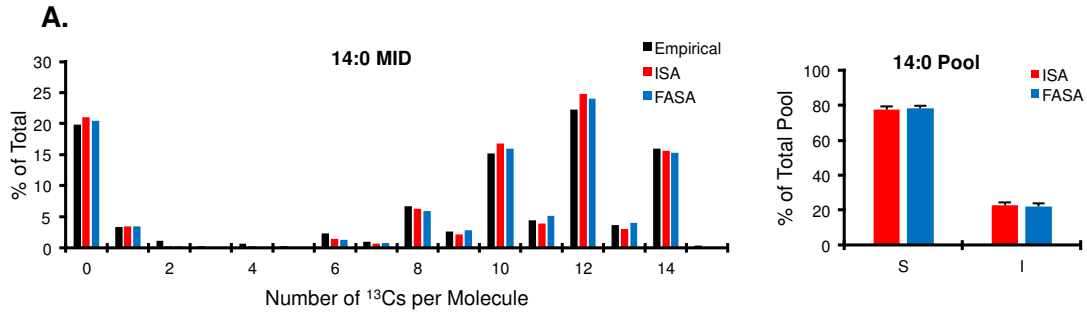


**Figure 8. Metabolic reprogramming of Fatty Acid Elongation Programs by TLRs.** BMDMs

were treated with vehicle, TLR2 agonist (PAM3 50 ng/mL), TLR3 agonist (Poly:IC 1000 ng/mL), TLR4 agonist (LPS 50 ng/mL), or  $\square$ -herpes virus 68 (MHV-68 MOI = 1) in media containing 100% U-<sup>13</sup>C<sub>6</sub>-glucose and 100% U-<sup>13</sup>C<sub>5</sub>-glutamine for 48 h. Cells were collected for

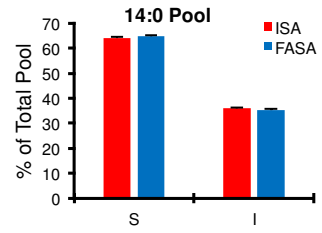
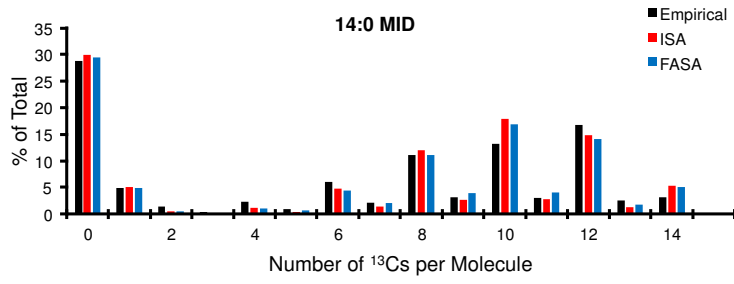
mRNA analysis after 24 h and for fatty acid analysis after 48 h as described in materials and methods. When applying FASA, values for *D* were fixed using results for 16:0 to facilitate modeling. Values represent average  $\pm$  standard deviation of biological quadruplicates. A) Accumulated SFA + MUFA lipids that were subject to the indicated elongation step for untreated (NT) and TLR activated macrophages. B) Accumulated lipids in cells that were synthesized by Fasn for untreated (NT) and indicated TLR activated macrophages. C) Accumulated n-6 PUFA lipid products that were elongated by the indicated step for NT and TLR activated macrophages. D) mRNA expression of Fasn and Elovl 1-7 for quiescent or TLR activated macrophages. E) Accumulated Fasn products for NT, Poly:IC, and MHV-68. F) Accumulated n-6 PUFA elongation products for NT, Poly:IC, and MHV-68. See supplemental methods for a complete description of all fatty acid origins included for each summation.



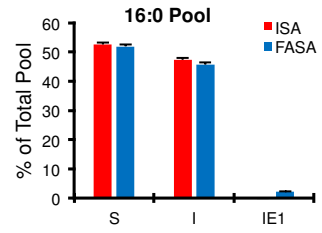
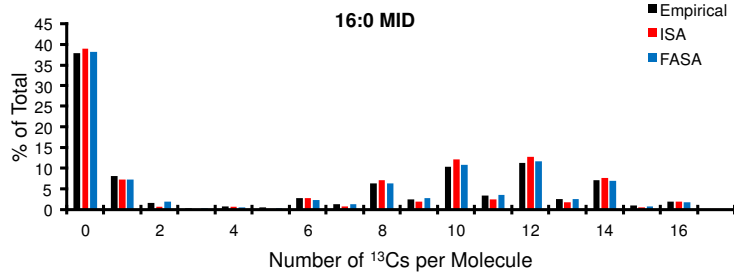
**Supplemental Figure 1. FASA Significantly Improves Fits for Fatty Acids Containing 18-24 Carbons in H1299 Cells.**

H1299 cells were cultured for 48 hours in DMEM containing 2% FBS, 100% U-<sup>13</sup>C<sub>6</sub>-glucose, and 100% U-<sup>13</sup>C<sub>5</sub>-glutamine. After labeling, cells were collected, derivatized, and analyzed as described in materials and methods. Representative empirical (black), ISA-derived (red), and FASA-derived (blue) MIDs as well as modeled fatty acid contribution parameters are shown for A) 14:0, B) 18:0, C) 22:0, and D) 24:0. Data shown for MIDs are representative singlets of biological quadruplicates. Data shown for pool contribution parameters are the average +/- standard deviation of biological quadruplicates.

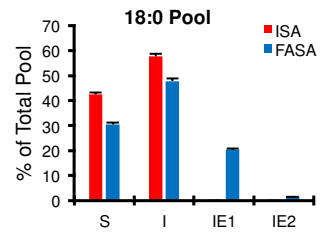
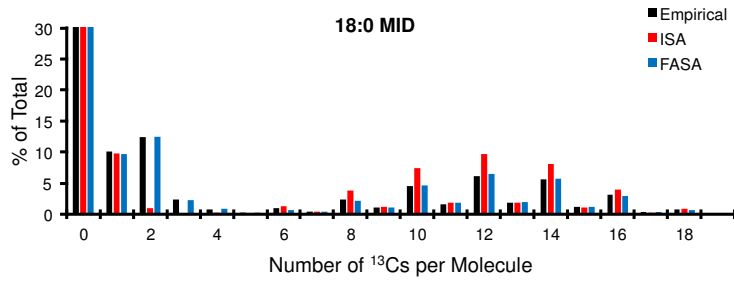
**A.**



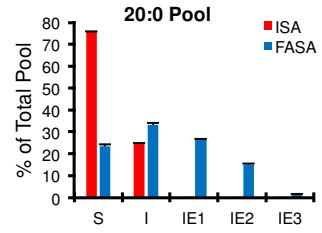
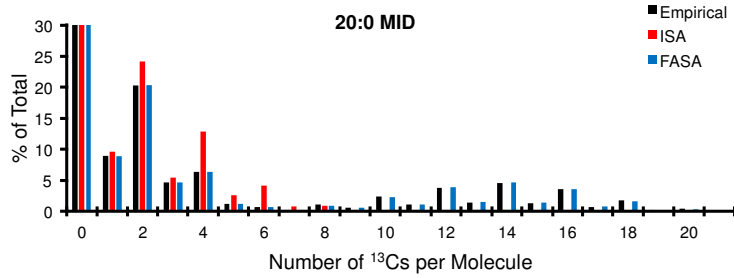
**B.**

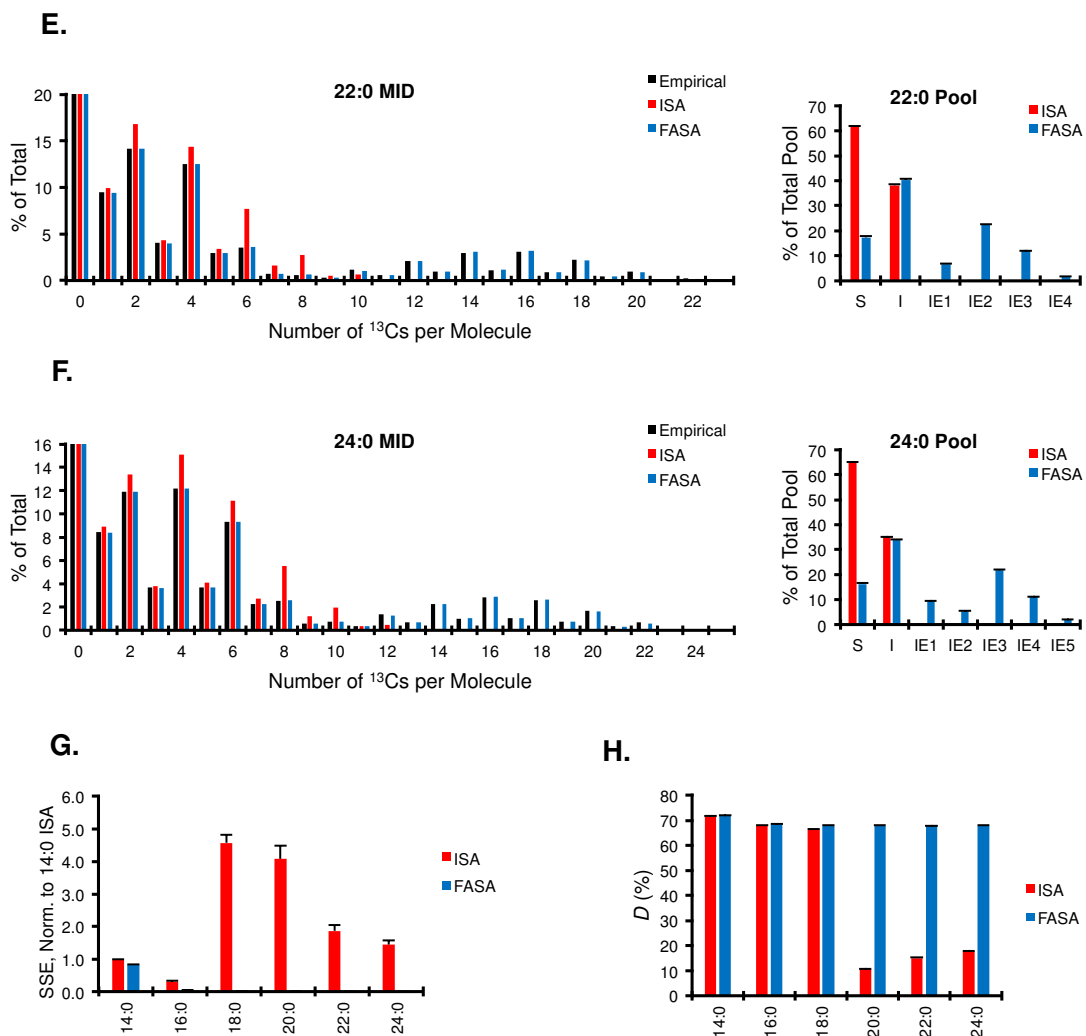


**C.**



**D.**

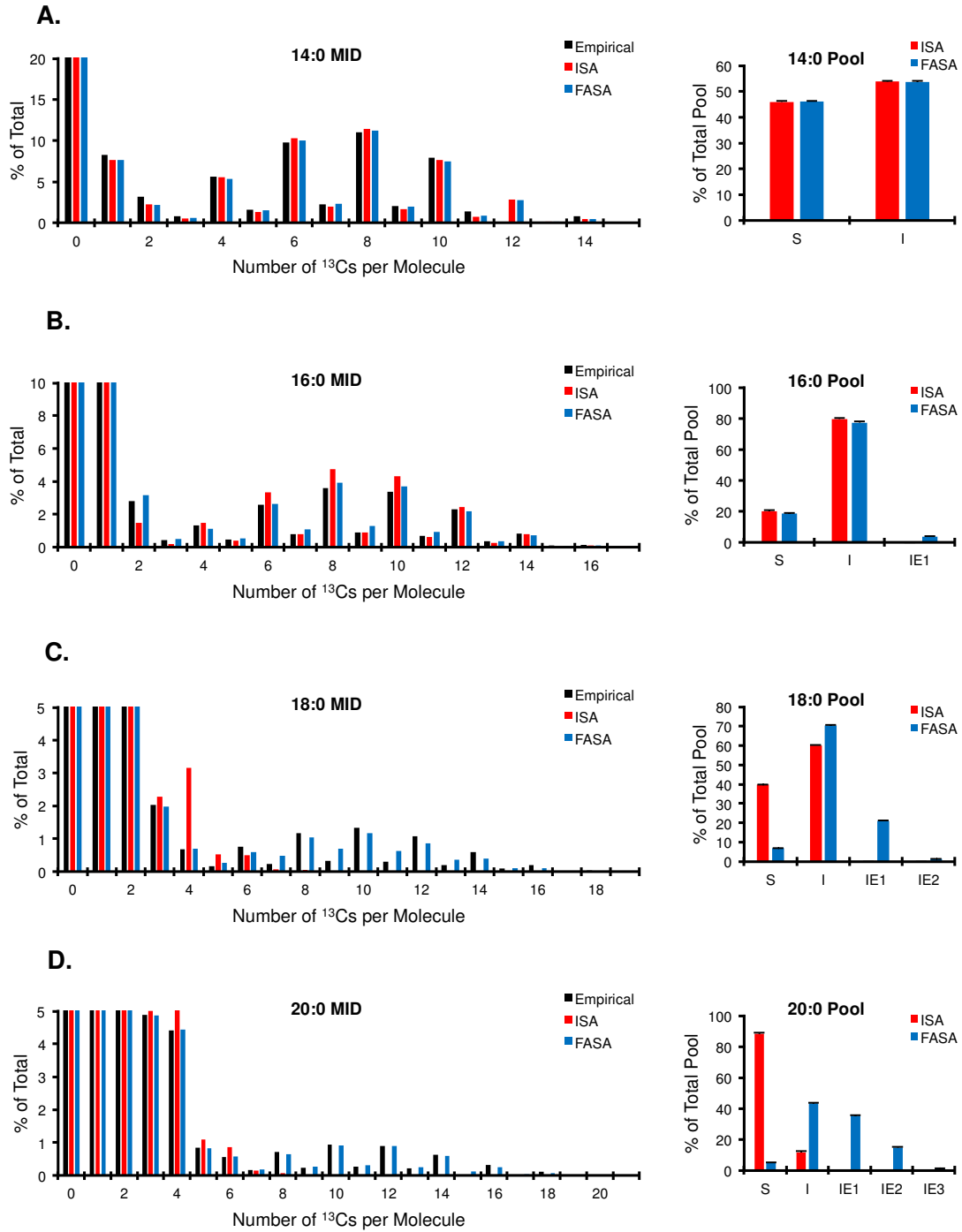


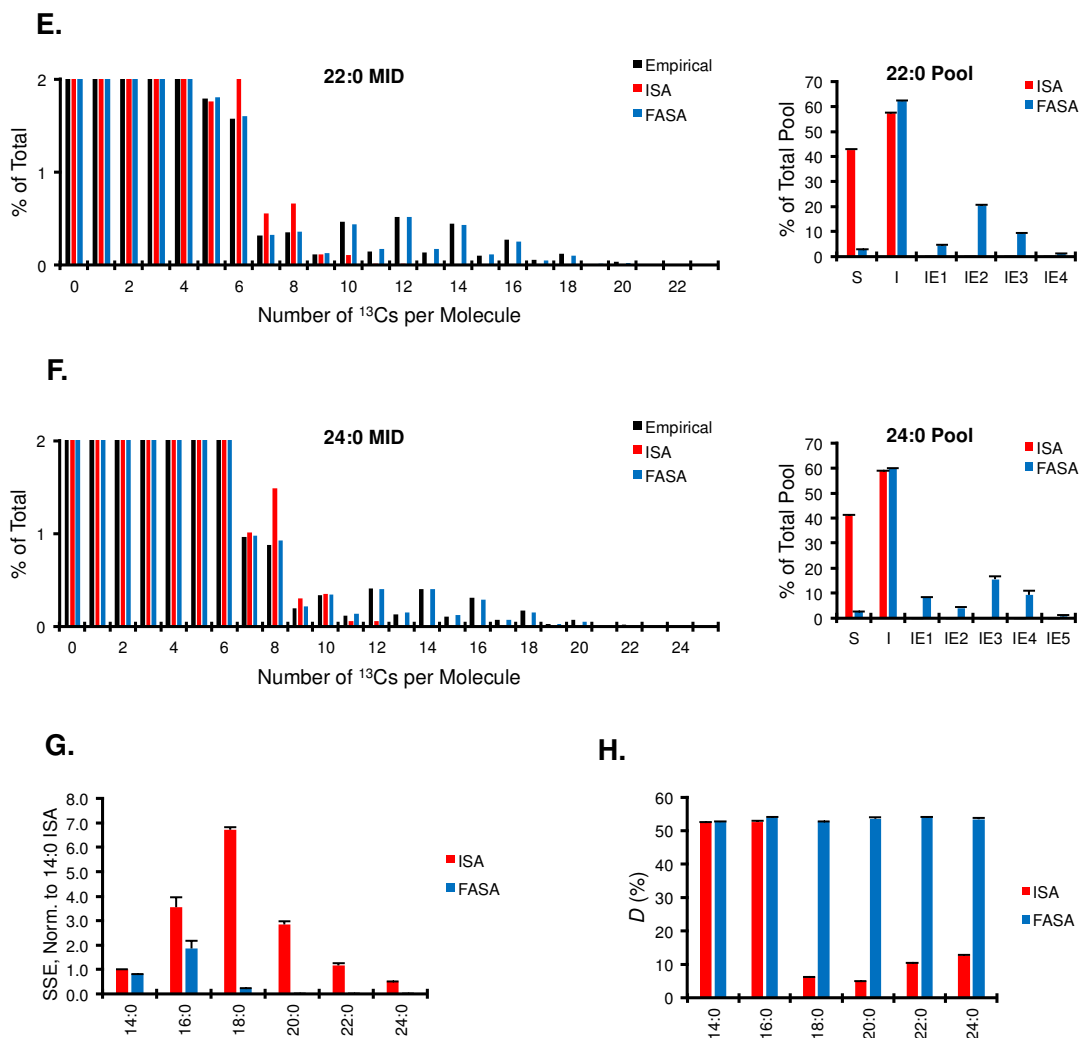


**Supplemental Figure 2. FASA Significantly Improves Fits for Fatty Acids Containing 18-24 Carbons in Murine Macrophages.**

BMDMs were cultured in media containing 100% U-<sup>13</sup>C<sub>6</sub>-glucose and 100% U-<sup>13</sup>C<sub>5</sub>-glutamine for 48 h. After labeling, cells were collected, derivatized, and analyzed as described in materials and methods. Representative empirical (black), ISA-derived (red), and FASA-derived (blue) MID as well as modeled fatty acid contribution parameters are shown for A) 14:0, B) 16:0, C) 18:0, D) 20:0, E) 22:0, and F) 24:0. G) Sum of Squared Error (SSE) for ISA and FASA,

normalized to 14:0. H) Acetyl-CoA enrichment parameter ( $D$ ) for indicated fatty acids using ISA (red) or FASA (blue). Data shown for MIDs are representative singlets of biological quadruplicates. Data shown for pool contribution parameters are the average  $\pm$  standard deviation of biological quadruplicates. Y-axes were modified for 20:0, 22:0, and 24:0 MIDs to better show the DNS distribution.

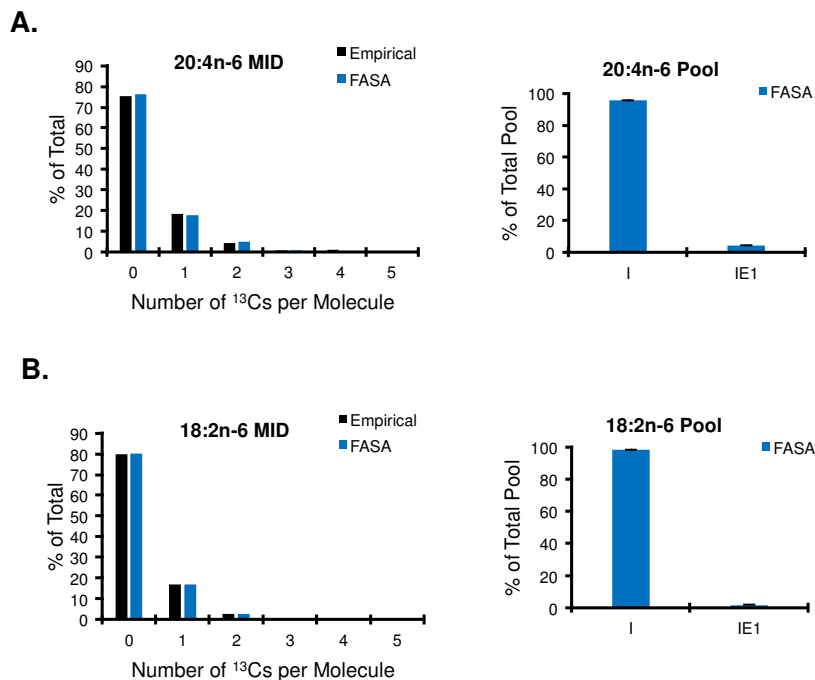




**Supplemental Figure 3. FASA Significantly Improves Fits for Fatty Acids Containing 18-24 Carbons in Primary Human Fibroblasts.**

Primary human fibroblasts were cultured in media containing 100% U- $^{13}\text{C}_6$ -glucose and 100% U- $^{13}\text{C}_5$ -glutamine for 72 h. After labeling, cells were collected, derivatized, and analyzed as described in materials and methods. Representative empirical (black), ISA-derived (red), and FASA-derived (blue) MID as well as modeled fatty acid contribution parameters are shown for A) 14:0, B) 16:0, C) 18:0, D) 20:0, E) 22:0, and F) 24:0. G) Sum of Squared Error (SSE) for

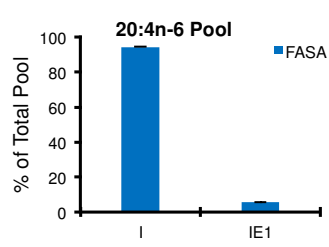
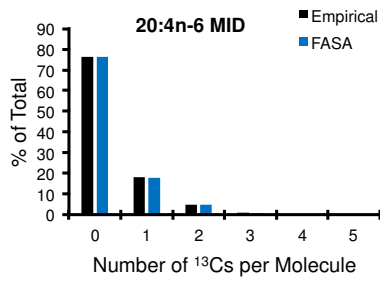
ISA and FASA, normalized to 14:0. H) Acetyl-CoA enrichment parameter (*D*) for indicated fatty acids using ISA (red) or FASA (blue). Data shown for MIDs are representative singlets of biological triplicates. Data shown for pool contribution parameters are the average +/- standard deviation of biological triplicates. Y-axis were modified for 18:0, 20:0, 22:0, and 24:0 MIDs to better show the DNS distribution.



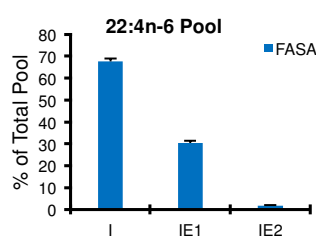
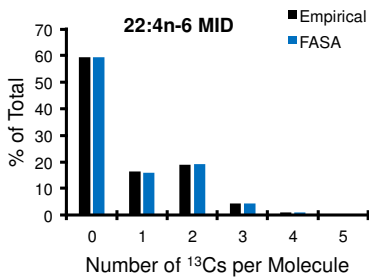
**Supplemental Figure 4. FASA Provides Excellent Fits for Polyunsaturated Fatty Acids in H1299 Cells.**

H1299 cells were cultured for 48 hours in DMEM containing 2% FBS, 100% U-<sup>13</sup>C<sub>6</sub>-glucose, and 100% U-<sup>13</sup>C<sub>5</sub>-glutamine. After labeling, cells were collected, derivatized, and analyzed as described in materials and methods. Representative empirical (black), ISA-derived (red), and FASA-derived (blue) MID as well as modeled fatty acid contribution parameters are shown for A) 20:4n-6 and B) 18:2n-6. Data shown for MID are representative singlets of biological quadruplicates. Data shown for pool contribution parameters are the average +/- standard deviation of biological quadruplicates.

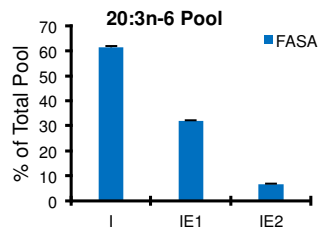
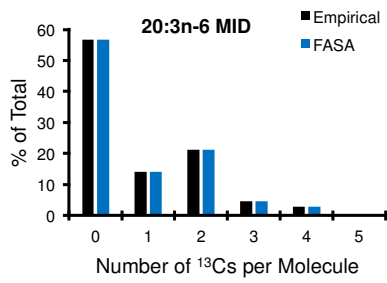
**A.**



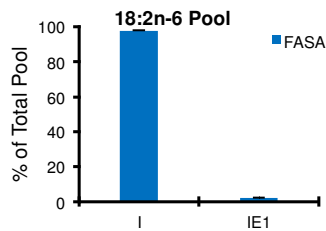
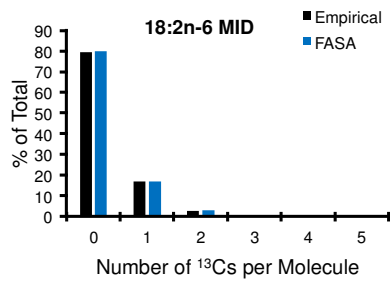
**B.**



**C.**



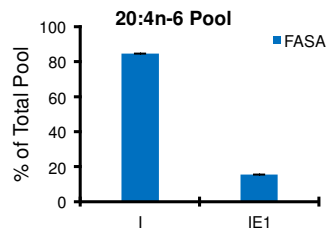
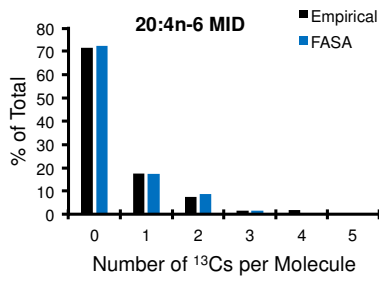
**D.**



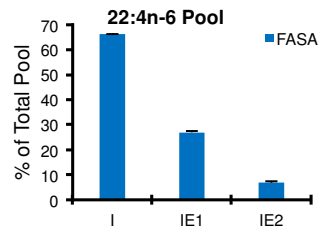
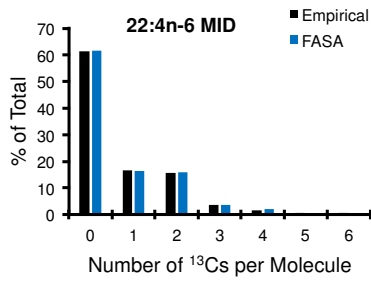
**Supplemental Figure 5. FASA Provides Excellent Fits for Polyunsaturated Fatty Acids in Murine Macrophages.**

BMDMs were cultured in media containing 100% U-<sup>13</sup>C<sub>6</sub>-glucose and 100% U-<sup>13</sup>C<sub>5</sub>-glutamine for 48 h. After labeling, cells were collected, derivatized, and analyzed as described in materials and methods. Representative empirical (black), ISA-derived (red), and FASA-derived (blue) MIDs as well as modeled fatty acid contribution parameters are shown for A) 20:4n-6, B) 22:4n-6, C) 20:3n-6, and D) 18:2n-6. Data shown for MIDs are representative singlets of biological quadruplicates. Data shown for pool contribution parameters are the average +/- standard deviation of biological quadruplicates.

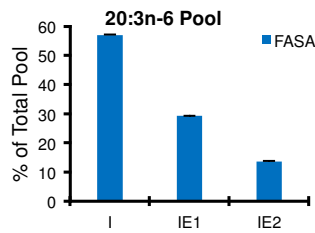
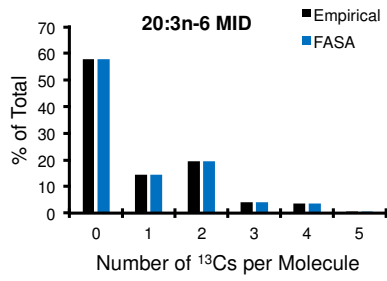
**A.**



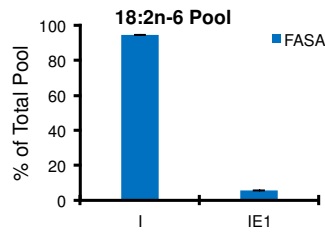
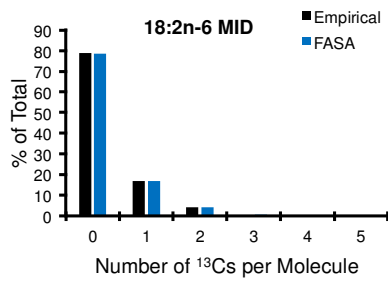
**B.**



**C.**

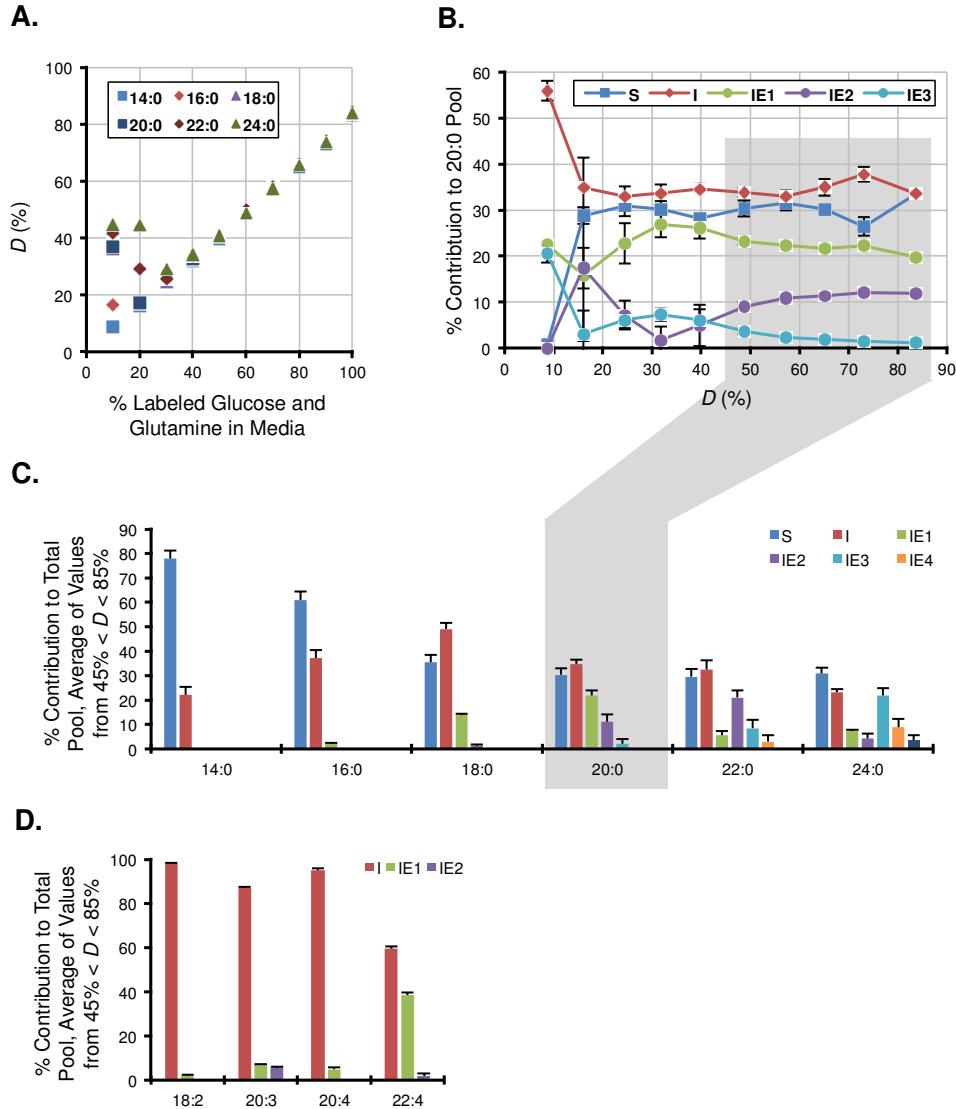


**D.**



**Supplemental Figure 6. FASA Significantly Improves Fits for Polyunsaturated Fatty Acids in Murine Macrophages.**

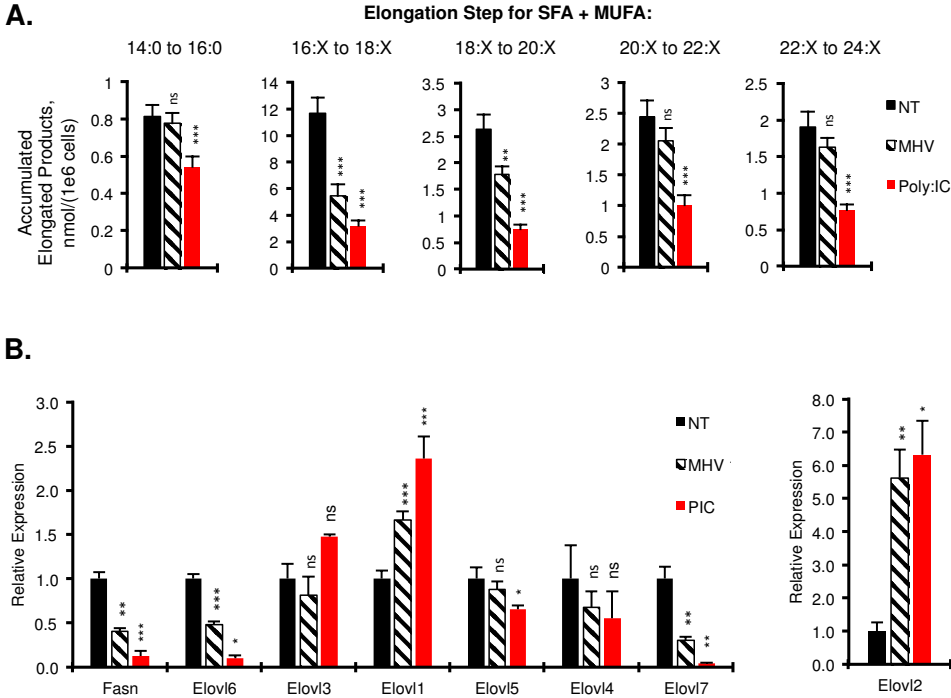
Primary human fibroblasts were cultured in media containing 100% U-<sup>13</sup>C<sub>6</sub>-glucose and 100% U-<sup>13</sup>C<sub>5</sub>-glutamine for 72 h. After labeling, cells were collected, derivatized, and analyzed as described in materials and methods. Representative empirical (black), ISA-derived (red), and FASA-derived (blue) MIDs as well as modeled fatty acid contribution parameters are shown for A) 20:4n-6, B) 22:4n-6, C) 20:3n-6, and D) 18:2n-6. Data shown for MIDs are representative singlets of biological triplicates. Data shown for pool contribution parameters are the average +/- standard deviation of biological triplicates.



**Supplemental Figure 7. Determining a Working Range for Lipogenic Acetyl-CoA Pool Labeling in FASA.**

H1299 cells with a stably incorporated, inducible shCON were cultured for 48 hours in DMEM containing 2% and 10%-100% U-<sup>13</sup>C<sub>6</sub>-glucose and U-<sup>13</sup>C<sub>5</sub>-glutamine. After labeling, cells were derivatized and analyzed as described in materials and methods. Values are average +/- standard deviation of biological triplicates unless otherwise noted. A) Modeled *D* is linear with percent of labeled glucose and glutamine in the media. Standard deviations are omitted for clarity, but were

< 0.5% for all points at or above 30% media label. B) For 20:0,  $S$ ,  $I$ , and  $IE_n$  parameter values are roughly consistent from at least 45% <  $D$  < 85%. C) Summary of parameter values for SFA. Values represent the average +/- standard deviation of all replicates where  $D > 45\%$ . D) Summary of parameter values for PUFA. Values represent the average +/- standard deviation of all replicates where  $D > 45\%$ .



**Supplemental Figure 8. Infection with MHV-68 Largely Recapitulates TLR3 Agonist Treatment.**

BMDMs were treated with vehicle, Poly:IC (1000 ng/mL, TLR3 agonist), or MHV-68 (MOI = 1) in media containing 100% U-<sup>13</sup>C<sub>6</sub>-glucose and 100% U-<sup>13</sup>C<sub>5</sub>-glutamine for 48 h. Cells were collected for mRNA analysis after 24 h and for fatty acid analysis after 48 h as described in materials and methods. When applying FASA, values for *D* were fixed using results for 16:0 to facilitate modeling. Values represent average ± standard deviation of biological quadruplicates.

A) Accumulated SFA + MUFA elongation products. B) mRNA expression of Fasn and Elov1-7. See supplemental methods for a complete description of all fatty acid origins included for each summation.

## References

1. Vance, D. E., and J. E. Vance (eds.). 2008. *Biochemistry of Lipids, Lipoproteins and Membranes*. 5th ed. Elsevier B.V., Oxford, UK.
2. Christie, W. W., and X. Han. 2010. *Lipid Analysis: Isolation, Separation, Identification, and Lipidomic Analysis*. 4th ed. The Oily Press, Bridgwater, England.
3. Menendez, J. A., and R. Lupu. 2007. Fatty acid synthase and the lipogenic phenotype in cancer pathogenesis. *Nat. Rev. Cancer*. **7**: 763–77.
4. Gerriets, V. a, and J. C. Rathmell. 2012. Metabolic pathways in T cell fate and function. *Trends Immunol.* **33**: 168–73.
5. Wakil, S. J. 1989. Fatty acid synthase, a proficient multifunctional enzyme. *Biochemistry*. **28**: 4523–4530.
6. Sassa, T., and A. Kihara. 2014. Metabolism of very long-chain Fatty acids: genes and pathophysiology. *Biomol. Ther. (Seoul)*. **22**: 83–92.
7. Kelleher, J. K., and T. M. Masterson. 1992. Model equations for condensation biosynthesis using stable isotopes and radioisotopes. *Am J Physiol Endocrinol Metab.* **262**: E118–E125.
8. Hellerstein, M. K., and R. A. Neese. 1992. Mass isotopomer distribution analysis: a technique for measuring biosynthesis and turnover of polymers. *Am. J. Physiol.* **263**: E988-1001.
9. Lee, W. N., S. Bassilian, H. O. Ajie, D. a Schoeller, J. Edmond, E. a Bergner, and L. O. Byerley. 1994. In vivo measurement of fatty acids and cholesterol synthesis using D2O and mass isotopomer analysis. *Am. J. Physiol.* **266**: E699–E708.
10. Oosterveer, M. H., T. H. van Dijk, U. J. F. Tietge, T. Boer, R. Havinga, F. Stellaard, A. K. Groen, F. Kuipers, and D.-J. Reijngoud. 2009. High fat feeding induces hepatic fatty acid

- elongation in mice. *PLoS One*. **4**: e6066.
11. Tredwell, G. D., and H. C. Keun. 2015. ConvISA: A simple, convoluted method for isotopomer spectral analysis of fatty acids and cholesterol. *Metab. Eng.* **32**: 125–132.
  12. York, A. G., K. J. Williams, J. P. Argus, Q. D. Zhou, G. Brar, L. Vergnes, E. E. Gray, A. Zhen, N. C. Wu, D. H. Yamada, C. R. Cunningham, E. J. Tarling, M. Q. Wilks, D. Casero, D. H. Gray, A. K. Yu, E. S. Wang, D. G. Brooks, R. Sun, S. G. Kitchen, T. T. Wu, K. Reue, D. B. Stetson, and S. J. Bensinger. 2015. Limiting Cholesterol Biosynthetic Flux Spontaneously Engages Type I IFN Signaling. *Cell*. **163**: 1716–1729.
  13. Argus, J. P., A. K. Yu, E. S. Wang, K. J. Williams, and S. J. Bensinger. 2017. An optimized method for measuring fatty acids and cholesterol in stable isotope-labeled cells. *J. Lipid Res.* **58**: 460–468.
  14. Lee, W., E. Bergner, and Z. Guo. 1992. Mass isotopomer pattern and precursor product relationship. *Biol. Mass Spectrom.* **21**: 114–122.
  15. Williams, K. J., J. P. Argus, Y. Zhu, M. Q. Wilks, B. N. Marbois, A. G. York, Y. Kidani, A. L. Pourzia, D. Akhavan, D. N. Lisiero, E. Komisopoulou, A. H. Henkin, H. Soto, B. T. Chamberlain, L. Vergnes, M. E. Jung, J. Z. Torres, L. M. Liao, H. R. Christofk, R. M. Prins, P. S. Mischel, K. Reue, T. G. Graeber, and S. J. Bensinger. 2013. An essential requirement for the SCAP/SREBP signaling axis to protect cancer cells from lipotoxicity. *Cancer Res.* **73**: 2850–62.
  16. Kelleher, J. K., and G. B. Nickol. 2015. *Isotopomer Spectral Analysis: Utilizing Nonlinear Models in Isotopic Flux Studies*. 1st Ed. Elsevier Inc.
  17. Buescher, J. M., M. R. Antoniewicz, L. G. Boros, S. C. Burgess, H. Brunengraber, C. B. Clish, R. J. DeBerardinis, O. Feron, C. Frezza, B. Ghesquiere, E. Gottlieb, K. Hiller, R. G.

- Jones, J. J. Kamphorst, R. G. Kibbey, A. C. Kimmelman, J. W. Locasale, S. Y. Lunt, O. D. Maddocks, C. Malloy, C. M. Metallo, E. J. Meuillet, J. Munger, K. Nöh, J. D. Rabinowitz, M. Ralser, U. Sauer, G. Stephanopoulos, J. St-Pierre, D. A. Tennant, C. Wittmann, M. G. Vander Heiden, A. Vazquez, K. Vousden, J. D. Young, N. Zamboni, and S.-M. Fendt. 2015. A roadmap for interpreting <sup>13</sup>C metabolite labeling patterns from cells. *Curr. Opin. Biotechnol.* **34**: 189–201.
18. Jonas, M. C., M. Pehar, and L. Puglielli. 2010. AT-1 is the ER membrane acetyl-CoA transporter and is essential for cell viability. *J. Cell Sci.* **123**: 3378–3388.
19. Wong, D. a, S. Bassilian, S. Lim, and W.-N. Paul Lee. 2004. Coordination of peroxisomal beta-oxidation and fatty acid elongation in HepG2 cells. *J. Biol. Chem.* **279**: 41302–9.
20. Bulusu, V., S. Tumanov, E. Michalopoulou, N. J. van den Broek, G. MacKay, C. Nixon, S. Dhayade, Z. T. Schug, J. Vande Voorde, K. Blyth, E. Gottlieb, A. Vazquez, and J. J. Kamphorst. 2017. Acetate Recapturing by Nuclear Acetyl-CoA Synthetase 2 Prevents Loss of Histone Acetylation during Oxygen and Serum Limitation. *Cell Rep.* **18**: 647–658.
21. Le, H. D., J. a Meisel, V. E. de Meijer, K. M. Gura, and M. Puder. 2009. The essentiality of arachidonic acid and docosahexaenoic acid. *Prostaglandins. Leukot. Essent. Fatty Acids.* **81**: 165–70.
22. Lagarde, M., B. Sicard, M. Guichardant, O. Felisi, and M. Dechavanne. 1984. Fatty acid composition in native and cultured human endothelial cells. *In Vitro.* **20**: 33–37.
23. Metallo, C. M., P. A. Gameiro, E. L. Bell, K. R. Mattaini, J. Yang, K. Hiller, C. M. Jewell, Z. R. Johnson, D. J. Irvine, L. Guarente, J. K. Kelleher, M. G. Vander Heiden, O. Iliopoulos, and G. Stephanopoulos. 2011. Reductive glutamine metabolism by IDH1 mediates lipogenesis under hypoxia. *Nature.* **481**: 380–384.

24. Abel, E. V., K. J. Basile, C. H. Kugel, A. K. Witkiewicz, K. Le, R. K. Amaravadi, G. C. Karakousis, X. Xu, W. Xu, L. M. Schuchter, J. B. Lee, A. Ertel, P. Fortina, and A. E. Aplin. 2013. Melanoma adapts to RAF/MEK inhibitors through FOXD3-mediated upregulation of ERBB3. *J. Clin. Invest.* **123**: 2155–2168.
25. Horton, J. 2002. SREBPs: activators of the complete program of cholesterol and fatty acid synthesis in the liver. *J. Clin. Invest.* **109**: 1125–1131.
26. Zhang, C., Y. Wang, F. Wang, Z. Wang, Y. Lu, Y. Xu, K. Wang, H. Shen, P. Yang, S. Li, X. Qin, and H. Yu. 2017. Quantitative profiling of glycerophospholipids during mouse and human macrophage differentiation using targeted mass spectrometry. *Sci. Rep.* **7**: 412.
27. O’Neill, L. A. J., and E. J. Pearce. 2016. Immunometabolism governs dendritic cell and macrophage function. *J. Exp. Med.* **213**: 15–23.

## CHAPTER FOUR:

### Future Directions

Over the course of my graduate studies, we have demonstrated the utility of stable isotope labeling, GC-MS, and modeling in measuring lipid metabolism (1–4). Furthermore, we have developed new analytical and mathematical tools for measuring very long chain fatty acid (VLCFA) metabolism (5, 6). In applying these tools, we have uncovered new aspects of fatty acid elongation and its regulation (6). Given the importance of VLCFA and their metabolism in basic biology and disease (7, 8), we anticipate that these new methods and findings will be of use to a wide variety of scientists. In addition to the significant progress made during this dissertation, this work has also created new areas for improvement and exploration.

Chapter Two of the dissertation outlined the method we have developed and optimized for derivatizing and analyzing fatty acids from stable isotope-labeled cells. Though this is the first method to have quantitative yields of fatty acid methyl esters (FAMES) from all major classes of mammalian lipids, and to yield high quality molecular ion mass isotopomer distributions (MIDs) for low abundance and/or highly unsaturated VLCFA (5), there are additional areas for improvement. One disadvantage of this method is that it is relatively long and labor-intensive; several areas could be streamlined. A liquid handler could be used for additions and extractions, particularly as sample number increases (9). The current acid-catalyzed methanolysis scheme (which requires a reaction time of 16-24 hrs) could be replaced with a base-catalyzed methanolysis followed by acid-catalyzed methanolysis (3-6 hrs) (10). This would combine strengths of base-catalyzed derivatization (high-speed transesterification of complex lipids under mild conditions) with the strengths of acid-catalyzed derivatization (high-speed esterification of free fatty acids under mild conditions) (11). Decreasing the number of hexane extractions from two to one and injecting a larger volume of sample would eliminate the need for sample

concentration and an associated transfer step. Though this would likely result in some loss of yield, we still anticipate having sufficient material and the time savings would be significant. Another challenge for this method is that it has been most thoroughly validated for cells collected *in vitro*. It is likely that the method could be adapted for serum, tissue, and even media with modest changes, particularly if the scheme involving base-catalysis followed by acid-catalysis is adopted. This would allow for measurement of VLCFA in a larger range of matrices, increasing the utility of the method overall.

Chapter Three of the dissertation explored the development and application of Fatty Acid Source Analysis (FASA), a model developed to translate the MIDs of stable isotope-labeled fatty acids (particularly VLCFA) into biologically useful information (6). Although we believe it moves the field forward as a first-of-its-kind framework, it also creates new questions and opens up new areas of study. We have tested the model in several systems (e.g. cancer cells, primary macrophages, primary fibroblasts, etc.) but it will be instructive to screen more cell types, particularly those where VLCFA concentrations are highest (e.g. glial cells (7)) or elongation-related genes are significantly regulated (e.g. browning adipose tissue (12)). Similarly, it will be instructive to test the model under different cell culture conditions. The cell culture conditions tested here contain low to modest levels of exogenous lipid available for scavenging (2-5% FBS). It would be interesting to determine how elongation is modified in media containing higher amounts of total lipids (10-20% FBS) or under loading conditions for specific lipids (e.g. BSA-conjugated 16:0 or 18:1). Under conditions of extreme lipid loading (20% FBS in addition to specific fatty acids supplemented at 100-500 $\mu$ M), it has been reported that the lipogenic acetyl-CoA pool for long and very long chain fatty acids can be significantly different in labeling

(13). This would cause a problem for FASA – thus, when using this method, it is important to validate that the modeled lipogenic acetyl-CoA pool enrichment is similar for all measured SFA and MUFA, particularly if the cells were cultured in a lipid-rich environment. Additionally, in the current studies, we have focused on information we can infer from single time points when fatty acid pools in cells are at steady state or before they have reached steady state. It is likely that we could gain additional information for the pre-steady state systems if we collected a time course (14). Given the complexity of fatty acid metabolic pathways (which include synthesis, degradation, interconversion, import, and export), collection of multiple early time points and fitting the data from FASA to a kinetic model would likely yield the best information on fatty acid metabolic fluxes (15).

Chapter Three of the dissertation also described how the application of FASA uncovered differential regulation of elongation in bone marrow-derived macrophages stimulated with different toll-like receptor (TLR) ligands. Given the striking differences conditions and the similarities between TLR3 and viral (MHV-68) responses, it is tempting to hypothesize that modulations in elongation play a functional role in a macrophage's response to specific pathogens. Also, given the upregulation of Elov12 and the accumulation of one of its products during labeling, 22:4n-6, it would be interesting to test if Elov12 overexpression or deletion modifies the functional response of macrophages to specific pathogens. If this functional difference is found, it would then be useful to determine what is controlling the upregulation of Elov12 and how it is changing the function of macrophages. Regulation of Elov12 is not well understood (8), and given that the substrates and products of Elov12 are VLC PUFAs (16),

decreases in the substrates or increases in the products could have direct effects on lipid signaling (e.g. eicosanoids) and/or membrane structure (17–19).

In sum, this dissertation work demonstrates the importance of measuring lipid metabolism using stable isotopes, GC-MS, and modeling. More specifically, we have developed novel analytical and modeling tools to measure VLCFA metabolism. We then applied these tools to relevant biological systems to learn new information about fatty acid elongation and how it is modulated. Given the importance of VLCFA to normal and pathophysiology, we anticipate this work will be useful to a wide variety of scientists in multiple fields.

## References

1. Williams, K. J., J. P. Argus, Y. Zhu, M. Q. Wilks, B. N. Marbois, A. G. York, Y. Kidani, A. L. Pourzia, D. Akhavan, D. N. Lisiero, E. Komisopoulou, A. H. Henkin, H. Soto, B. T. Chamberlain, L. Vergnes, M. E. Jung, J. Z. Torres, L. M. Liao, H. R. Christofk, R. M. Prins, P. S. Mischel, K. Reue, T. G. Graeber, and S. J. Bensinger. 2013. An essential requirement for the SCAP/SREBP signaling axis to protect cancer cells from lipotoxicity. *Cancer Res.* **73**: 2850–62.
2. Kidani, Y., H. Elsaesser, M. B. Hock, L. Vergnes, K. J. Williams, J. P. Argus, B. N. Marbois, E. Komisopoulou, E. B. Wilson, T. F. Osborne, T. G. Graeber, K. Reue, D. G. Brooks, and S. J. Bensinger. 2013. Sterol regulatory element-binding proteins are essential for the metabolic programming of effector T cells and adaptive immunity. *Nat. Immunol.* **14**: 489–99.
3. York, A. G., K. J. Williams, J. P. Argus, Q. D. Zhou, G. Brar, L. Vergnes, E. E. Gray, A. Zhen, N. C. Wu, D. H. Yamada, C. R. Cunningham, E. J. Tarling, M. Q. Wilks, D. Casero, D. H. Gray, A. K. Yu, E. S. Wang, D. G. Brooks, R. Sun, S. G. Kitchen, T. T. Wu, K. Reue, D. B. Stetson, and S. J. Bensinger. 2015. Limiting Cholesterol Biosynthetic Flux Spontaneously Engages Type I IFN Signaling. *Cell.* **163**: 1716–1729.
4. Mercer, J. L., J. P. Argus, D. M. Crabtree, M. M. Keenan, M. Q. Wilks, J.-T. A. Chi, S. J. Bensinger, C. P. Lavau, and D. S. Wechsler. 2015. Modulation of PICALM Levels Perturbs Cellular Cholesterol Homeostasis. *PLoS One.* **10**: e0129776.
5. Argus, J. P., A. K. Yu, E. S. Wang, K. J. Williams, and S. J. Bensinger. 2017. An optimized method for measuring fatty acids and cholesterol in stable isotope-labeled cells. *J. Lipid Res.* **58**: 460–468.

6. Argus, J. P., M. Q. Wilks, Q. D. Zhou, W. Hsieh, E. Khialeeva, V. Bui, S. Xu, A. K. Yu, E. S. Wang, H. R. Herschman, K. J. Williams, and S. J. Bensinger. Development and Application of Fatty Acid Source Analysis (FASA), A New Model for Quantifying Fatty Acid Metabolism Using Stable Isotope Labeling. *Manuscript in Preparation*.
7. Sassa, T., and A. Kihara. 2014. Metabolism of very long-chain Fatty acids: genes and pathophysiology. *Biomol. Ther. (Seoul)*. **22**: 83–92.
8. Jakobsson, A., R. Westerberg, and A. Jacobsson. 2006. Fatty acid elongases in mammals: their regulation and roles in metabolism. *Prog. Lipid Res.* **45**: 237–49.
9. Lin, Y. H., N. Salem, E. M. Wells, W. Zhou, J. D. Loewke, J. A. Brown, W. E. M. Lands, L. R. Goldman, and J. R. Hibbeln. 2012. Automated high-throughput fatty acid analysis of umbilical cord serum and application to an epidemiological study. *Lipids*. **47**: 527–539.
10. Christie, W. W., and X. Han. 2010. Lipid Analysis: Isolation, Separation, Identification, and Lipidomic Analysis. 4th ed. The Oily Press, Bridgwater, England.
11. Carrapiso, A. I., and C. García. 2000. Development in lipid analysis: some new extraction techniques and in situ transesterification. *Lipids*. **35**: 1167–77.
12. Jakobsson, A., J. A. Jørgensen, and A. Jacobsson. 2005. Differential regulation of fatty acid elongation enzymes in brown adipocytes implies a unique role for Elovl3 during increased fatty acid oxidation. *Am. J. Physiol. Endocrinol. Metab.* **289**: E517–E526.
13. Wong, D. a, S. Bassilian, S. Lim, and W.-N. Paul Lee. 2004. Coordination of peroxisomal beta-oxidation and fatty acid elongation in HepG2 cells. *J. Biol. Chem.* **279**: 41302–9.
14. Buescher, J. M., M. R. Antoniewicz, L. G. Boros, S. C. Burgess, H. Brunengraber, C. B. Clish, R. J. DeBerardinis, O. Feron, C. Frezza, B. Ghesquiere, E. Gottlieb, K. Hiller, R. G. Jones, J. J. Kamphorst, R. G. Kibbey, A. C. Kimmelman, J. W. Locasale, S. Y. Lunt, O.

- D. Maddocks, C. Malloy, C. M. Metallo, E. J. Meuillet, J. Munger, K. Nöh, J. D. Rabinowitz, M. Ralser, U. Sauer, G. Stephanopoulos, J. St-Pierre, D. A. Tennant, C. Wittmann, M. G. Vander Heiden, A. Vazquez, K. Vousden, J. D. Young, N. Zamboni, and S.-M. Fendt. 2015. A roadmap for interpreting <sup>13</sup>C metabolite labeling patterns from cells. *Curr. Opin. Biotechnol.* **34**: 189–201.
15. Wiechert, W., and K. Nöh. 2013. Isotopically non-stationary metabolic flux analysis: Complex yet highly informative. *Curr. Opin. Biotechnol.* **24**: 979–986.
16. Bond, L. M., M. Miyazaki, L. M. O'Neill, F. Ding, and J. M. Ntambi. 2016. *In Biochemistry of Lipids, Lipoproteins and Membranes*. 6th Ed., pp. 185–208. , Elsevier, Amsterdam.
17. Smith, W. L., and R. C. Murphy. 2016. *In Biochemistry of Lipids, Lipoproteins and Membranes*. 6th Ed, pp. 259–296. , Elsevier, Amsterdam.
18. Serhan, C. N. 2014. Pro-resolving lipid mediators are leads for resolution physiology. *Nature*. **510**: 92–101.
19. Dowhan, W., M. Bogdanov, and E. Mileykovskaya. 2016. *In Biochemistry of Lipids, Lipoproteins and Membranes*. 6th Ed., pp. 1–37. , Elsevier, Amsterdam.